Coupling of the deoxygenation of benzoic acid with the oxidation of propylene as a new tool to elucidate the architecture of Mo-based oxide catalysts.

Frédéric Dury

Acknowledgements

Au terme de ces quatre années de recherche, je souhaite remercier toutes les personnes qui ont participé, de près ou de loin, à l'élaboration de cet ouvrage.

Mes premiers remerciements s'adressent à feu le Professeur Paul Grange. En m'accueillant il y a cinq ans au sein de l'unité de catalyse et de chimie des matériaux divisés, il a insufflé, un peu à mon insu, le goût pour la recherche fondamentale.

Je tiens naturellement à adresser mes remerciements à mon promoteur de thèse, le Professeur Eric Gaigneaux ainsi qu'à tous les membres de ce jury de thèse, le Professeur Patrick Bertrand, le Professeur Michel Devillers, le Professeur Patricio Ruiz, le Professeur Frédéric Meunier et le Docteur Véron Nsunda pour leurs remarques constructives dans l'élaboration de cette thèse.

Je remercie le F.R.I.A. pour l'octroi de deux bourses de doctorat.

Une activité de recherche telle que celle qui fut la mienne pendant ces quatres années est difficilement concevable sans le soutien intellectuel, technique et logistique apporté par chaque membre du laboratoire mais également par plusieurs stagiaires que j'ai eu l'opportunité d'encadrer ; je souhaite leur exprimer à travers ces quelques lignes toute ma gratitude pour leur aide très précieuse.

Je ne voudrais pas manquer d'exprimer mes remerciements envers mes amis avec qui j'ai partagé d'excellents moments de détente, condition *sine qua none* pour maintenir une motivation à toute épreuve.

Enfin, j'adresse un merci tout particulier à ma famille et à mes parents pour leur aide, leurs encouragements répétés et leur foi en mon travail.

Beaucoup d'événements auront jalonné cette période de ma vie mais c'est sans nul doute ta rencontre qui aura été déterminante dans l'accomplissement de cette thèse. Merci, Ingrid, pour ta présence et tes encouragements quotidiens.

Contents

Part I

General introduction

The general introduction aims at presenting and justifying the purposes of the present work in the field of heterogeneous catalysis, more precisely in the selective oxidation of propylene and propane. By a short review of the history and actual needs of these reactions, we will develop our point of view about the pertinence of the present work.

Chapter 1

State of the art

Chemistry is everywhere, Chemistry can (almost) do everything. From the very little carbon nanotube or silicium microchip to the enormous tire of the new Airbus A380, *via* the clothes or the cosmetic products, Chemistry is impossible to circumvent.

The domains which are dealing with Chemistry are numerous. One of them is a primordial field : petrochemistry. Fuels, plastics, resins, rubbers, food additives, medical molecules, etc are derived from petrochemistry intermediates. It is thus obvious that a large amount of daily essential objects for our consumer society are the fruit of hydrocarbon molecules. From an economic point of view, Chemistry represents a market of about 1300 billions Euros. Among the related products, 90 percent are based on the use of a catalyst in a chemical process. The catalysts market is thus flourishing: in 2003, the global market for catalysts was 10 billions euros [1, 2, 3]. The forecasts show a growth of 3.4 percent per year only in the field of petrochemical intermediates. The demand for all the products based on hydrocarbons increases each year and justifies the investments made in the research field of petrochemistry and catalysis.

More precisely, the industrial and academic research in the heterogeneous catalysis domain is very active. Indeed, the heterogeneous catalysis presents

some advantages for the chemical industries compared to the homogeneous catalysis like (i) easy recovering of the catalyst, (ii) environmentally safer, (iii) possibility to work in the gaseous phase, etc. At this time, many resources are engaged to develop some heterogeneous catalytic systems which could allow the direct transformation of alkane to some more added value molecules, by the way of a selective oxidation reaction. Among the different strategies imagined by the research teams all over the world, one of them consists to transpose and to adapt the existing catalytic systems used in the transformation of olefins. Such a choice of strategy involves to imagine some new techniques and methods to study and to understand the molecular mechanisms subjacent to the activation and reactivity of the alkenes and/or alkanes on a solid catalyst.

1.1 The selective oxidation of propylene

The production of acrolein by the selective oxidation of propylene and propane follows the general guideline previously described.

Acrolein is not used as such but, as it is essential for the production of other essential compounds, it is of first importance. Acrolein is mainly used as a precursor in the synthesis of methionine or as an intermediate in the production of acrylic acid. Methionine is an amino acid used as a food additive for animals while acrylic acid is used primarily: as a starting chemical polyacrylate (surface coatings), polyacrylic acid and salts, including super-absorbent polymers, detergents, water treatment and dispersants, textiles and non-wovens, adhesives and sealants.

At this time, acrolein is mainly produced by the selective oxidation of propylene (eq. 1.1).

$$C_3H_6 + O_2 \rightarrow CH_2 = CH - CHO + H_2O \tag{1.1}$$

The main technologies commercially available have been developed by Nippon Shokubai [4], by Sohio (now known as British Petroleum) and by

BASF [5, 6] and are based on the supported multicomponent catalysts (see table 1.1). This reaction is carried out in the gas phase [7, 8] at a temperature in the range 600-723K, with a gas hourly space velocity (GHSV) of 1330-2600 h^{-1}, at a pressure of 2.026 10^5-2.53 10^5 Pa. An oxygen to propylene molar ratio around 1.6 is used, i.e. that for a propylene inlet concentration of 5-8 mol%, oxygen concentration may lie between 8 and 12.3%. These reaction conditions allow to reach 95% propylene conversion and a selectivity of 83% to acrolein for the best catalyst of which the key element formulation are Bi and Fe molybdates ($Mo_{12}BiFe_3Co_{4.5}Ni_{2.5}Sn_{0.5}K_{0.1}O_X$). Acrylic acid and total oxidation products are the main by-products. Other important groups like Mitsubishi Chemical Corporation, LG Chemical LTD, Nippon Catalytic Chemical Industries, Atofina (Total) are very active in the field of the heterogenous catalysis with a very high number of patents [4, 9, 10, 11].

The oxidation of propylene to acrolein is exothermic ($\Delta H = -340\,kJ\,mol^{-1}$ [8]) and proceeds, according to Grasselli [12], on bismuth molybdates, by the way of the molecular mechanism presented in figure 1.1. It is postulated that propylene can first coordinate to surface Mo^{6+} through a π donation bond. The bismuth oxygen bond in the vicinity of the molybdenum center proceeds to the α hydrogen abstraction. This step appears to be the rate limiting step. The transition state involves the formation of a CH-O bond between the molybdenum center and the hydrocarbon leading to the stabilization of the complex. Next, the new acrolein molecule is released thanks to the removal of a hydrogen atom by a neighbouring oxygen lattice bonded to a molybdenum atom. After the desorption of acrolein, water is released and the oxygen vacancy is postulated to migrate to the site of earlier oxygen reduction where it is reoxidized thanks to the oxygen from the gas phase.

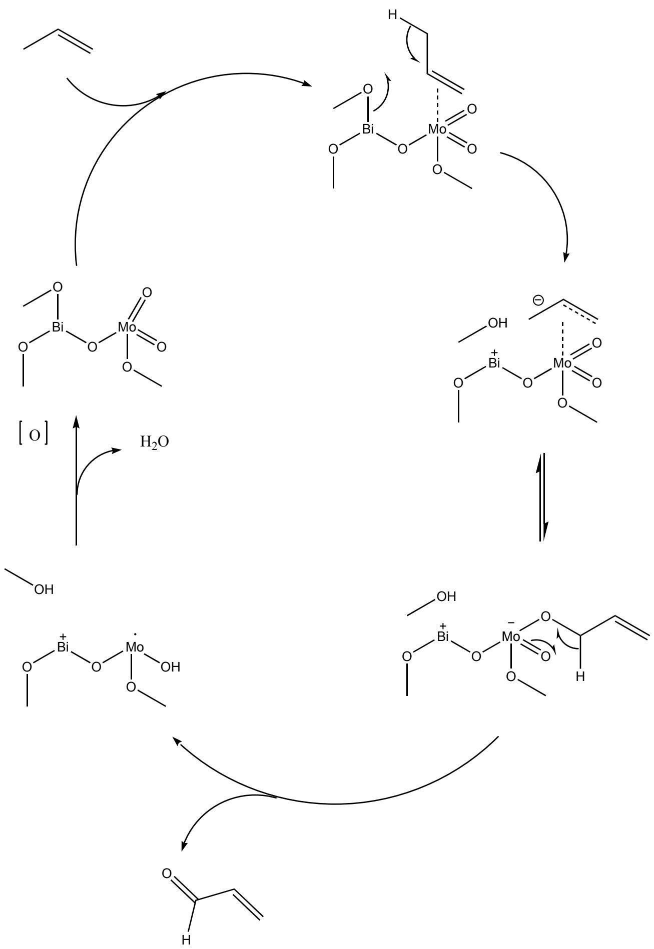

Figure 1.1: Reaction scheme of the oxidation of propylene on bismuth molybdate according to Grasselli [12].

Table 1.1: Commercial catalysts developed for the oxidation of propylene to acrolein.

Catalyst	*Year of commercial use*
$CuO\text{-}SiO_2$	1950
$Bi/Mo/P/O\text{-}SiO_2$	1957
$Bi/Mo/P/Fe/O\text{-}SiO_2$	1959
$Bi/Mo/P/Fe/Co/Ni/O\text{-}SiO_2$	1964
$Bi/Mo/P/Fe/Co/Ni/K/O\text{-}SiO_2$	1970
$Bi/Mo/P/Fe/Co/Ni/K/W/O\text{-}SiO_2$	1972

1.2 The catalysts

The catalysts used in the industrial process of propylene oxidation to acrolein have been improved over the years (table 1.1). The first catalyst based on CuO, developed by Shell between 1940 and 1955 gave acrolein with high selectivity (60%) but at low conversion of propylene (20%). Improvements have been obtained by the use of bismuth phosphomolybdate based catalysts developed by Standard Oil of Ohio between 1957 and 1962. The third generation of catalysts used in the selective oxidation of propylene to acrolein were multicomponents molybdate based catalysts (Co, Ni, Fe, Bi, K, W, P, Si). This late generation of catalysts, with the following composition, $Mo_{12}BiFe_3Co_{4.5}Ni_{2.5}Sn_{0.5}K_{0.1}O_X$, shows a good activity which allows to reach a selectivity to acrolein of 83% and 95% conversion at 593K [7].

The determination of these complex industrial formulations was boosted thanks to the fundamental research done by the Academics in the field of propane (amm)oxidation and propylene oxidation. Several researches were led to determine and characterize the catalytic sites active in such reactions.

During this late decade, three well-known groups respectively headed by Ueda, Grasselli and Schlögl have performed some crucial advances in the discovery of some highly efficient oxidation catalysts. These authors have contributed to the better understanding of several multicomponent catalysts based on the Mo-V-O formula. The main contribution of both Ueda and Grasselli was the establishment of the link between the catalytic performances and the crystalline structure of the multicomponent catalysts [13, 14, 15, 16]. They systematically studied the influence of some elements substitutions on the catalytic activity [15]. Thus, Te and Nb were respectively demonstrated to enhance the promotion of propylene intermediate and the selectivity to acrylic acid in the oxidation of propane. Group of Schlögl, based on the experimental fact that such high-performance catalysts are all predominated by structures of the Mo_5O_{14} type, focussed their work on the characterization of this kind of structure [17]. For that purposes, the authors have studied by transmitting electron microscopy the structure of the molybdenum (sub)oxides as several model catalysts [18].

All these research programs indirectly highlight the importance of several subjacent concepts like, crystal face structure, lattice oxygen, defects, metal oxygen bond strength, redox properties, etc.

1.3 Some critical concepts

Catalytic performances are often explained in agreement with one or several concepts. Many of them are used or considered in this work to explain the catalytic results. Hereafter, some major theories are described.

Haber has contributed to demonstrate that the selective oxidation of propylene occurs on (100) and (101) faces of MoO_3 whereas total oxidation is induced on faces (010) [19]. Many years before, Volta was arguing that selective catalytic sites for acrolein were located on the (020) crystal face [20]. These contradicting results were thus the starting point of several new research programs in order to precise the exact role of some specific crystal

faces [21, 22, 23].

Whatever the right hypothesis, this view of the active site is still too rigid and too general to fully explain the mechanisms taking place at the atomic scale. In fact, this crystal face dependent behaviour is the reflect of some specificity in the Mo-O bonds present at the surface of these particular crystal faces. It highlights that a single bonded or double bonded Mo-O will have some intrinsic electronic properties. These can be modified by the near or far electronic environment, i.e. the presence and the oxidation state of the other elements. Some of these electronic properties were investigated using a probe reaction. Thus, experiments of 1-butanol dehydration by Haber strongly suggested that the selectivity to oxidation products was correlated to the exchangeability of the superficial oxygen atoms [23]. Moreover, dehydration of 2-butanol on MoO_3 indicated that the oxidative activity was improved when the surface of the catalyst was slightly reduced [24].

These experimental facts are obviously correlated to the metal oxygen bond strength and/or length. It has been shown several times that the incorporation or the substitution of one or several elements in a crystal structure was contributing to enhance the conversion and/or the selectivity to the oxidation products. This concept is critical in the multicomponent catalyst as shown by Grasselli, Ueda and Schlögl [13, 16, 17]. It is claimed that these isolated elements could contribute to change the critical length of some bonds which are thus more geometrically adapted to the organic reactant. The substitution of elements could also allow to tune the redox properties of the catalysts.

Besides the hypothesis concerning the cations, bulk and superficial oxygen atoms of the catalyst probably constitute the core of an oxidation reaction. Indeed, it is now well established that most of the oxidation reactions take place with the participation of the oxygen lattice. In fact, several equilibria between the adsorbed oxygen, the superficial oxygen, the bulk oxygen and the gaseous oxygen dictate the catalytic performances of an oxidation reaction. In a similar way, the selectivity of the oxidation reaction is influenced by

the electronic characteristics of the oxygen species. One distinguishes the superoxide (O_2^-), the peroxide (O_2^{2-}), the monoatomic "electrophilic" oxygen (O^-) and monoatomic "nucleophilic" oxygen (O^{2-}). $O^-$is often associated with the total oxidation while O^{2-} is associated with the selective "mild" oxidation but all can be generated at the surface of a same catalyst depending on the reaction conditions. Conversion and selectivities in an oxidation reaction are thus connected by the oxygen species and their related equilibria. For example, when an oxygen atom is used by the organic reactant, some oxygen defects are generated at the surface of the oxide. Several possibilities exist to minimize the impact of the oxygen vacancy on the catalyst stability. In some cases, bulk oxygen atoms can migrate to the surface and fill the oxygen defects. As a consequence, this leads to the formation of a bulk oxygen defect. In other cases, gaseous molecular oxygen is activated on the surface of the catalyst and migrates to the defect point to regenerate the superficial oxygen lattice. Other possibilities for the system to minimize the instability caused by the oxygen abstraction is to reorganize its crystalline structure by the generation of some shear structures or some modifications in the coordination of the cations. The reorganized oxide can be called suboxides.

Other mechanisms exist but they all contribute to increase the mobility of the remaining oxygen lattice and as a direct consequence, the catalytic activity. This enhanced activity favoured by the presence of some bulk oxygen defects (or shear structures) was demonstrated by Gaigneaux in the oxidation of isobutene to methacrolein [25]. The activity of MoO_3 was compared with the activity of Mo_8O_{23}. These experiments highlighted that the initial activity was higher in the presence of the molybdenum suboxides before its further oxidation to MoO_3. However, the best activity was maintained because a specific under-stoichiometry between the molybdenum and the oxygen atoms was preserved during the reaction by the formation of a new molybdenum suboxides, namely $Mo_{18}O_{52}$.

1.4 The improvements to be realized

In the past, methods used to reach a performing catalyst were quite empiric but nevertheless successful. However, some drawbacks have not been avoided. As mentioned in section 1.1, the acrolein is not used as such but serves mainly as an intermediate compound. The selective oxidation of propylene to acrolein is in fact often incorporated in a two-step process to produce acrylic acid. This is imposed by the available catalysts since the reaction conditions in each step of the catalytic process are different. Currently, many research programs are active to develop a catalyst which could be used in a one-step process, i.e. to produce acrylic acid starting from propylene. These attempts are not so concluding as the single-step process remains at a research level. Thus, the improvement of the existing two-step processes and their related oxide catalysts is still the best way to obtain the highest yield in the production of acrylic acid.

Whatever the pathway to maximize the production of acrylic acid, acrolein or propylene are some obliged products. Until now, the main source of propylene comes from the steam cracking of naphta which also leads to a huge production of ethylene. Since propylene is also the main building block of polypropylene, industrials are seeking for some new sources of propylene. A promising source of the olefin is the dehydrogenation of the corresponding alkane. In the view of producing propylene and acrolein for the acrylic acid multi-step process or its direct use in a single-step process, propane offers several economical and industrial advantages. Indeed, propane is available in large quantities and is poorly used. But, major improvements are still necessary in the field of the catalysts. The main problem encountered when using the propane to produce acrylic acid in a single-step process is the reactivity of the acid and its further degradation. When propane is used as the feedstock to produce propylene or acrolein, a large amount of the hydrocarbons is burned into CO and CO_2 by releasing large quantities of heat. The control of the by-products and the side reactivity goes necessarily through

the optimization of the existing oxide catalysts. Such an optimization must be accomplished by the way of a better knowledge of the oxidation active site and an extensive comprehension of the molecular mechanisms occurring during the oxidation of propane and propylene.

Chapter 2

Overview of the thesis

2.1 Purposes

The previous chapter has shown that the catalysis of oxidation is widely used for the production of many added value molecules. Whereas the oxide catalysts dedicated to their synthesis and the corresponding processes are successfully used in the petrochemical industries, some improvements are needed. Thus, it is still possible to improve the catalysts for (i) better catalytic performances (no by-products, higher yields), (ii) a better lifetime of the active phases and (iii) a more simple catalytic process, i.e. single-step instead of multi-step processes.

Since several decades, the old static view of the catalyst, namely the rigid definition of a catalytic entity[1], has been progressively amended by some new theories highlighting the modifications undergone by the catalysts during the catalytic reaction. The new dynamic view of the heterogeneous catalysis has emerged to explain the good performances measured on some new complex oxide catalytic phases. Among these dynamic phenomena, one can cite the formation of a new amorphous or crystalline phase from the starting material or the development of a particular plane [28, 29, 22, 30, 31, 32, 33, 34, 35], the

[1] a substance, usually used in small amounts relative to the reactants, that modifies and increases the rate of a reaction without being consumed in the process [26, 27].

modification of the oxidation level in the bulk or at the surface of the catalyst [24, 36, 37, 38, 39, 40], the reconstruction of some specific crystalline plane by the action of some surface mobile species [25, 41, 42, 43, 44, 45, 46, 47, 48] and the creation at the surface of the catalyst of some cationic and anionic vacancies [21, 49, 50, 51, 52]. More precisely, the presence of oxygen vacancies seems to be a critical parameter for an improved catalytic activity in terms of hydrocarbon conversion and selectivity to oxidized products. Indeed, some authors claimed that an oxide catalyst of which the surface is lightly reduced, namely of which the surface presents some oxygen vacancies, exhibits higher catalytic performances [24].

Thus, it becomes necessary to develop some new tools to detect and to monitor the dynamic modifications undergone by the catalyst. The crystallographic modifications and the variations of the oxidation state can be quite easily measured *ex-situ* by some specific, but rather heavy, methods based on X-ray radiations, photoelectron spectroscopy or more generally on the core electron study. Unfortunately, the creation of oxygen vacancies is often badly understood since both powerful, cheap and easy characterization techniques are not available. However, the comprehension of this superficial dynamic modification could be of great importance to improve the oxide catalysts. Indeed, in a majority of oxidation reactions realized on the molybdenum based oxide catalysts, a Mars & Van Krevelen mechanism (MVK) is observed . In such a mechanism, the hydrocarbon is oxidized, in a first step, by the oxygen atoms coming from the catalyst, namely lattice oxygens. In a second step, the oxygen vacancies resulting from the abstraction of the oxygen atoms in step one are filled by the decomposition of the gaseous oxidant which could be molecular oxygen, N_2O,... [53, 54] (figure 2.1). This constitutes an equilibrium between two reaction rates which can be displaced in favor of the oxidizing/reducing step depending on (i) the strength of the oxidizing/reducing gas, (ii) the capacity of the catalyst to activate the molecules. The position of the oxidizing/reducing equilibrium can thus lead to the formation of some oxygen vacancies related to a particular oxidation state and to some further

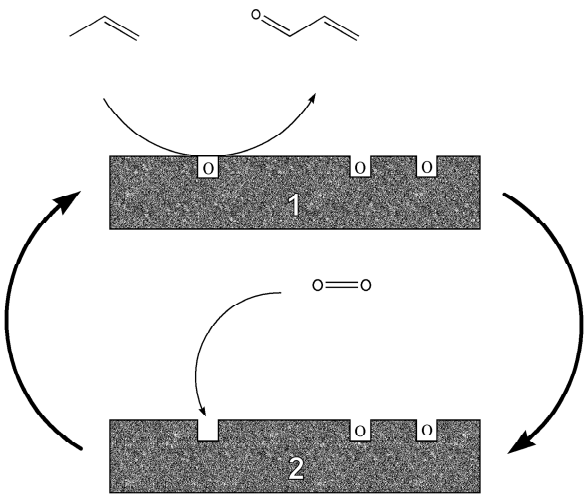

Figure 2.1: Scheme of the Mars & Van Krevelen mechanism observed in several oxidation reactions.

improved catalytic performances.

Thus, the challenge is to detect any modifications of the catalyst at the atomic scale. Some new physico-chemical characterization techniques like the atomic force microscopy (AFM) or the scanning tunneling microscopy (STM) have been used and have provided some spectacular results. In particular, STM and AFM have allowed to image the modifications undergone by a molybdenum oxide during a specific reaction [55, 56, 57, 58]. Whereas AFM and STM (and all the complex techniques) provide some quite dramatic and useful information, they are not flexible enough to be used during a catalytic reaction and cannot thus provide any "real" observations caught when the catalyst is "at work". One can imagine to obtain these information "at the atomic scale" with some spectroscopic techniques used *in-situ* or *operando*, but many technical and economic limitations still prevent from reaching the goal.

To compensate for these drawbacks, we propose to develop a new probe

reaction in which the products formed could characterize the surface of the oxide catalysts in term of atomic vacancies. More precisely, we focus our attention on the lattice oxygens and their related vacancies at the surface of the molybdenum based oxide catalysts. In the perspective of improving the performances of the oxide catalysts by a better comprehension of the dynamic transformations undergone by the active catalytic site, it becomes evident that some major information could be obtained from the characterization of the oxygen vacancies. This suggests that the number and the mutual disposition of the lattice oxygen (and their related vacancies) within a catalytic site is a determining factor of the conversion level and the selectivity in an oxidation reaction run on oxide catalysts. It is also obvious that the oxygen vacancies could be intimately correlated with the oxidation state of the metallic elements and their coordination.

Among the reactions involving some oxygen transfer to the catalysts, the deoxygenation of benzoic acid to benzaldehyde and toluene could be an adequate candidate to probe the oxygen vacancies. Indeed, the conversion of the acid and the different selectivities have been reported in the literature to be dictated by the number and the mutual disposition of the oxygen vacancies available at the surface of an oxide catalyst [59, 60]. The use of such a probe-reaction coupled with an oxidation reaction in conjunction with the classical methods of characterization (X-ray diffraction, X-ray photoelectron spectroscopy, Raman spectroscopy,...), will allow us to precise “in real-time” the nature of the catalytic site according to its oxygen vacancies. For this purpose, an original coupling between the deoxygenation of benzoic acid and the oxidation of propylene is developed in the second part of this work. The catalytic system can thus be summarized like this : oxygen atoms needed to oxidize propylene into acrolein or CO/CO_2 comes by the intermediate of the lattice oxygen, from the benzoic acid (instead of molecular oxygen in a conventional system) transformed in benzaldehyde or toluene (figure 2.2). Finally, the coupling is used to characterize the molybdenum oxide based catalysts in term of oxygen vacancies when they are used in the oxidation of

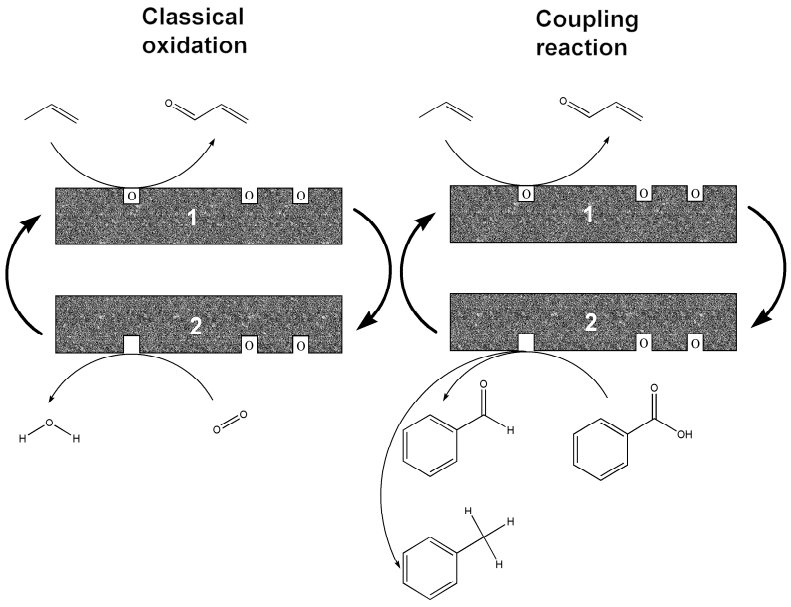

Figure 2.2: Schematic view of the classical MVK mechanism and the coupling reaction.

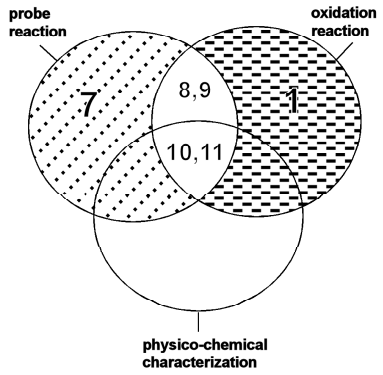

Figure 2.3: Global strategy of this work. Numbers symbolize the chapters of this thesis.

propylene according to the MVK mechanism [54].

2.2 Research strategy

The strategy for developing the new tool presented in section 2.1 can be summarized into two major steps : (i) development of the probe reaction in the presence of hydrogen and testing of its potentialities (part III), (ii) development of the coupling between the probe reaction and the oxidation of propylene, use of the coupling to probe/characterize the surface of some selected molybdenum oxide catalysts (part IV).

The strategy is represented by the schema of the figure 2.3. After a short review of the state of the art in the oxidative heterogeneous catalysis field (chapter 1), the objectives will be defined and justified in the chapter 2. Chapters 3 to 5 are concerned with the description of the experimental work.

The first step of this strategy aims to evaluate the deoxygenation of the benzoic acid in the conditions reported in the literature, i.e. in the presence of hydrogen on the molybdenum (sub)oxides. Thus, it is essential to check the reactivity and the stability of the catalysts in this reducing condition (chapter

6). Moreover, the systematic characterization of the catalysts before and after the reaction combined with the results provided by the probe reaction itself must allow to validate this reaction to probe the oxygen vacancies (chapter 7). This step directly conditions the realization of the second one since it allows to understand how to interpret the results provided by the probe reaction.

The second step is the core of this research. Indeed, the coupling between the probe reaction and the oxidation of propylene must demonstrate that the probe reaction is an adequate tool to characterize "in real time" the active catalytic site in an oxidation reaction. Therefore, the coupling is performed on the selected molybdenum (sub)oxides (chapter 8) then on some metal molybdates as a model of the industrial catalysts (chapter 9). This allows to demonstrate, in chapter 10, that the coupling follows the MVK mechanism and is thus adequate as a probe reaction of the oxygen vacancies. Finally, thanks to some correlations between the information provided by the probe reaction and some physico-chemical characterizations, we precise the nature of the catalytic site active in oxidation (chapter 11).

2.2.1 Description of the probe reaction

The deoxygenation of benzoic acid was first used by Sakata et al. on oxide catalysts to study the general reaction pathway [59]. Their motivation was the improvement of the aromatic aldehyde production thanks to a deeper understanding of this reaction. Indeed, the demand for such molecules is growing. Moreover, the production of aldehydes from carboxylic acids knows an increasing interest among the industrial producers who are seeking an alternative process to the Rosenmund reduction[2]. However, some work is still needed to increase the selectivity to the desired products since several by-products are synthesised during the catalytic reaction. The authors have studied the oxides of Mg, Pb, Cr, La, Pr, Yb, Mn, Fe, Co, Zn, Zr and Ce in the presence of hydrogen as the reductant for the direct hydrogenation of the

[2]The Rosenmund reduction proceeds with an halogenation of the benzoic acid followed by a hydrogenation.

benzoic acid. This screening allowed to distinguish two categories of catalysts in relation to the selectivity pattern. Two basic mechanisms have thus been highlighted : (i) group I (MgO, PbO, Cr_2O_3, La_2O_3) of which reactivity is dictated by their *basic* properties. The main products (benzene and phenol) are formed by a radical-like mechanism. (ii) group II (MnO_2, Fe_2O_3, ZnO, ZrO_2,etc.) of which reactivity is controlled by their *redox* properties. These oxides mainly produce benzaldehyde and toluene with a selectivity governed by the reduction degree of the oxide.

A second research group (de Lange, van Ommen and Lefferts) had also performed several investigations on the formation of the selective product (benzaldehyde) and by-products (benzene, phenol, benzophenone, benzylalcohol, etc.) during the direct hydrogenation of benzoic acid on ZnO and ZrO_2 [60, 61]. They conclude, like Sakata, that the formation of benzaldehyde proceeds by a reverse Mars & van Krevelen mechanism : the molecular hydrogen reduces the catalyst, leading to the formation of some oxygen vacancies, then the catalyst is re-oxidised by the benzoic acid. By-products like benzylalcohol are generated via secondary reactions of benzaldehyde when the conversion of benzoic acid is complete. It has been shown that the production of by-products depends on the amount of molecular hydrogen provided to the catalytic system. When the feed is rich in molecular hydrogen, benzaldehyde and toluene are favoured. In the other extreme cases, when there is no hydrogen, benzene and benzophenone are the only products formed but with a very low rate.

Although no information was available on the feasibility of such a reaction on molybdenum based oxide catalysts and on the further coupling with the oxidation of propylene (instead of the use of the molecular hydrogen), it was choosen to exploit the reverse Mars & van Krevelen mechanism claimed by Sakata. This property could be used to develop a new probe reaction of the oxygen vacancies created during an oxidation reaction.

To be an adequate probe reaction, Tatibouet mentioned that the deoxygenation of benzoic acid must fulfill several conditions [62] : "*A good*

surface probe obviously should be influenced by the nature of the catalytic surface, i.e., the chemical composition or arrangement of the surface atoms. This means that the reaction used must be sensitive to the structure of the catalyst surface to permit a meaningful comparison among the catalysts tested. The test reaction should also present a wide selectivity pattern, for which at least two intermediates follow separate routes leading to the different final products. The ideal situation is obviously obtained when each route is determined by a specific property such as Lewis or Brönsted acidity or by different arrangement of surface atoms (structure sensitivity)". This first criterion makes the deoxygenation a strong candidate as a probe reaction. Indeed, the structure sensitivity is claimed by Sakata et al. who have tested this specific reaction on several basic and acidic metal oxides [59]. The deoxygenation of benzoic acid is clearly dependent on such properties since the presence/absence of oxygen vacancies is the determining factor for the formation of benzaldehyde, toluene and benzene.

Tatibouet also highlights a second condition to validate a specific reaction as a probe reaction [62] : *"Moreover, the test reaction should be useful at a temperature where no surface reconstruction occurs during the catalytic cycle"*. The thermal stability of the catalyst is more difficult to evaluate *a priori.* But, the high calcination temperature of all the catalysts used in this work (upper than 823K, the maximum reaction temperature) is a security factor which could minimize such a reconstruction phenomenon.

The reaction mechanism should be known according to Tatibouet [62] : *"Finally, a good knowledge of the reaction mechanism is necessary to permit the correct interpretation of the variations in the catalytic behaviour observed from studies of a series of catalysts*". Many authors, including Sakata, have devoted a long time to improve the understanding of the reaction pathway leading to the formation of the three main products, namely benzaldehyde, toluene and benzene [59, 60, 63].

As revealed in the previous section, the deoxygenation of benzoic acid in the presence of hydrogen is described in the literature as a reaction with

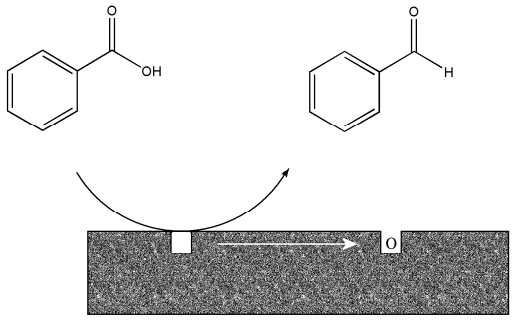

Figure 2.4: Principle of formation of a benzaldehyde molecule from one benzoic acid molecule according to Sakata et al.

selectivities to the different products depending on the arrangement of oxygen vacancies (O_V) at the surface of the oxide catalysts. Sakata and Ponec have proposed that, on oxides like ZrO_2, Mn_3O_4 or MgO, benzaldehyde can be produced at the surface of catalysts exhibiting isolated oxygen vacancies (eq. 2.1, figure 2.4) [64, 65, 60].

$$C_6H_5COOH + O_V \rightarrow C_6H_5COH + O_L \tag{2.1}$$

Moreover, twin oxygen vacancies, namely vacancies close to each other, catalyze the formation of toluene (eq. 2.2, figure 2.5). In such a mechanism, the oxygen vacancies (O_V) are filled with the oxygen atoms coming from the benzoic acid.

$$C_6H_5COOH + 2\,O_V + 2H \rightarrow C_6H_5CH_3 + 2\,O_L \tag{2.2}$$

with O_L representing lattice oxygen atoms and O_V representing oxygen vacancies.

A third product, benzene, can also be produced by a radical-like

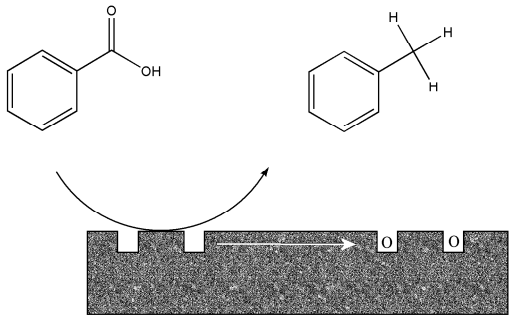

Figure 2.5: Principle of formation of a toluene molecule from one benzoic acid molecule according to Ponec et al.

mechanism but without requiring oxygen vacancies [59, 64, 65].

Following the performances of the deoxygenation of benzoic acid thus clearly allows to probe the catalysts surface state in terms of density and relative arrangement of the oxygen vacancies.

2.2.2 Catalysts used in this research

Since our main objective is to develop a tool that will probe the oxygen vacancies of an oxide catalyst during its use in an oxidation reaction, we have focused our choice on molybdenum based catalysts since they are widely used in the heterogeneous catalysis field. In a more targeted way, we have chosen to use the molybdenum (sub)oxides (MoO_{3-X}) and some metal molybdates. Molybdenum (sub)oxides will be used to optimize and to test the potentialities of the deoxygenation of benzoic acid as a probe reaction whereas the metal molybdates will be mainly used in the coupling reaction as a model of the industrial catalysts. More details concerning the catalyst are provided in the annexes.

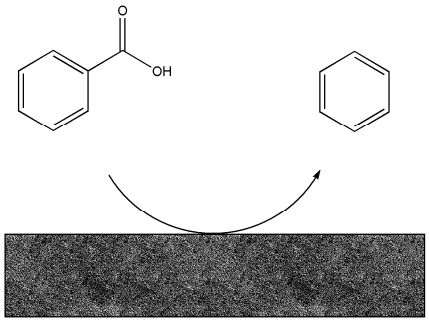

Figure 2.6: Principle of formation of a benzene molecule from one benzoic acid molecule according to Ponec et al.

Part II

Experimental

This part lays out all the experimental methods used in the present work. On several occasions, the reader is invited to refer to the chapters 3 to 5 to obtain the precise protocol of the experiments.

Chapter 3

Catalysts preparation

3.1 Molybdenum (sub)oxides

The preparation of molybdenum suboxides, i.e. molybdenum oxides with oxygen defects in the bulk structure, needs much attention. Molybdenum suboxides are very sensitive to oxidizing or reducing atmospheres and have thus poor structural stability. That characteristic is also responsible for the difficulties met when we tried to obtain a specific molybdenum suboxide phase with a high purity level.

Magneli and after him, Kilhborg were the pioneers in the controlled preparation of molybdenum suboxides [66, 67, 68, 69, 70, 71, 72, 73, 74, 75]. Their method was quite simple but requires much care in the preparation step. We will call it "Solid state method" hereafter. The principle was very simple and consisted in controlling the total molybdenum and oxygen contents in the final solid. These authors considered that molybdenum suboxides have an oxidation stage which is intermediate between MoO_2 and MoO_3. The desired oxidation level corresponding to a particular molybdenum suboxide was obtained by simply mixing together a precise amount of MoO_2 and MoO_3 in a closed volume under vacuum. The temperature and the time of calcination was apparently determined empirically by the authors. But, these

Table 3.1: Parameters for the preparation of molybdenum suboxides by the solid state method.

Molybdenum suboxide	*Temperature of calcination (K)*	*Time of calcination (h)*	*Amount of MoO_2 (moles)*	*Amount of MoO_3 (moles)*
Mo_4O_{11}	973	120	1	3
Mo_8O_{23}	1023	96	1	7
Mo_9O_{26}	916	72	1	8

parameters were chosen in such a way that the migration of molybdenum and oxygen atoms permits the formation of the new crystalline structure. Table 3.1 summarizes the different parameters used for the synthesis of Mo_8O_{23}, Mo_9O_{26} and Mo_4O_{11}.

Practically, MoO_2 (Aldrich, 99%) was pre-treated under a 60 ml min^{-1} flow of 5% H_2 in nitrogen at 723K/1h to reduce the potential oxidized species at the surface of the powder. Similarly, MoO_3 (Aldrich, 99.5%) was oxidized in a 60 ml min^{-1} flow of pure oxygen at 623K/2h. The pretreated molybdenum dioxide was used as fast as possible since no particular precautions were taken to avoid the oxidation of MoO_2 in air. Predetermined amounts of "reduced" MoO_2 and "oxidized" MoO_3 were closely mixed by hand in an Agathe mortar during 20 minutes. The granulometry was thus not checked. Ten grams of the obtained grey powder were introduced in a specific quartz reactor between two walls of quartz wool (figure 3.1). The quartz reactor was then sealed under a vacuum of 10^{-3} Pa. The cell was heated under static vacuum according to the parameters described in table 3.1. Times of calcination were taken from the literature [67, 69, 71].

Stoichiometric oxides, namely MoO_2 and MoO_3, were used in the catalytic tests after the respective pre-treatments described above in the preparation procedure of molybdenum suboxides.

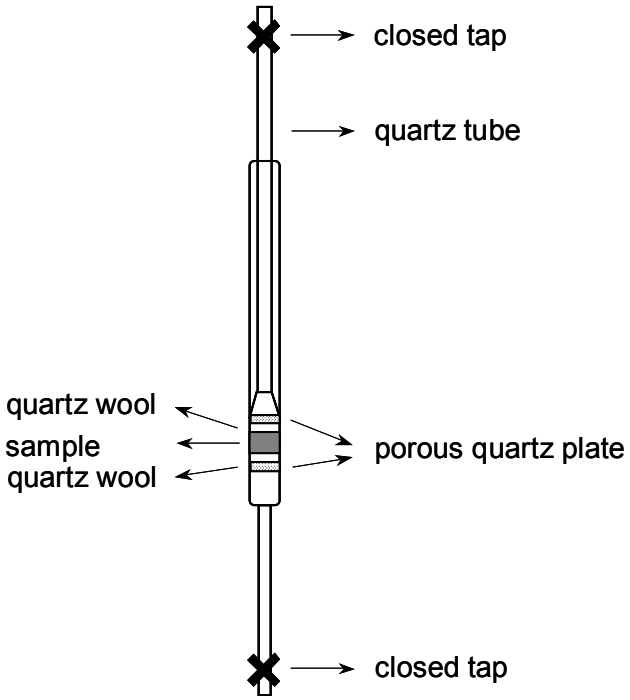

Figure 3.1: Simplified scheme of the quartz reactor used for the synthesis of molybdenum suboxides.

3.2 Metal molybdates

Six metal molybdates were prepared. Fe molybdate was synthesised by the co-precipitation method whereas Co, Ni and three Bi molybdates were obtained thanks to the citrate method.

3.2.1 Fe molybdate

13,6438 g of $Fe(NO_3)_3.9H_2O$ (Merck, 99%) were dissolved in 100 ml of distilled water (solution A). A second solution was obtained by dissolving 8,9466 g of $(NH_4)_6Mo_7O_{24}.4H_2O$ (Aldrich, ACS reagent) in 100 ml of distilled water (solution B). Its pH was adjusted to 2 with nitric acid (Aldrich, 25%). Then, the solution A was added drop by drop in solution B. The mixed solutions were stirred for three hours in the glass vessel at 90°C. During that time the colour of the solution has changed from yellow to green. The precipitate was filtered, dried at 393K/12h and finally calcined at 648K/10h. The obtained phase was $(Fe_2(MoO_4)_3$ [76].

3.2.2 Co, Ni and Bi molybdates

For the following catalysts, we have used an identical synthesis protocol. Precursors and quantities are summarized in table 3.2.

Precursors A and B were dissolved separately in 100 ml of distilled water at room temperature (solutions A and B). When complete dissolution was reached, the mixture of the solutions A and B was adjusted to pH 1 with nitric acid (Aldrich, 25%). Then, the appropriate amount of citric acid (Merck, 99%) dissolved in 100 ml of distilled water, was added drop-wise to the mixed precursors solution. Afterwards, water was evaporated at 310K under reduced pressure and the obtained solid was dried overnight at 353K under vacuum. The dried solid was calcined in air first at 573K during 20 hours then a second time at 723K during 20 hours.

Table 3.2: Amount of precursors for the preparation of molybdate catalysts by the “citrate method”.

Metal molybdate	***Precursor A***	***Precursor B***	***Amount of A (g)***	***Amount B (g)***	***Amount of citric acid (g)***
$CoMoO_4$	$(NH_4)_6Mo_7O_{24}.4H_2O$ (Aldrich, ACS reagent)	$Co(NO_3)_2.6H_2O$ (Merck, 99%)	8.0337	13.2855	12.5241
$NiMoO_4$	$(NH_4)_6Mo_7O_{24}.4H_2O$ (Aldrich, ACS reagent)	$Ni(NO_3)_2.6H_2O$ (Merck, 99%)	8.0285	13.2589	12.5464
$Bi_2Mo_3O_{12}$	$(NH_4)_6Mo_7O_{24}.4H_2O$ (Aldrich, ACS reagent)	$Bi(NO_3)_3.5H_2O$ (Aldrich, 98%)	10,9209	20.0273	25.0273
$Bi_2Mo_2O_9$	$(NH_4)_6Mo_7O_{24}.4H_2O$ (Aldrich, ACS reagent)	$Bi(NO_3)_3.5H_2O$ (Aldrich, 98%)	7.3371	20.0683	20.0723
Bi_2MoO_6	$(NH_4)_6Mo_7O_{24}.4H_2O$ (Aldrich, ACS reagent)	$Bi(NO_3)_3.5H_2O$ (Aldrich, 98%)	3.6489	20.0606	17.3382

Chapter 4

Catalytic tests

4.1 Catalytic apparatus

All the catalytic tests involving the deoxygenation of benzoic acid (BA) reaction were performed in a custom-made (designed and built) catalytic apparatus. The high solidification temperature of the benzoic acid (T_s=394K) has imposed us to maintain at 405K all the parts where benzoic acid could be present. The system is illustrated in figure 4.1. It is composed of a saturator-condenser where the solid benzoic acid was warmed at 364K, several lines which could receive either hydrogen, propylene or oxygen and a hot box where all the gases were mixed together. The gaseous mixture fed a stainless steel fixed bed micro-reactor. The reactants and products were analysed by on-line gaseous chromatography.

4.2 Reaction conditions

The total flow is 100 ml min^{-1} for all the catalytic tests and the granulometry of the catalyst is included between 200 and 315 μm. The flow of the gaseous reactants and the amount of catalysts were adapted according to the reaction conditions (these data will be provided later in the text). The reactor was heated

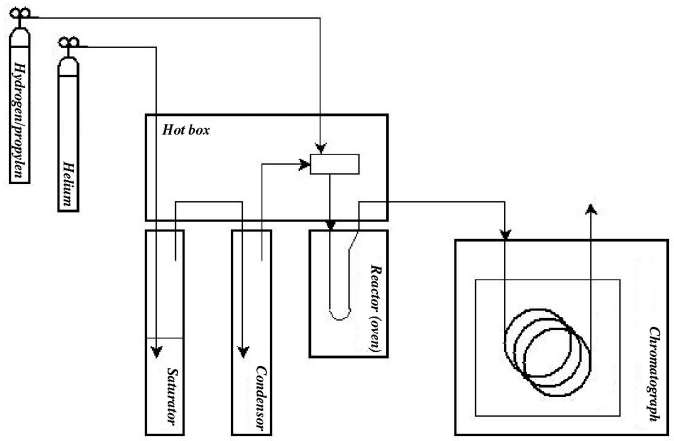

Figure 4.1: Catalytic apparatus used for the deoxygenation of benzoic acid.

under the reaction mixture with a rate of 10K min^{-1}. The catalytic activity was measured between 623K and 723K after a stabilisation time of 90 minutes. After the catalytic test, the reactor was cooled under reaction mixture to room temperature at an estimated rate of 105K min^{-1}. The concentration of the different reactants was measured in absence of conversion. The transformation of the benzoic acid, alone, in presence of hydrogen and/or propylene was determined to take place above 773K in absence of any catalytic species.

On-line chromatographic analyses were performed every 22 minutes during the whole duration of a catalytic test by using a flame ionization detector (FID) for the detection of the reactants (benzoic acid and/or propylene) and the selective products (benzene, toluene, benzaldehyde, acrolein) and a catharometric detector (TCD) for the detection of CO and CO_2. Since quantities involved during the reaction are very low (maximum 954 ppm), the errors made on the measured raw data are not negligible and must be considered for the selectivities calculation. For information purposes, error on the benzoic acid, benzaldehyde, benzene, propylene, CO and CO_2

concentrations correspond respectively to 10, 1, 4, 4, 1 and 1 ppm[1]. Moreover, due to the system design and the use of benzoic acid which requires high temperature in whole the catalytic system (temperature higher than 405K to avoid the solidification of the acid), we were unable to detect acrolein in a quantitative way. Moreover, the small potential amount of acrolein formed during the reaction (maximum 318 ppm) is below the threshold of detection of the GC apparatus (2000 ppm).

[1]The reproducibility of the catalytic tests was evaluated to be in the range of the error made on the measured raw data.

Chapter 5

Physico-chemical characterizations

All characterizations were carried out *ex situ*. The possibility that the obtained data do not reflect the real state of the catalyst at work must however be discarded, as a very rapid cooling rate (105K min^{-1}) under reaction mixture has been applied at the end of each test.

Tendencies in the characterization data reported hereafter can be correlated with the catalytic performances.

5.1 Surface area measurements - SBET

Specific areas were measured with a Micromeritics ASAP 2000 instrument using the adsorption of Kr at 77K. Before the analyse, 100 mg of sample were degassed at 10^{-1} Pa and 423K for 1 h.

5.2 X-ray diffraction - XRD

X-ray diffraction analyses were performed at room temperature on a Siemens Kristalloflex D5000 diffractometer using the nickel filtered Kα radiation of

Cu (λ=1.5418 $\dot{A}$). The samples were prepared on a silicium mono-crystal sample holder. Diffraction patterns were recorded in continuous mode over 2θangles between 5° and 80° at a rate of 1.2° min^{-1}. The crystalline structure identification was done by comparing the obtained diffractogram with those reported in the JCPDS database from the International Centre for Diffraction Data.

5.3 X-ray photoelectron spectroscopy - XPS

Mo based oxide samples were analyzed with an Axis Ultra spectrometer from Kratos working with a monochromatic Al Kα radiation (15 kV, 10 mA) and the charge compensation device provided by the supplier (charge balance fixed at -2.3 V). Pass energy for the analyzer was 40 eV and the spot size was 700 μm x 300 μm corresponding to a FWHM of 0.92 eV for the Ag 3d5/2 band of a freshly sputtered silver standard.

The binding energies were calibrated by fixing the C-(C, H) contribution of the C 1s adventitious carbon at 284.8 eV. Peaks were considered to be combinations of Gaussian and Lorentzian functions in a 70/30 ratio, working with linear baseline (following recommendations from the supplier). For the quantification of the elements, sensibility factors provided by the manufacturer were used.

Decomposition of the Mo 3d doublets to Mo^{n+} species was done by fixing an energy gap of 3.13 eV, and an area ratio of 2/3 between the Mo 3d3/2 and the Mo 3d5/2 bands. FWHM of Mo 3d doublet were linked together. Solutions of the decomposition were afterwards validated by checking that the binding energies for the different Mo^{n+} eventually found, fitted with those commonly accepted and that an energy gap around 1.2 eV existed between corresponding bands of two successive Mo^{n+} species. Oxygen (O 1s) and carbon (C 1s) peaks were also decomposed into several species by imposing the same FWHM between the different contributions of a same element.

5.4 Scanning electron microscopy - SEM

Scanning electron microscopy (SEM) was realized on a PHILIPS XL30 ESEM-FEG microscope in high vacuum mode using secondary electrons and an acceleration tension of 10 or 20 kV. Catalysts were analyzed by spreading them on a carbon tape.

5.5 Temperature programmed reduction - TPR

TPR was performed by using a 100 ml min^{-1} flow of 5% H_2 diluted in helium. The reduction was followed by monitoring the water formation with a GC/ion-Trap Mass Spectrometer (HP G1800A GCD system) coupled to the reactor. The temperature was increased from 323K to 723K at a constant rate of 5K min^{-1}.

Part III

Deoxygenation of benzoic acid in the presence of hydrogen on molybdenum oxides and suboxides

This part of the thesis sets out the first step of the strategy introduced above, i.e. the development of the deoxygenation of benzoic acid as a probe reaction of the oxygen vacancies at the surface of the oxide catalysts. This reaction was already tested by Sakata [59, 65] on oxide catalysts like MgO, La_2O_3, ZrO_2,etc but not on molybdenum based oxide. The main objective is thus to evaluate the potentialities and drawbacks of the probe reaction when used on molybdenum based oxide catalysts. It is expected that the probe reaction will exhibit drastically different behaviours in terms of catalytic performances (both conversion and selectivities) according to the used molybdenum (sub)oxide.

Chapter 6

H_2-TPR of MoO_{3-x}

Abstract

Since this kind of crystallographic phases will be used in some catalytic tests in the presence of a large excess of molecular hydrogen, the reducibility of molybdenum (sub)oxides is investigated by hydrogen TPR experiments and XRD analysis . Consequently, the evaluation of their stability is very important for the understanding of their catalytic behaviour. The results show that the stability of the molybdenum (sub)oxides are very different in spite of their structural similarities.

6.1 Introduction

The nature of the molybdenum suboxide, i.e. a molybdenum oxide with several oxygen atom defaults in the crystallographic structure compared with the molybdenum atoms content, is a major argument for the determination of its stability in a reducing atmosphere. It could be expected that the under-stoichiometry in oxygen could facilitate the modification of the mean oxidation level during a determined reaction by some atoms diffusion phenomena [77, 18, 78]. Moreover, these phases are often reported as intermediate active

site formed *in situ* during some oxidation reactions [79, 25, 24].

Knowing that the deoxygenation of benzoic acid is performed with a ratio hydrogen/benzoic acid higher than one, it was thus justified to evaluate the behaviour of all the molybdenum suboxides.

6.2 Experimental

6.2.1 Sample preparation

MoO_2 (Aldrich, 99%) and MoO_3(Aldrich, 99.5%) were used as received from the producer. Mo_4O_{11}, Mo_9O_{26} and Mo_8O_{23} were prepared according to the "solid state method". Prior to the TPR analyses, the purity of each sample was determined by X-ray diffraction. XRD measurements were also realized after the TPR to correlate the final phase with the reduction phenomena.

6.2.2 TPR analysis

Several hydrogen temperature programmed reduction experiments were performed according to the parameters provided in section 5.5. 100 mg of each catalyst (granulometry : 100-315 μm) was used in a quartz reactor. The temperature was increased from 323K to 723K at a constant rate of 5K min^{-1} and then maintained 1 hour at 723K. No thermal pretreatment was applied to the samples in order to avoid a superficial reduction of the sample.

6.3 Results

TPR results are presented in figure 6.1. Three categories can be distinguished among the five samples : (i) MoO_3 and Mo_9O_{26} do not show any reduction peak, (ii) Mo_4O_{11} and Mo_8O_{23} have both one peak of reduction centered at about 723K and (iii) MoO_2 has two reduction peaks centered at about 603K and 723K. Moreover, concerning MoO_2, it is noticed that a significant amount of water is detected between 323K and 423K.

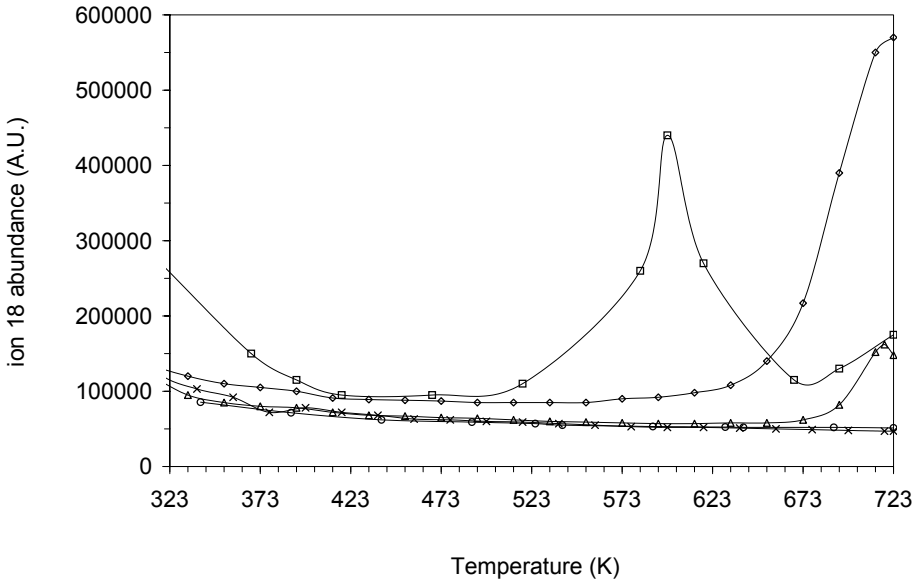

Figure 6.1: TPR results of MoO_2(□), Mo_4O_{11}(△), Mo_8O_{23} (◊), Mo_9O_{26} (×) and MoO_3 (⊘) performed under 5% H_2 in helium.

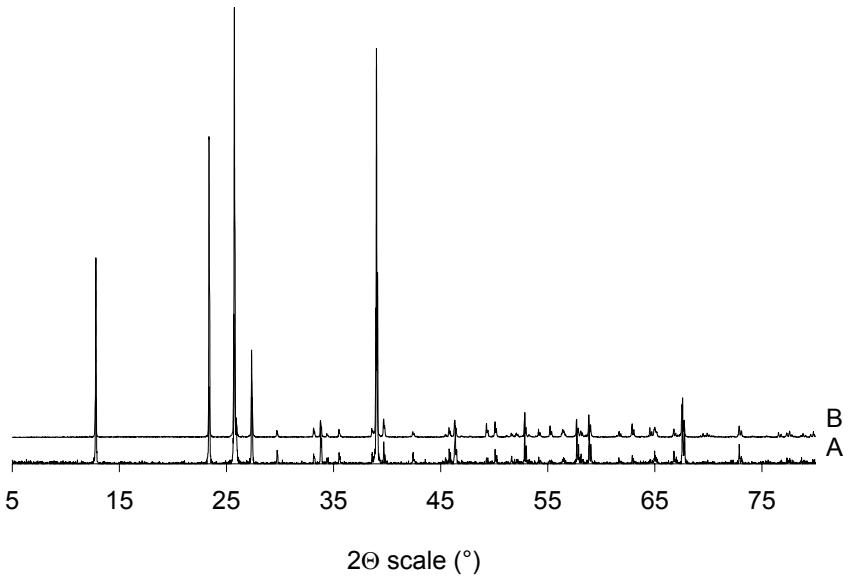

Figure 6.2: XRD results on fresh MoO_3 (JCPDS n°5-0508) (A) and after TPR experiment (B). All peaks are attributed to MoO_3.

Figure 6.2 to 6.6 present the XRD analysis performed before and after TPR experiments respectively on each available suboxides. These data show that all the fresh samples correspond to the expected crystalline phase. However, some impurities (Mo_9O_{26}) are present in Mo_8O_{23}.

X-ray diffraction reveals that the crystalline phase of three samples, MoO_3, $Mo_4O_{11}$and MoO_2 remain unchanged after TPR experiment. Some modifications are observed in the relative intensity of the peaks. However, no precautions were taken to ensure a quantitative analysis of the different samples. Thus, we will not discuss these modifications.

Whereas the TPR experimental conditions are undoubtedly reducing, the Mo_9O_{26} diffractogram exhibits two small peaks attributed to a more oxidized

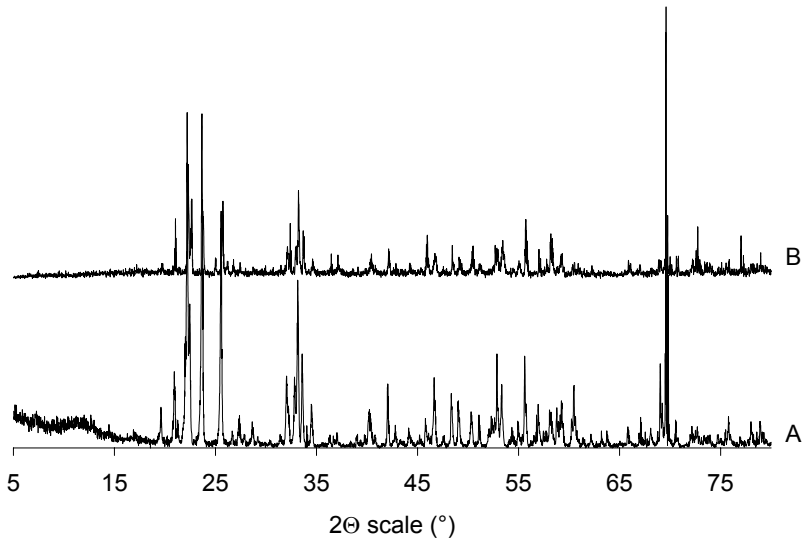

Figure 6.3: XRD results on fresh Mo_4O_{11} (JCPDS n°5-0337) (A) and after TPR experiment (B). All peaks are attributed to Mo_4O_{11}.

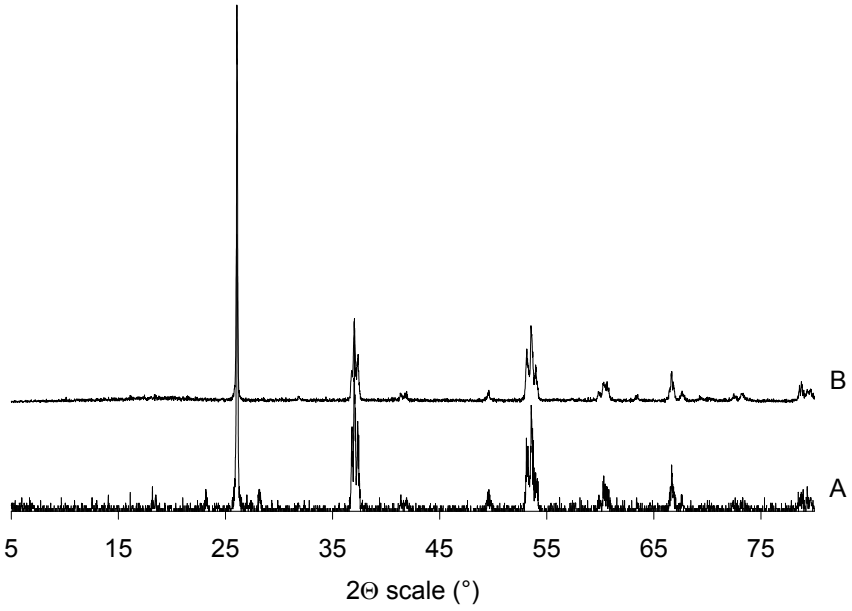

Figure 6.4: XRD results on fresh MoO_2 (JCPDS n°32-0671) (A) and after TPR experiment (B). All peaks are attributed to MoO_2.

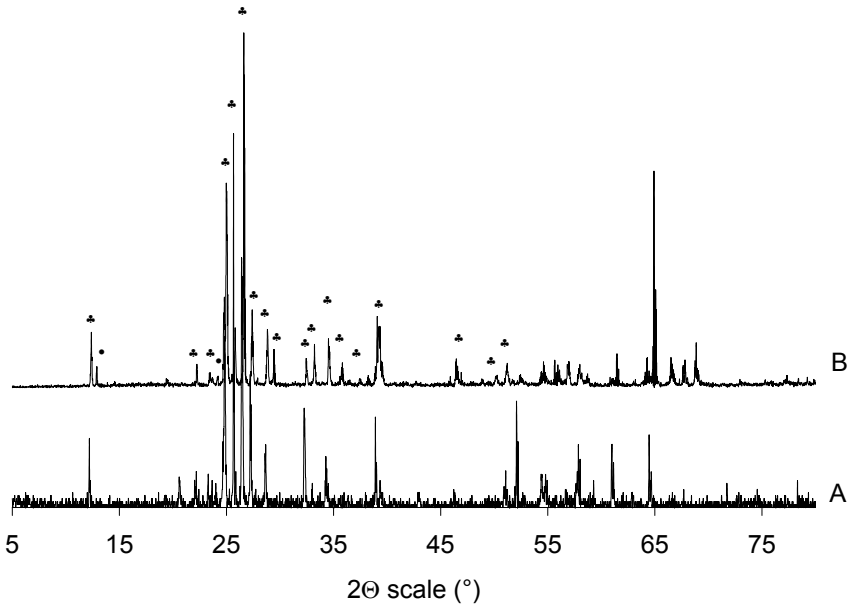

Figure 6.5: XRD results on fresh Mo_9O_{26} (A) and after TPR experiment (B). Symbols ♣ represent peaks attributed to Mo_9O_{26} (JCPDS n°12-0753) and symbols • identify the peaks corresponding to MoO_3 (JCPDS n°5-0508) both in A and B. Peaks not marked are not identified or not reported in the database.

crystalline phase, namely MoO_3.

The last molybdenum suboxide, Mo_8O_{23}, undergoes a bulk reduction : Mo_4O_{11} is detected as a new phase and no peaks corresponding to Mo_8O_{23} remain after TPR experiment. The Mo_9O_{26} contamination seen in the fresh catalyst is still present after the temperature programmed reduction experiment.

The fresh samples were analysed by XPS to determine the molybdenum species present at the surface of the samples (figure 6.7). MoO_3 only exhibits fully oxidized molybdenum species. Mo_9O_{26} and Mo_8O_{23} have both Mo^{6+} and Mo^{5+} while Mo_4O_{11} and MoO_2 present some molybdenum atoms at +6,

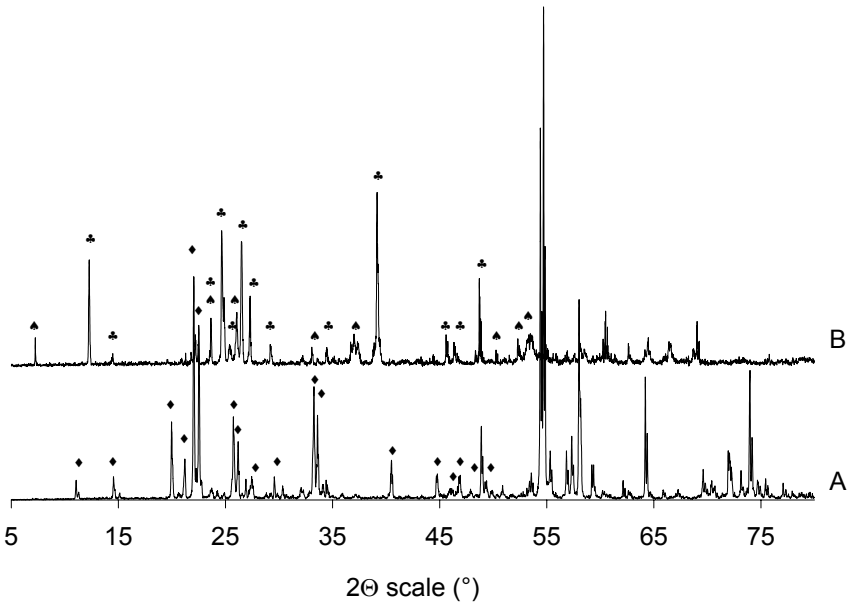

Figure 6.6: XRD results on fresh Mo_8O_{23} (A) and after TPR experiment (B). ♦ indicate peaks corresponding to Mo_8O_{23}(JCPDS n°5-0339), ♣ represent peaks attributed to Mo_9O_{26} (JCPDS n°12-0753) and ♠ identify the peaks corresponding to Mo_4O_{11} (JCPDS n°5-0337). Peaks not marked are not identified or not reported in the database beyond 2θ =49°.

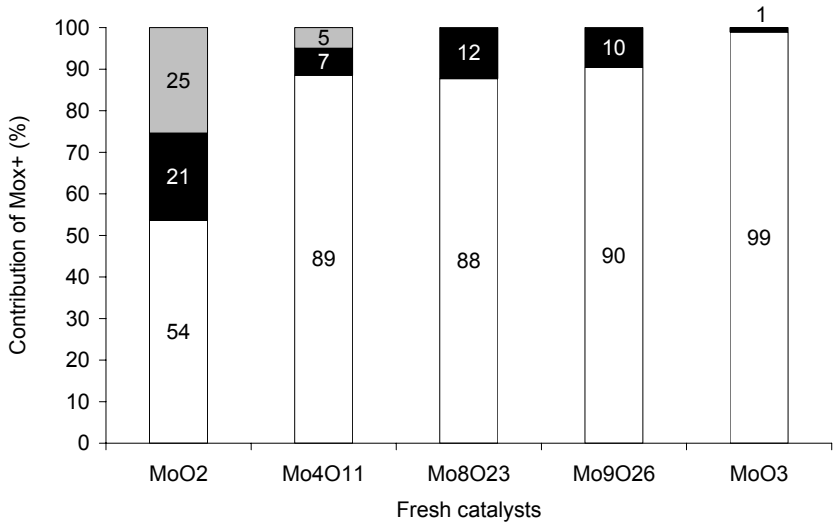

Figure 6.7: Importance of the Mo^{6+}(white), Mo^{5+}(black) and Mo^{4+} (grey) contributions found by XPS for the fresh molybdenum (sub)oxides.

+5 and +4 oxidation level.

6.4 Discussion

XRD and TPR results exposed in this chapter show that a reduction detected by TPR is not always reflected by XRD. We will thus examine independently the case of each sample.

Whereas two peaks of reduction are detected for MoO_2, XRD analyses does not show any more reduced phase than MoO_2. No metallic molybdenum or any intermediate crystalline phases between MoO_2 and metallic molybdenum were detected. The formation of Mo was observed by Arnoldy [80] but at about 950K. Moreover, the peak observed in our experiment at 603K was not detected by this author. Thus, the reduction seen by TPR does not induce the formation of a new crystalline phase. Consequently, two hypotheses must be envisaged : (i) the reduction leads

to the formation of an amorphous reduced phase or (ii) the reduction of the MoO_2 sample is only superficial, i.e. the as-received MoO_2 from the supplier is slightly oxidized at its surface. A reduction of MoO_2 to an amorphous phase has never been reported in the available literature. Moreover, the XPS analysis of the fresh sample reported in figure 6.7 allows us to definitively validate the second hypotheses and to reject the first one. We have reported the different Mo^{x+} contributions detected at the surface of the fresh catalysts. Whereas one could expect that only Mo^{4+} is found at the surface of MoO_2, a large amount of Mo^{5+} and Mo^{6+} is detected, respectively representing 21 and 25% of the molybdenum atoms. One can assume that these oxidized molybdenum species are thus responsible for the detection of two peaks in the TPR experiments. Whereas XPS analyses do not allow to determine which species are reduced at 603K and 723K, these superficial oxidized species at the surface of the as-received MoO_2 catalyst are different by their reducibility.

Mo_4O_{11} exhibits a small reduction peak at about 723K. Whereas no new phases were detected by XRD, one can notice that some peaks have vanished after TPR experiment. Two cases must be envisaged : (i) a preferential reduction of some specific crystalline faces. This preferential reduction would not be sufficient to induce the formation of a new phase like MoO_2, (ii) Remembering that Mo_4O_{11} is constituted of MoO_6 octahedra and MoO_4 tetrahedra connected by sharing oxygen corner, the reduction could affect one of these molybdenum species. In fact, these two hypotheses are connected. Indeed, one could assume that the modification of a molybdenum species could induce a modification of a characteristic crystalline face, for example, by a change in the coordination of the molybdenum. Since the XRD analyses are not quantitative, they only allow to notice the variation of the relative peak intensity. The main phase being not changed after TPR experiment, the modifications undergone by the sample are not induced by a reduction due to the presence of hydrogen but rather by a recrystallization due to the high temperature of the experiment.

The XRD and TPR results concerning MoO_3 and Mo_9O_{26} are well

correlated. They demonstrate that until 723K, these phases are very stable and do not undergo a significant bulk reduction. This seems in contradiction with the result described by Arnoldy : he observed a small reduction peak on MoO_3 at about 620K when the sample was heated with a rate of 5K min^{-1} [80]. We do not observe such a reduction peak probably because the conditions used by Arnoldy were more drastic (67% H_2/Ar). However, the two peaks corresponding to MoO_3 highlight a partial oxidation of Mo_9O_{26} in the presence of 5% H_2/He at high temperature. This observation reinforces the fact that Mo_9O_{26} is very stable in a reducing atmosphere. Indeed, the formation of a more oxidized molybdenum oxide under reducing conditions indicates that the high temperature is critical but not the presence of hydrogen. Thus, a temperature of 723K can induce the crystallisation of amorphous material to MoO_3 or the stabilisation of some imperfect Mo_9O_{26} structures to molybdenum trioxide. Such a transformation is not impossible since MoO_3 and Mo_9O_{26} have very similar crystalline structure.

Mo_8O_{23} is clearly the most unstable sample of the investigated (sub)oxides. It is reduced to Mo_4O_{11} at 723K as shown by XRD measurements. This sample also confirms that Mo_9O_{26} is a very stable suboxide against reducing conditions since the contamination detected in Mo_8O_{23} sample, i.e. Mo_9O_{26}, remains present after TPR experiment. Moreover, it seems that the amount of contamining Mo_9O_{26} in Mo_8O_{23} after TPR experiment increases whereas the experimental conditions are reducing. Once again, like for Mo_4O_{11}, the temperature factor is stronger than the presence of hydrogen.

The information revealed are the following : (i) MoO_3 and Mo_9O_{26} are the most stable and resistant sample against the bulk reduction, (ii) the surface of the as-received MoO_2 is slightly oxidized, the oxidized species are reduced at 603K and 723K, (iii) some crystallographic planes of Mo_4O_{11} seem to be reduced at 723K but without forming any new phase, (iv) Mo_8O_{23} is partially reduced to Mo_4O_{11} at 723K.

6.5 Conclusions

These results are quite basic. However, three observations must be highlighted : (i) MoO_2, even after a reducing treatment, will never exhibit a fully reduced surface, (ii) Mo_9O_{26} is very resistant against the reduction by molecular hydrogen and (iii) Mo_8O_{23} and Mo_9O_{26}, whereas they are similar in terms of oxygen defects, have an opposite behaviour in term of stability. This last observation could be of great importance in the understanding of the reactivity of molybdenum suboxides.

Chapter 7

Monitoring the reduction state of MoO_{3-x}[1]

Abstract

The very first catalytic tests of deoxygenation of benzoic acid on molybdenum (sub)oxides in the presence of a large excess of hydrogen have highlighted some interesting hysteresis phenomena in the course of a temperature cycle.

Thanks to several catalytic tests run in isothermal conditions and to the results exposed in chapter 6, we suggest that the variation of the catalytic performances both in conversion and selectivities are linked to the sequential reduction of the molybdenum (sub)oxides towards MoO_2. Indeed, it appears that some specific molybdenum suboxides are rather selective to one product of deoxygenation. Mo_8O_{23} produces toluene, Mo_4O_{11} is very selective in benzene while MoO_2 mainly produces benzaldehyde. The hysteresis is thus the consequence of the sequential appearance and disappearance of such molybdenum (sub)oxides as a function of the reaction temperature.

Even if these results confirm that the molybdenum suboxides are rather

[1]Results concerning Mo_8O_{23} are published in Catalysis Today 91-92 (2004) 111-116 following the EUROPACAT VI (The European Catalysis Forum) and ISO2003 (The 7th European Workshop Meeting on Selective Oxidation) Innsbruck, September 2003.

unstable and tend to be deeply reduced in presence of hydrogen at higher temperature, they encourage us to continue our investigations. They illustrate the good specificity of the new probe reaction towards the presence and the arrangement of the oxygen vacancies at the surface of the oxide catalysts. Moreover, they confirm that the deoxygenation of benzoic acid can be an adequate tool to monitor the oxidation level of the molybdenum oxide based catalysts.

7.1 Introduction

It progressively becomes well accepted that a key to optimize the performances of Mo oxide catalysts in some selective oxidation processes is to stabilize them in a slightly reduced state during the reaction [24, 40, 41, 59]. Now, a crucial aspect to be understood in order to further improve performances of such processes is to identify the optimal reduction state of the catalysts in terms of location and of concentration of the reduced features.

To progress in this direction, a major difficulty comes from the fact that Mo oxides "at work" are not static during oxidation reactions. The bulk and the surface can equilibrate their coordination and structure with the composition (i.e. the reduction/oxidation strength) of the reaction gas and the temperature, eventually resulting in reconstruction phenomena [41, 81]. *In situ* characterization (with the catalysts maintained in reaction conditions during the characterization) and *operando* characterization (an *in situ* characterization coupled to a simultaneous measurement of the catalytic performances) are efficient approaches to handle such a delicate behaviour. But this work aims at developing a parallel approach, namely the use of probe reactions, the deoxygenation of benzoic acid, that allows to monitor the properties of the catalysts through the distribution of the reaction products. We directed our attention to correlate the performances (conversion and selectivities) with the modifications undergone by the catalysts in the course of a temperature cycle catalytic test.

7.2 Experiments

7.2.1 Preparation of the catalysts

Mo_8O_{23}, Mo_9O_{26} and Mo_4O_{11} were synthesized by heating a mixture of MoO_3 (Aldrich, 99.5% pure) and MoO_2 (Aldrich, 99% pure) according to the "solid state method" described in section 3.1. Commercial MoO_2 (Aldrich, 99% pure) and MoO_3 (Aldrich, 99.5% pure) were respectively reduced and oxidized according to the conditions described in section 3.1.

7.2.2 Catalytic activity measurements

Deoxygenation of benzoic acid was performed at atmospheric pressure in a stainless steel fixed bed micro-reactor on MoO_3, Mo_8O_{23}, Mo_9O_{26}, Mo_4O_{11} and MoO_2. The reaction feed contained 574 ppm of benzoic acid (Aldrich, 99% pure) and 50000 ppm of hydrogen (Indugas, 99.95% pure) while helium (Indugas, 99.99% pure) was the gas balance. The total flow was adjusted to 100 ml min^{-1} . One hundred milligram of catalyst with a granulometry of 100-315 μm were used. Two series of catalytic tests were realized : (i) in isothermal conditions (623K/9h or 673/9h or 723K/9h) (ii) in a three-step temperature cycle. The performances were first measured at 473, 523, 573, 623, 638, 653, 673 and 723 K, then at the same temperatures during the cooling down of the reactor, then again during a second rise of temperature. The reaction was run at each temperature during 2 hours.

Additional experiments were conducted following the same procedure but stopped at different moments of the test. In all cases, catalysts were recovered after a fast cooling to room temperature (105K min^{-1}) in the flow of reaction gas. Remaining acid, benzaldehyde, toluene and benzene were measured at the reactor outlet by on-line GC-FID. Further details are available at chapter 4.

7.2.3 Characterization

The catalysts were characterized before and after the catalytic reactions by specific area measurement, X-ray diffraction, X-ray photoelectron spectroscopy and scanning electron microscopy. Specifications and detailed information are given elsewhere (section 5 on page 49).

7.3 Results

7.3.1 Catalytic activity measurements

7.3.1.1 Isothermal catalytic tests

Catalytic performances measured in the course of the isothermal catalytic procedure are presented in figures 7.1 to 7.4. The three tested temperatures are reported in a same plot for the sake of clarity whereas they are three independent catalytic tests.

The data plotted in figure 7.1 indicate that MoO_2 is not active at 623K. A small conversion of benzoic acid is measured at 673K at the beginning of the catalytic test. It increases to 9% during the second hour of reaction and slightly decreases to 2% after 9 hours. Benzaldehyde is the only product detected through the whole duration of the catalytic test. The initial conversion of benzoic acid is much higher at 723K (48%) and decreases to 10% at the end of the catalytic reaction procedure. Three products are formed on MoO_2 during the first hour of reaction. Toluene, benzene and benzaldehyde are respectively produced with a selectivity of 4, 20 and 76%. After the first hour of catalytic test, toluene was not detected anymore. Starting from the second hour of reaction, the selectivity of benzene increases to 47% to the detriment of benzaldehyde.

The data collected during the evaluation of the catalytic performance of Mo_4O_{11} are summarized in figure 7.2. No conversion of benzoic acid is observed at 623K. Four hours of reaction are also necessary before detecting the transformation of benzoic acid to toluene and benzene at 673K. The

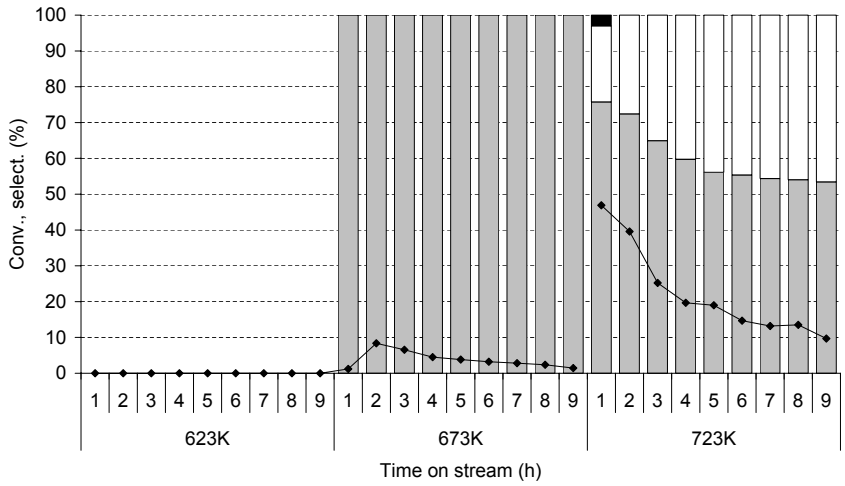

Figure 7.1: Evolution of the conversion of benzoic acid (plain line) and the selectivities in benzaldehyde (grey), benzene (white) and toluene (black) on MoO_2 through the three temperatures of reaction.

conversion is initially of about 1% and increases to 28% after 9 hours. Benzaldehyde is formed after 7 hours of reaction but the selectivity, although increasing, remains below 10%. The production of toluene and benzene are stable with a selectivity of respectively 30 and 60%. At 723K, the behaviour of the catalyst is more complex. At the initial time, 9% of the benzoic acid is converted to benzaldehyde (61% of selectivity) and benzene (39% of selectivity). Next, the conversion increases to 61% in 9 hours. After 3 hours of reaction, toluene is produced to the detriment of the benzaldehyde selectivity. The selectivity to benzene does not evolve much and seems stabilized at about 64%.

Mo_8O_{23} is the only active catalyst at the three explored temperatures (figure 7.3). In all the cases, the initial conversion is low but increases with time on stream. The maximum conversion is in the range of 20-30% at 623, 673 and 723K. This maximum of conversion is reached before the end of the

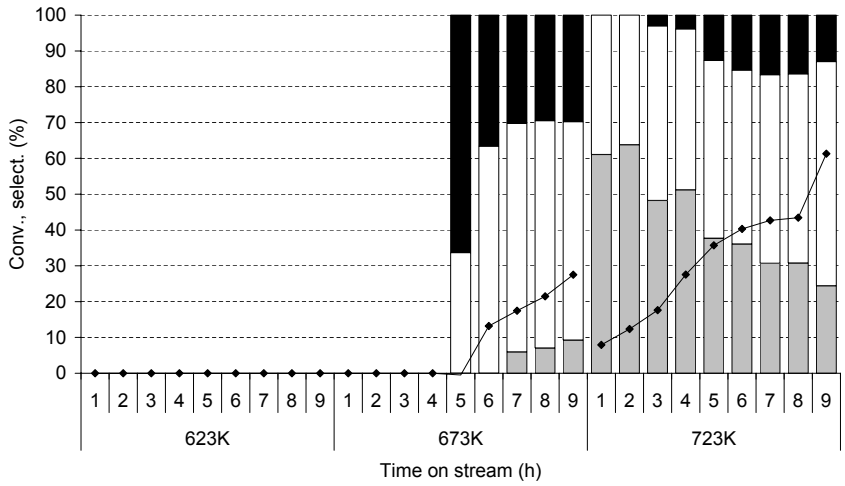

Figure 7.2: Evolution of the conversion of benzoic acid (plain line) and the selectivities in benzaldehyde (grey), benzene (white) and toluene (black) on Mo_4O_{11} through the three temperatures of reaction.

catalytic test, respectively at the 8th hour for the lowest temperatures and at the 4th hour for the highest temperature of reaction. The profile of selectivity at 623K can be distinguished from the others. Indeed, when benzoic acid starts to be converted, only toluene is produced with the maximum selectivity. During the second hour of reaction, benzaldehyde is generated with a selectivity of 36% and toluene with a selectivity of 64%. No benzene is detected. From the third hour of reaction, a small amount of benzene is produced to the detriment of toluene. After, the selectivity of benzene remains low to vanish in the last hour of the catalytic test. Finally, benzaldehyde is produced with 98% of selectivity. The carbon balance is completed by a small amount of toluene.

Mo_9O_{23} was tested in the same experimental conditions as the other molybdenum suboxides. No catalytic activity was detected whatever the temperatures of reaction.

The last molybdenum oxide, namely MoO_3, is inactive at 623K and 673K

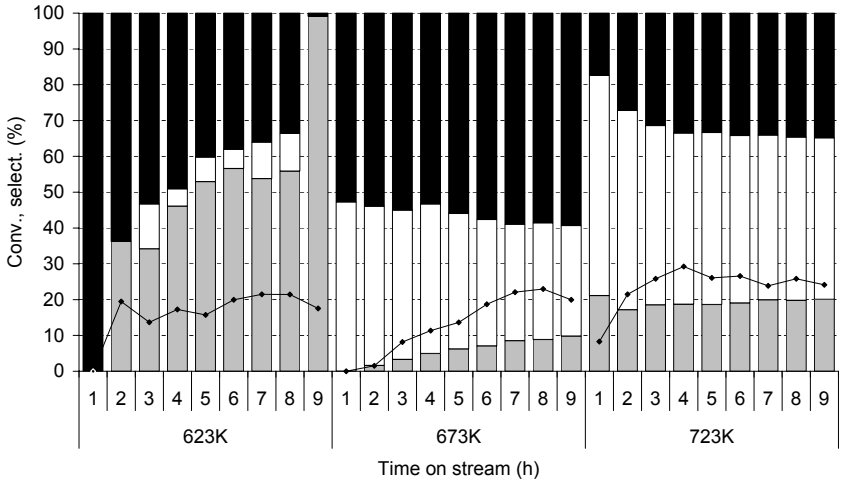

Figure 7.3: Evolution of the conversion of benzoic acid (plain line) and the selectivities in benzaldehyde (grey), benzene (white) and toluene (black) on Mo_8O_{23} through the three temperatures of reaction.

(figure 7.4). A rather constant conversion between 8 and 10% is measured at 723K. Benzene is the major product of reaction during the first 5th hours of reaction with a constant selectivity of about 30 %. Benzaldehyde is the second product detected at the same time. From the 6th hour of reaction, a growing amount of toluene is measured.

7.3.1.2 Temperature cycle catalytic tests

Catalytic performances obtained in the course of the temperature cycle are plotted in figures 7.5 to 7.8. No catalytic activity was measured on Mo_9O_{26}. The results between 638K (decrease) and 638K (2nd rise) are not reported since no catalytic activity was observed.

Comparing the different steps of the cycle, hysteresis are observed for the conversion of benzoic acid and the selectivities to the different products on all the tested catalysts except for MoO_2 (figure 7.7). Thus, the catalytic

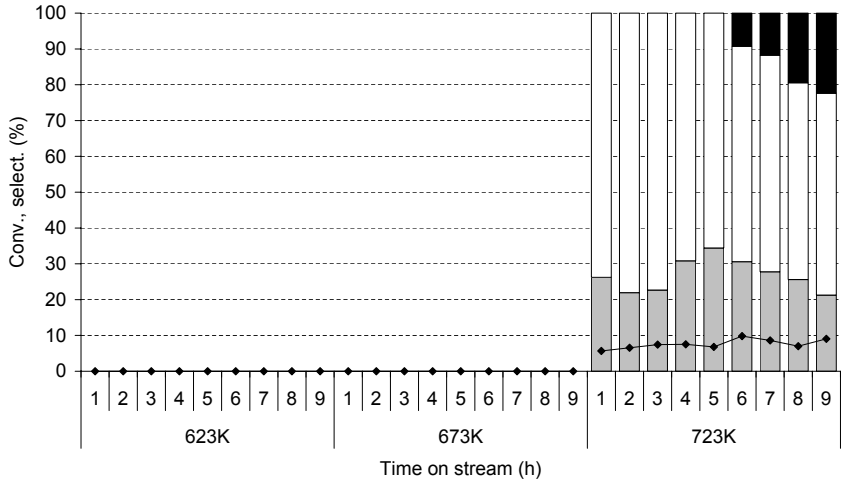

Figure 7.4: Evolution of the conversion of benzoic acid (plain line) and the selectivities in benzaldehyde (grey), benzene (white) and toluene (black) on MoO_3 through the three temperatures of reaction.

test performed on Mo_8O_{23} shows that : in the first rise of temperature, the conversion of benzoic acid at 653K is 2% whereas at the same temperature, it is respectively, 12 and 31% in the decrease and the second rise of temperature. Similar tendencies are observed at the other temperatures. Conversions are thus systematically higher at a given temperature following the order : first rise < decrease < second rise. Only one exception is found at 723K (second rise) during which the conversion of benzoic acid drops dramatically to 4%, i.e. below the level that was obtained in the first rise. At 653K (first rise) only benzaldehyde and toluene are formed. But in all other cases, benzaldehyde, toluene and benzene are always formed together. In the first rise of the cycle, the increase of temperature induces an increase of the selectivity to benzene while the selectivities to toluene and benzaldehyde both decrease. During the cooling step, an opposite tendency is found, namely a decrease of the selectivity to benzene and an increase of the selectivity to benzaldehyde. The

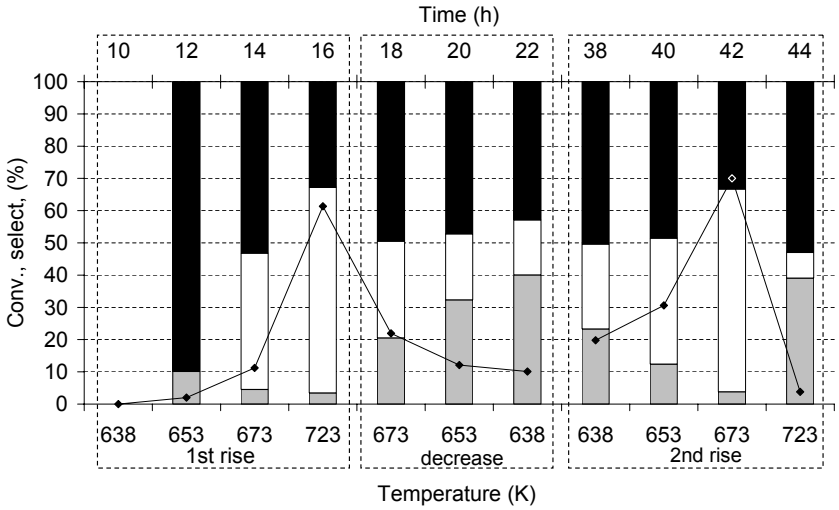

Figure 7.5: Evolution of the conversion of benzoic acid (plain line) and the selectivities in benzaldehyde (grey), benzene (white) and toluene (black) through the three steps of the catalytic test performed on Mo_8O_{23}. No activity was observed at temperatures lower than 638K and was not reported for the sake of clarity.

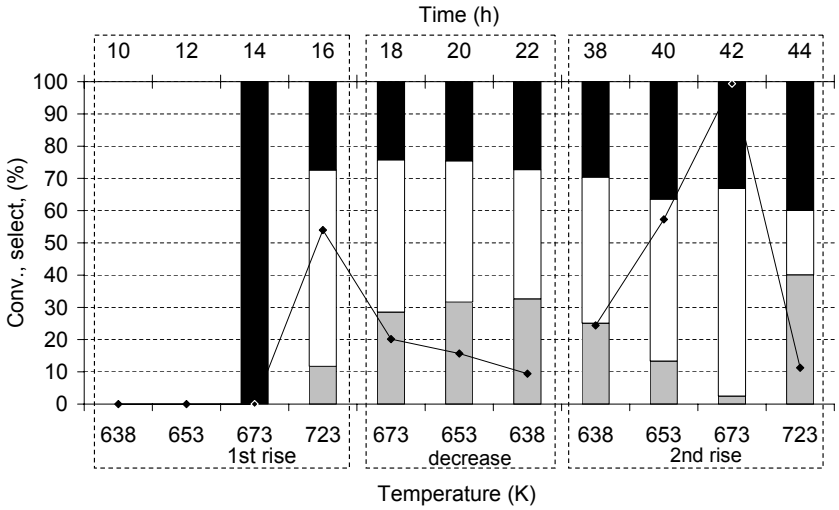

Figure 7.6: Evolution of the conversion of benzoic acid (plain line) and the selectivities in benzaldehyde (grey), benzene (white) and toluene (black) through the three steps of the catalytic test performed on Mo_4O_{11}. No activity was observed at temperatures lower than 638K and was not reported for the sake of clarity.

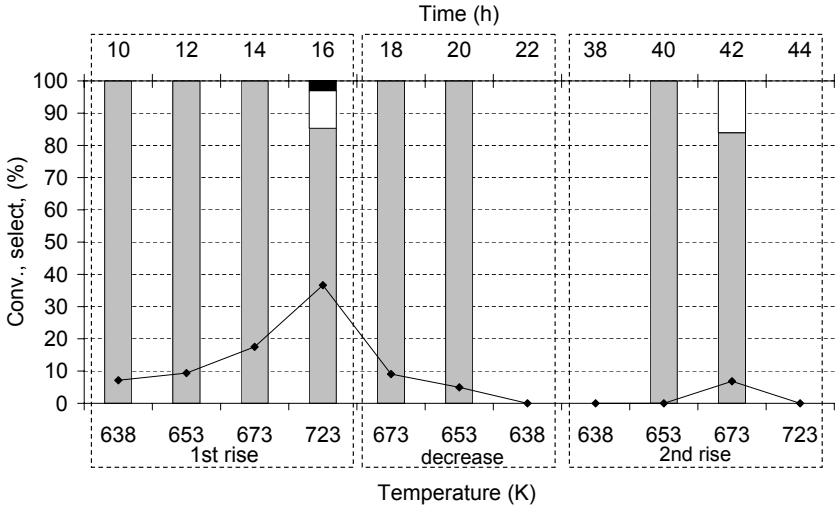

Figure 7.7: Evolution of the conversion of benzoic acid (plain line) and the selectivities in benzaldehyde (grey), benzene (white) and toluene (black) through the three steps of the catalytic test performed on MoO_2. No activity was observed at temperatures lower than 638K and was not reported for the sake of clarity.

selectivity to toluene only slightly decreases. In the second rise of temperature, two tendencies are distinguished: (i) from 638 to 673 K, the tendency is identical to the first rise: selectivities to toluene and benzaldehyde decrease and the selectivity to benzene strongly increases, (ii) at a higher temperature (723 K), the selectivity to benzaldehyde and toluene suddenly increases and the selectivity to benzene decreases. Let us remind that at the same moment of the test, the conversion of acid undergoes a dramatic drop.

Rather similar tendencies are observed for MoO_3 and Mo_4O_{11} but not for MoO_2 (figure 7.7). In that last case, the conversion increases in the first step but drops in the second one under the corresponding conversion level obtained previously. Moreover, no more activity is detected at 638K in the second rise of temperature. Benzaldehyde is the only product detected during the three

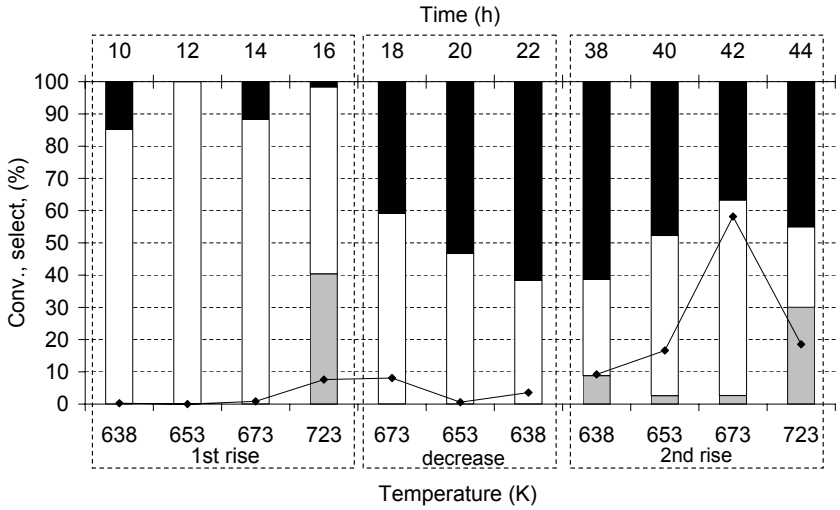

Figure 7.8: Evolution of the conversion of benzoic acid (plain line) and the selectivities in benzaldehyde (grey), benzene (white) and toluene (black) through the three steps of the catalytic test performed on MoO_3. No activity was observed at temperatures lower than 638K and was not reported for the sake of clarity.

Table 7.1: Crystalline phases detected by XRD after isothermal catalytic tests.

Crystalline phases detected before catalytic test (JCPDS number)	*Crystalline phases detected after catalytic test at 623K (JCPDS number)*	*Crystalline phases detected after catalytic test at 673K (JCPDS number)*	*Crystalline phases detected after catalytic test at 723K (JCPDS number)*
MoO_2 (32-0671)	MoO_2 (32-0671)	MoO_2 (32-0671)	MoO_2 (32-0671)
Mo_4O_{11} (5-0337)	Mo_4O_{11} (5-0337)	Mo_4O_{11} (5-0337) MoO_2 (32-0671)	MoO_2 (32-0671)
Mo_8O_{23} (5-0339) Mo_9O_{26} (12-0753)	Mo_8O_{23} (5-0339) Mo_9O_{26} (12-0753) MoO_2 (32-0671) Mo_4O_{11} (5-0337)	Mo_8O_{23} (5-0339) Mo_9O_{26} (12-0753) MoO_2 (32-0671) Mo_4O_{11} (5-0337)	Mo_8O_{23} (5-0339) Mo_9O_{26} (12-0753) MoO_2 (32-0671)
Mo_9O_{26} (12-0753)	Mo_9O_{26} (12-0753)	Mo_9O_{26} (12-0753)	Mo_9O_{26} (12-0753)
MoO_3 (05-0508)	MoO_3 (05-0508)	MoO_3 (05-0508)	MoO_3 (05-0508) MoO_2 (32-0671)

steps of the catalytic cycle excepted at 723K (1st rise) and 673K (2nd rise), i.e. when the conversion of benzoic acid is maximum, where benzene and/or toluene are also formed.

7.3.2 Characterization

7.3.2.1 Isothermal catalytic tests

X-ray diffraction analyses were performed before and after catalytic tests. Results are summarized in table 7.1. Two catalysts keep the same crystalline phase as the fresh sample whatever the temperature of the isothermal catalytic test : Mo_9O_{26} and MoO_2. Mo_4O_{11} is unchanged after the reaction at 623K but is partially reduced to MoO_2 after the test at 673K. The same catalyst recovered after the catalytic test at 723K is fully reduced to MoO_2. Mo_8O_{23} is deeply reduced after the reaction : Mo_4O_{11} and MoO_2 are detected after the

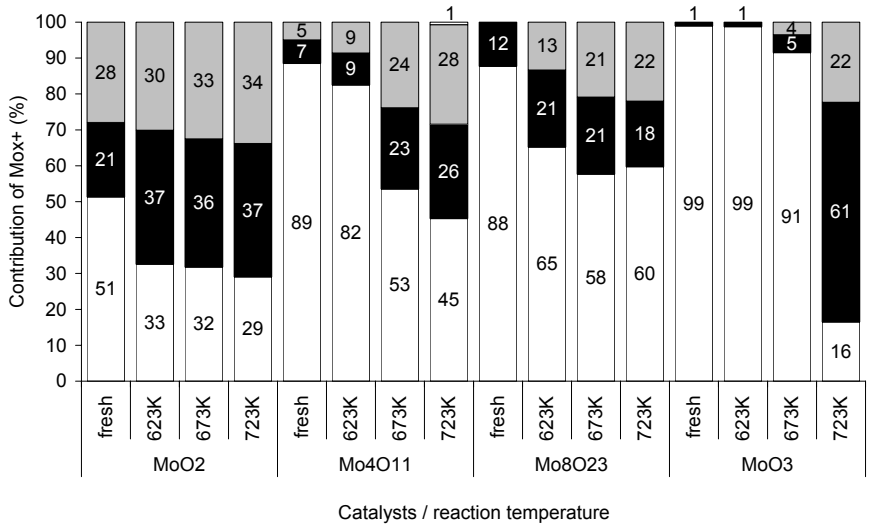

Figure 7.9: Atomic percentage of Mo^{6+}(white), Mo^{5+}(black), Mo^{4+} (grey) and Mo^{3+} (hatched) measured by XPS on fresh molybdenum suboxides and after isothermal catalytic tests.

test at 623K and 673K whereas a small amount of Mo_9O_{26} (already revealed in figure 6.6) contaminating the fresh Mo_8O_{23} is always detected whatever the reaction temperature. MoO_3 remains unreduced below 723K. Above this temperature, some peaks attributed to MoO_2 are detected.

XPS analyses of the superficial oxidation state of the molybdenum (sub)oxides are reported in figure 7.9. In general, the behaviour of the surface is similar to the bulk. Thus, the higher the reaction temperature is, the lower the Mo^{6+} content is. Concerning MoO_2, Mo_4O_{11} and Mo_8O_{23}, the reduction with the temperature also appears through the progressive formation of Mo^{5+} and Mo^{4+} species. MoO_3 does not follow the same behaviour since no Mo^{4+} is detected at 623K. Moreover, the reduction is very pronounced at 723K with only 16.5% of Mo^{6+}remaining at the surface of the catalyst.

Table 7.2: Specific area of molybdenum suboxides fresh and after temperature cycle catalytic tests.

Catalyst	*Specific area of the fresh catalysts* ($m^2 g^{-1}$)	*Specific area after catalytic test* ($m^2 g^{-1}$)
MoO_2	5.00	5.51
Mo_4O_{11}	0.04	3.29
Mo_8O_{23} Mo_9O_{26}	0.17	3.02
Mo_9O_{26}	0.06	0.40
MoO_3	0.2	1.07

7.3.2.2 Temperature cycle catalytic tests

Tables 7.2 respectively summarizes the specific areas measured before/after catalytic tests on the molybdenum (sub)oxides. The specific area of all the catalysts increases after catalytic test. It must be also highlighted that the increase of the surface of the most stable catalysts (Mo_9O_{26} and MoO_3 according to the TPR experiments, see chapter 6) is lower than the other catalysts. XRD analyses (table 7.3) show that Mo_4O_{11}, Mo_8O_{23} and MoO_3 are reduced after the catalytic test : Mo_4O_{11} is totally reduced to MoO_2, Mo_8O_{23} is totally reduced to Mo_4O_{11} and MoO_2 (once more, one should notice that the contamination is still present). The last catalyst, namely MoO_3, is partially reduced to MoO_2 since MoO_3 is still detected by XRD. MoO_2 and Mo_9O_{26} are unchanged after the reaction.

The molybdenum oxidation level of the fresh catalysts and the catalysts recovered after catalytic test was investigated by XPS and reported in figure 7.10. These data confirm that like the bulk, the surface gets reduced in the course of the catalytic test. The reduction is particularly marked at the surface of MoO_2, Mo_4O_{11} and Mo_8O_{23} which contained the lowest values of

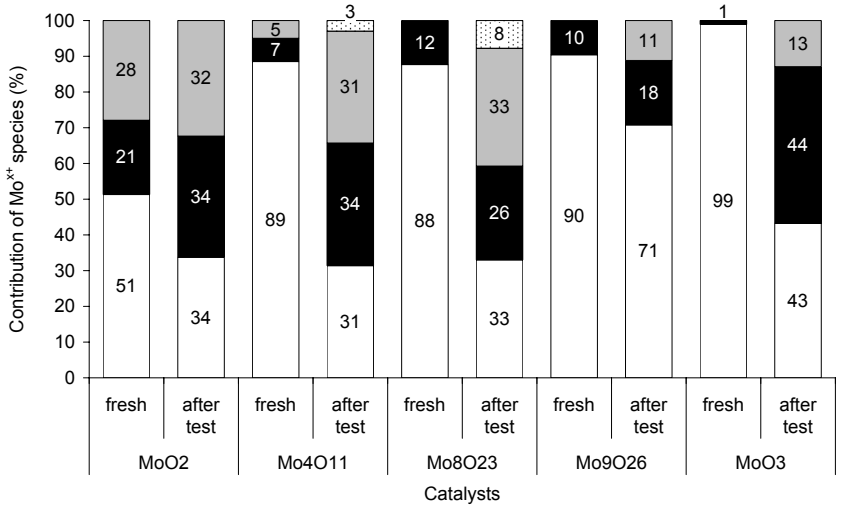

Figure 7.10: Atomic percentage of Mo^{6+}(white), Mo^{5+}(black), Mo^{4+} (grey) and Mo^{3+} (hatched) measured by XPS on fresh molybdenum suboxides and after temperature cycle catalytic tests.

Table 7.3: Crystalline phases detected by XRD after temperature cycle catalytic tests.

Crystalline phases detected before catalytic test (JCPDS number)	*Crystalline phases detected after catalytic test (JCPDS number)*
MoO_2 (32-0671)	MoO_2 (32-0671)
Mo_4O_{11} (5-0337)	MoO_2 (32-0671)
Mo_8O_{23} (5-0339) Mo_9O_{26} (12-0753)	MoO_2 (32-0671) Mo_9O_{26} (12-0753) Mo_4O_{11} (5-0337)
Mo_9O_{26} (12-0753)	Mo_9O_{26} (12-0753)
MoO_3 (12-0753)	MoO_3 (12-0753) MoO_2 (32-0671)

Mo^{6+}(about 33%). Concerning these two last samples, some deeply reduced molybdenum species were detected at a binding energy of 228.6 eV (figure 7.11). According to the literature, this reduced molybdenum species can be interpreted as Mo^{3+} [82]. It is generally detected in some molybdenum containing samples used in hydrodesulfurization processes [82, 83, 84]. The figure 7.10 also reinforces the fact that Mo_9O_{26} is very stable in a reducing atmosphere : in addition to being inactive during the catalytic reaction, its surface is only slightly reduced compared to the other catalysts recovered after the cycling reaction.

To understand the transformations undergone by the catalysts during the hysteresis phenomena, we have focused our efforts on Mo_8O_{23} which presents the more complex behaviour. The temperature cycle catalytic tests were repeated several times according to the same procedure, stopped at different moments of the reaction then characterized by XRD, XPS and scanning electron microscopy (SEM). The phases found along the test are summarized

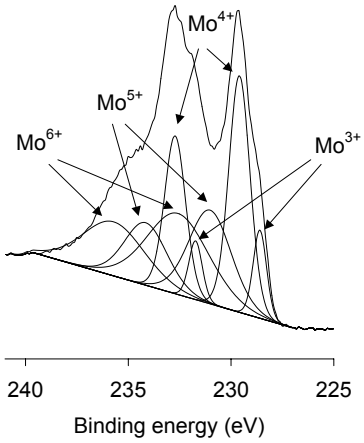

Figure 7.11: Spectra of Mo 3d obtained by X-ray photoelectron spectroscopy on Mo_8O_{23} recovered after the temperature cycle catalytic test.

in table 7.4.

The main XRD peaks for the fresh sample are typical of Mo_8O_{23} (JCPDS n°5-0339). The presence of Mo_9O_{26} (JCPDS n°12-0753) is also revealed. Mo_8O_{23} and Mo_9O_{26} are still present after the first rise of temperature. But Mo_4O_{11} (JCPDS n°5-0337) and MoO_2 (JCPDS n°32-0671) appear as two minor phases after the first step of the reaction test. After the cooling step and the second rise of temperature, three main phases are detected: Mo_9O_{26}, Mo_4O_{11} and MoO_2. After these treatments, the lines of Mo_8O_{23} have totally vanished. For the samples recovered at intermediate moments, progressing along the test, Mo_4O_{11} first becomes the main phase until 673K (first rise) but then vanishes, likely transforming to MoO_2. Small peaks attributed to Mo_9O_{26} are still present.

Figure 7.12 summarizes the different Mo^{n+} contributions found by XPS for fresh Mo_8O_{23} and the samples recovered at different moments of the catalytic test. For comparison, corresponding data are also given for the other

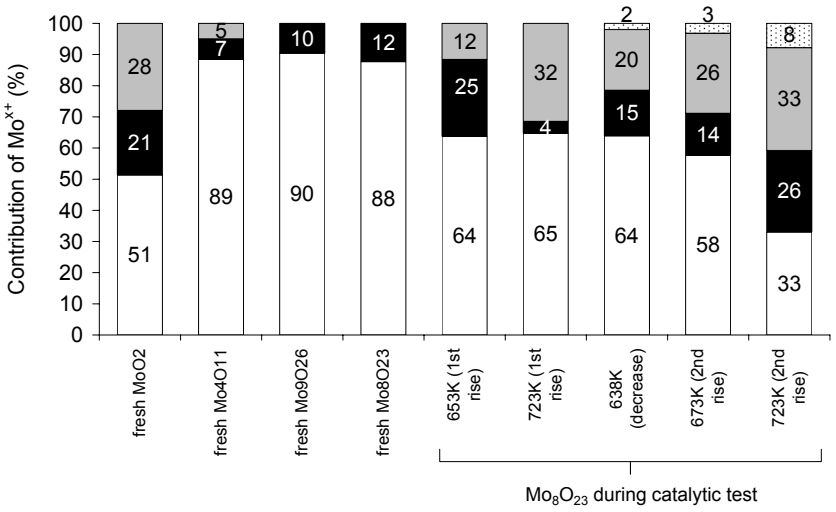

Figure 7.12: Importance of the Mo^{6+}(white), Mo^{5+}(black), Mo^{4+} (grey) and Mo^{3+} (hatched) contributions found by XPS for fresh Mo_8O_{23} and catalysts recovered at different moments of the catalytic tests. Data for fresh MoO_2, Mo_4O_{11} and Mo_9O_{26} reference compounds are also given.

Table 7.4: Crystalline phases detected by XRD for fresh Mo_8O_{23} and the same catalysts recovered at different moments of the catalytic test after a fast cooling down to room temperature. The qualitative amount of crystalline phases is determined thanks to the absolute intensity of the main peak of the different phases.

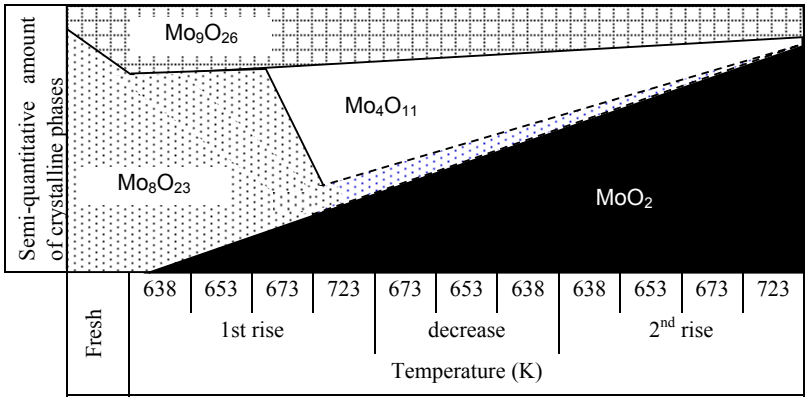

suboxides in their fresh state. Fresh Mo_8O_{23} exhibits mainly Mo^{6+} and a small amount of Mo^{5+} species. A surface reduction of Mo_8O_{23} starts during the first rise of temperature, as a significant increase of the Mo^{5+} contribution is observed for the sample recovered at 653K (first rise), while Mo^{4+} species appear. Correspondingly the Mo^{6+} contribution decreases. Further in the cycle, Mo^{6+} contribution then remains constant with time-on-stream, but it decreases significantly at the end of the test (723 K, third step). Concerning the evolution of Mo^{5+} and Mo^{4+} species, the situation is more delicate. When the reaction is stopped during a rise of temperature, the Mo^{4+} content tends to increase while that of Mo^{5+} tends to decrease. Again, a different behavior is observed at the end of the second rise of temperature where the Mo^{5+} content increases likely at the detriment of Mo^{6+}. Mo^{3+} [82] is an additional species that appears in the second rise of temperature with a contribution always remaining below 10%.

SEM reveals an important transformation of Mo_8O_{23} with time-on-stream (figure 7.13 on the next page). Fresh Mo_8O_{23} exhibits particles with a lamellar

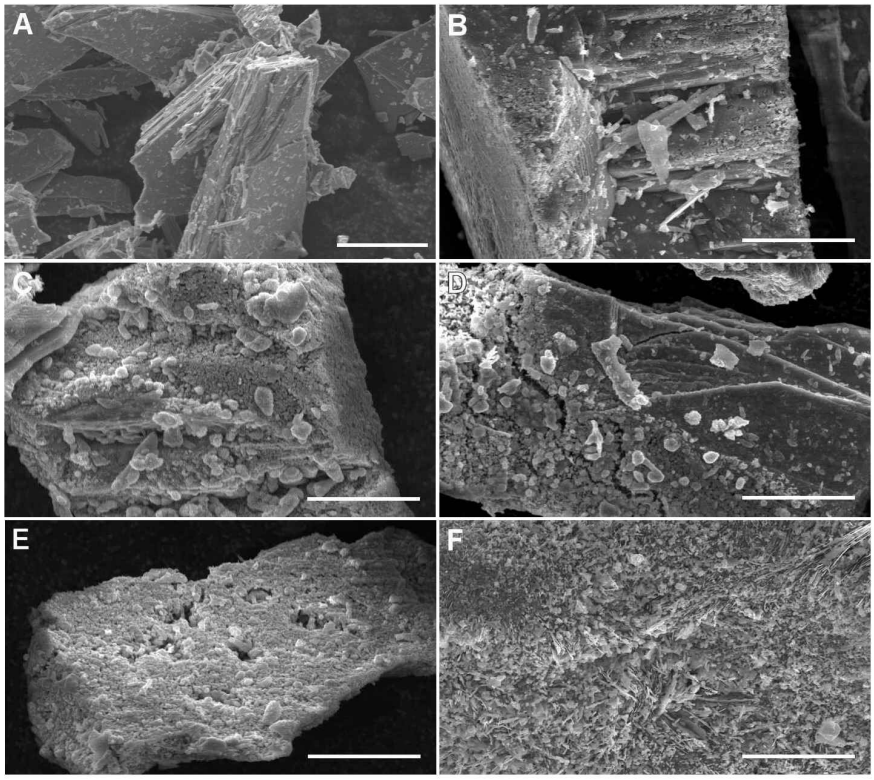

Figure 7.13: SEM image of fresh Mo_8O_{23} (A) and at different moments of the catalytic test: (B) first rise at 653 K; (C) first rise at 723 K; (D) decrease at 638 K; (E) second rise at 673 K; (F) second rise at 723 K. White lines represent 20 μm.

structure. But, after the reaction is stopped at 653K (first rise), the extremities of the lamellae get fragmented and pits appear in the middle of the crystal faces. The crystal size is not significantly modified. The same tendency is more clearly observed for the catalysts recovered when the reaction is stopped at 723 (first rise) and 638K (cooling step). After the reaction is stopped at 673K (second rise), lamellae are no more visible, and the crystals appear completely reorganized, having undergone a recrystallization. This is further confirmed by the observation of the sample recovered at the very end of the test. Such a recrystallization is consistent with the increase of specific area with time-on-stream.

7.4 Discussion

Since we have more deeply studied the hysteresis phenomenon on Mo_8O_{23}, we will base the discussion on this catalyst. However, the same reasoning applies to all (sub)oxides.

Several mechanisms accounting for the reduction of MoO_3 to MoO_2 have been proposed in the literature. According to Ressler et al. [85], the reduction pathway, precisely the formation or not of intermediate species, depends on the reduction temperature. Below 698 K, MoO_3 would reduce directly to MoO_2 without any intermediate species. But above 698 K, the MoO_2 resulting from the direct reduction of MoO_3 would react *in situ* with the not yet reduced remaining fraction of MoO_3, leading to the formation of a third phase with a more distorted structure, namely Mo_4O_{11}. The evolution of the crystalline phases throughout our catalytic tests suggests that the reduction scheme described by Ressler also applies in our case. One nuance must be evoked, namely the fact that we work with Mo_8O_{23} (in mixture with a small amount of Mo_9O_{26}) rather than with MoO_3. This difference is, however, not an argument to rule down the parallelism with the experiments of Ressler, on the contrary. Mo_8O_{23} and Mo_9O_{26} have indeed a structure very similar to that of MoO_3 (see section A). As a reminder, these suboxides can be

roughly described as a stacking of strips with corner-sharing arrangements of MoO_6 octahedra exactly as in MoO_3, glued together along shear planes [69, 71, 74, 75]. The shear planes consist in edge sharing arrangements of octahedra compensating the oxygen deficiency of the suboxides. The main difference between MoO_3 and Mo_8O_{23}/Mo_9O_{26} is thus the presence of shear planes. But these are known to allow easy diffusion of oxygen atoms from the bulk to the surface [86]. They thus most likely facilitate the reaction with MoO_2, which involves a transfer of oxygen to form Mo_4O_{11}.

Now, one can now explain the evolution of the catalytic performances of Mo_8O_{23} shown in figure 7.14 on the basis of the behaviour of the other (sub)oxides. As a reminder, (i) MoO_2 produces benzaldehyde with a high selectivity but it loses its activity at the end of the cycle due to a severe surface reduction, (ii) Mo_9O_{26} remains inactive and stable independently of the temperature investigated, (iii) the performances of Mo_4O_{11} strongly depend on the temperature. Indeed, an activity is obtained at 623K provided that an activation of 4 hours under the reaction conditions is respected. Then, benzene is the main product with small amounts of toluene. At 723 K, Mo_4O_{11} does not need any activation period and produces benzene (main product) and benzaldehyde. Among the phases investigated, Mo_4O_{11} is the most active phase at temperatures higher than 673 K, and progressively reduces to MoO_2. At 653K (first rise of temperature), Mo_8O_{23} induces the production of toluene and benzaldehyde which reflects the presence of twin and single oxygen vacancies at their surface (figures 2.4 on page 32 and 2.5 on page 33). MoO_2 resulting from the direct reduction of Mo_8O_{23} at low temperature also likely contributes partially to the production of benzaldehyde. Increasing the temperature, and thus getting closer to the critical point of 698K mentioned by Ressler, the formation of Mo_4O_{11} is favored. This accounts for the observed increases of activity and of the selectivity to benzene. The latter suggests a lower concentration of oxygen vacancies at the surface of Mo_4O_{11}. In the cooling step, particularly below 698 K, two phenomena must be taken into account: (i) Mo_4O_{11} formed during the first step of the cycle becomes inactive;

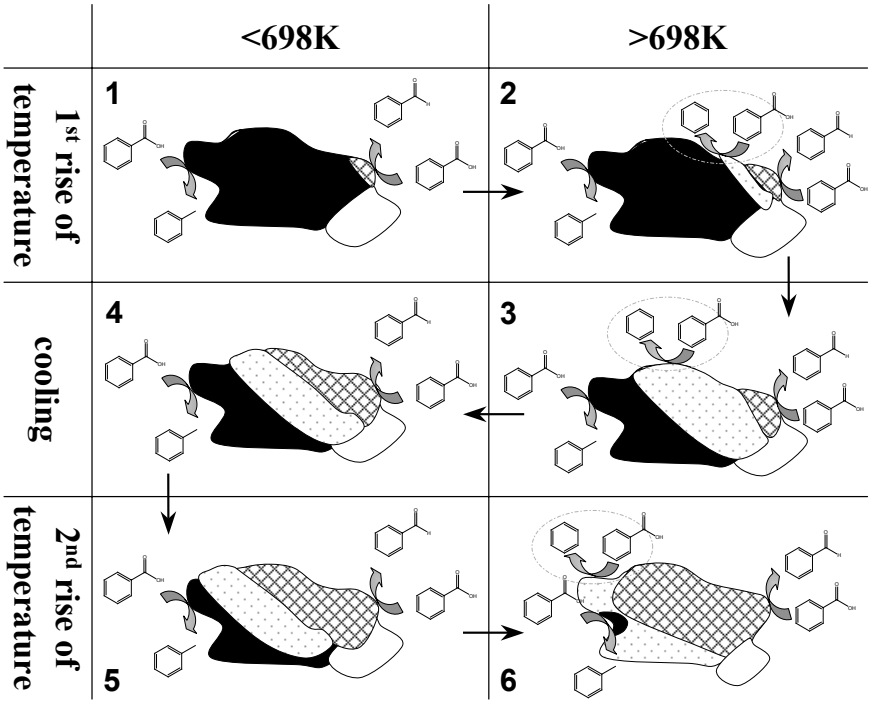

Figure 7.14: Reduction scheme of Mo_8O_{23} in the course of the increase and decrease of temperature. Black is Mo_8O_{23}, white is Mo_9O_{26}, points represents Mo_4O_{11} and hatched is MoO_2. Discontinued circle indicates the activation of the deoxygenation of benzoic acid to benzene on Mo_4O_{11} at high temperature. The numbers show the steps as a function of the time.

(ii) the in situ formation of additional Mo_4O_{11} is stopped. The consequences are the observed decrease of conversion and the shift of selectivity from the formation of benzene to benzaldehyde and toluene. The selectivity to benzaldehyde in the cooling step (which is higher than in the first rise) suggests the presence of a larger amount of MoO_2 in the catalyst. The first part of the second rise of temperature (up to 673 K) is explained by the same behavior as evoked for the first. The explanation of the severe loss of activity observed at the end of the second rise is more delicate. It results from a combination of several phenomena. (i) Mo_8O_{23} and Mo_9O_{26} have completely disappeared from the system as a result of their reduction either to MoO_2 or to Mo_4O_{11}. (ii) The absence of Mo_8O_{23} and Mo_9O_{26} inhibits the further *in situ* formation of Mo_4O_{11}, which together with (iii) its progressive reduction to MoO_2, leads to (iv) the progressive decrease of the Mo_4O_{11} content in the system. The sudden increase of selectivity to toluene and benzaldehyde definitely argues in favor of this hypothesis. Other elements may additionally reinforce the variations of performances, as (v) a deeper reduction of MoO_2 and (vi) a possible poisoning of the surface by an accumulation of carbonaceous compounds due to the formation of benzene [65]. The above hypothesis to explain the catalytic behavior of Mo_8O_{23} rests on the interpretation of XRD data that the catalyst undergoes a series of recrystallization with time-on-stream. Nevertheless, this interpretation is supported by the H_2-TPR results exposed in the previous chapter. It was found that Mo_9O_{26} is resisting very much against the reduction by the hydrogen while Mo_8O_{23} get reduced towards MoO_2 at 723K. Moreover, SEM pictures actually strongly support this view, showing indeed the occurrence of such a phenomenon at the surface and in the bulk of the catalyst. Photoelectron spectroscopy data also support our hypothesis since the fluctuations between Mo^{5+} and Mo^{4+} (figure 7.12) fit quite well with the different crystalline phases met during the catalytic test. By comparison with the fresh reference compounds, more Mo^{5+} (and less Mo^{4+}) species would mean that Mo_8O_{23} is the phase at the surface of the catalyst during the first catalytic step and that MoO_2 is the superficial phase during the very last step.

On the contrary, less Mo^{5+} (and more Mo^{4+}) could indicate the presence of Mo_4O_{11} as the superficial phase.

7.5 Conclusion

Mo_8O_{23} undergoes a reduction to MoO_2 in the course of the deoxygenation of benzoic acid in the presence of hydrogen. The phenomenon is temperature dependent. Below 698K, Mo_8O_{23} reduces directly to MoO_2. But, above 698K, the reduction proceeds through the formation of Mo_4O_{11} as an intermediate phase. Measuring the performances of the phases involved in this reduction pathway reveals that Mo_4O_{11} mainly produces benzene, Mo_8O_{23} mainly produces toluene and MoO_2 mainly produces benzaldehyde. The combination of these data allows us to account for the achievement of a hysteresis when following the performances of Mo_8O_{23} in the deoxygenation reaction carried out along a temperature cycle. Following the opposite approach, it should thus be possible, on the basis of its selectivity to the different products of the deoxygenation of benzoic acid, to predict the stabilized phases in a molybdenum oxide-based catalyst at work. In this way, the deoxygenation of benzoic acid appears as a promising probe of the reduction state of catalysts of the MoO_{3-x} series at work.

Part IV

Coupling the deoxygenation of benzoic acid with the selective oxidation of propylene on molybdenum based oxide catalysts

The previous part confirmed the deoxygenation of benzoic acid in presence of hydrogen as an adequate reaction to probe both the presence of oxygen vacancies and the oxidation state at the surface of the molybdenum oxide based catalysts. Now, to meet our objectives, i.e. to develop a new tool to characterize the oxygen vacancies on oxide catalysts "at work" in *an oxidation reaction*, we will couple, the deoxygenation of benzoic acid with the oxidation of propylene in an original reaction.

Chapter 8

Reducing gas primacy on the probe reaction[1]

Abstract

This work compares the reactivity of a molybdenum suboxide, Mo_8O_{23}, in the deoxygenation of benzoic acid in the presence of hydrogen or propylene. Major differences are highlighted with Mo_8O_{23} as the active phase. When the reaction is performed in the presence of hydrogen as the reducing gas, benzoic acid is converted to benzaldehyde, toluene and benzene. If molecular hydrogen is replaced by propylene as a weaker reducing gas, the only product formed during the reaction is benzaldehyde. It is demonstrated that, in absence of molecular hydrogen in the reaction mixture, a large amount of benzoic acid remains irreversibly adsorbed at the surface of the catalyst. The comparison of the two series of catalytic tests allows to somehow discriminate how the nature and the mobility of the hydrogen atoms involved in the reaction dictate the behaviour of the catalyst.

[1] accepted in Catalysis Today following the Concorde (CO-ordination of Nanostructured Catalytic Oxides Research and Development in Europe) meeting in Louvain-la-Neuve (Belgium), January 2005

8.1 Introduction

The previous chapter showed that the deoxygenation of benzoic acid cannot be performed on molybdenum (sub)oxides in the presence of hydrogen without leading to the deep reduction of the catalyst. The present chapter is thus dedicated to the evaluation of the catalytic activity of the molybdenum suboxides when the molecular hydrogen is replaced by a weaker reducing gas : propylene. By such a change in the experimental method, we can approach the main objective of this thesis.

The comparison of the catalytic behaviour of Mo_8O_{23} in the presence of hydrogen or in the presence of propylene provides some insight into the nature of the hydrogen species involved in the deoxygenation of benzoic acid. Some understanding on the role of hydrogen mobility in such a system is additionally obtained.

8.2 Experiments

8.2.1 Preparation of the catalysts

Mo_8O_{23} was synthesized by heating a mixture of commercial MoO_3 and MoO_2 in a quartz reactor. The cell was heated under vacuum at 1023K during 96h. The molar ratio between the two precursor compounds was adjusted to obtain the appropriate mean oxidation state in the final phase [67].

8.2.2 Catalytic activity measurements

Deoxygenation of benzoic acid was performed at atmospheric pressure in a stainless steel fixed bed micro-reactor with 100mg of catalyst. The reaction mixture invariably contained 574 ppm of benzoic acid (Aldrich, 99% pure) which was mixed with either 50000 ppm hydrogen (Indugas, 99.95% pure) (experiment H) or 167000 ppm of propylene (Indugas, 99.8% pure) (experiment P). In both cases, helium was the gas balance. Total flow was

adjusted to 100 ml min^{-1} with helium (Indugas, 99.996%). All catalytic tests were performed at 723K for 10 hours. Benzoic acid, propylene, benzaldehyde, toluene, benzene, CO_2 and CO were analysed by gas phase chromatography.

8.2.3 Characterization

The catalysts were characterized before and after the catalytic reactions and additional experiments by specific area measurements, X-ray diffraction and X-ray photoelectron spectroscopy. Specifications and detailed information are given elsewhere (section 5 on page 49).

8.3 Results

8.3.1 Catalytic activity measurements

Results from experiment H are presented in Figure 8.1. In the presence of hydrogen as reducing agent, the conversion of benzoic acid increases with time on stream and reaches 35% after five hours. Next, the conversion is around 30% until the end of the catalytic test. Initially, benzene and toluene are formed respectively with 79% and 21% of selectivity. But, after sixty minutes of reaction, benzaldehyde is produced to the detriment of benzene. Meanwhile, the selectivity to toluene increases. After ten hours of catalytic reaction, selectivities to benzaldehyde, toluene and benzene are respectively : 20%, 45% and 35%. In experiment P, the conversion of propylene is very low (less than 5% of conversion) and can thus not be discussed in detail. Concerning the conversion of benzoic acid (Figure 8.2), major differences with experiment H appear : (i) the conversion of benzoic acid for the first three hours is less than 10% and increases only to 18%), (ii) only benzaldehyde is detected and (iii) a lack in the total selectivity indicates a large deficit in the carbon balance while the carbon balance was reached in experiment H. In order to understand the origin of these differences, experiment P was reproduced two times under identical conditions but after three hours of reaction, the gas feed

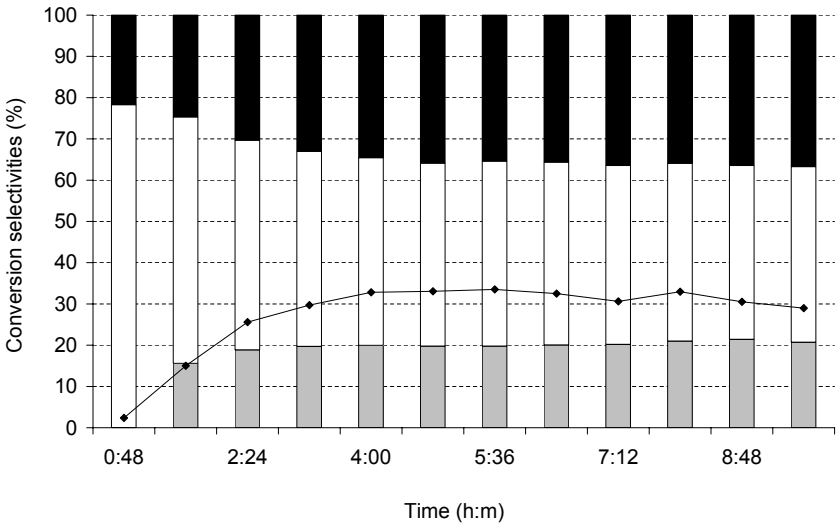

Figure 8.1: Conversion of benzoic acid (black line) and selectivities to benzaldehyde (grey), toluene (black) and benzene (white) during experiment H.

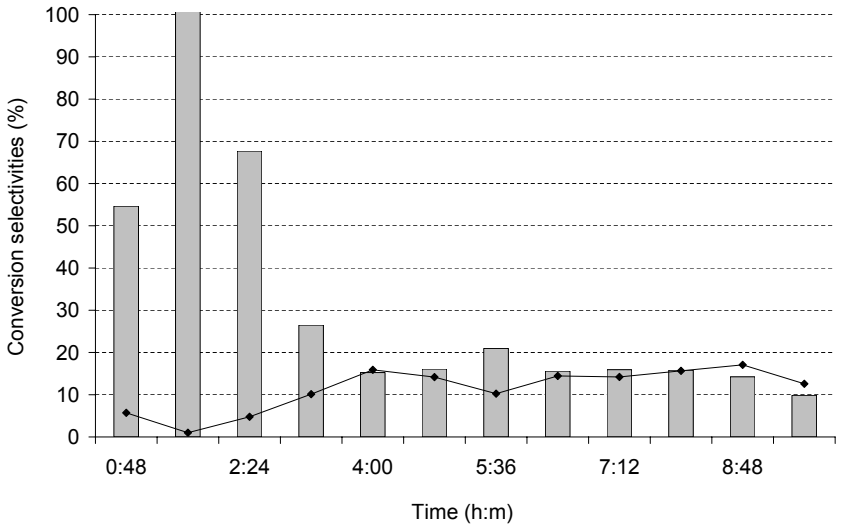

Figure 8.2: Conversion of benzoic acid (black line) and selectivities to benzaldehyde (grey) during experiment P.

was suddenly changed either to pure helium or to 5% hydrogen in helium. No more benzoic acid nor propylene were thus added to the feed. No products were detected while flushing under pure helium at 723K. Figure 8.3 illustrates the compounds detected at the outlet of the reactor during the flushing with hydrogen at 723K. No benzaldehyde is detected. On the contrary, significant amounts of benzene and toluene are desorbed from the catalyst (respectively 25 and 20 ppm during the very first minutes). The desorption proceeds during three hours, with the concentrations of desorbed benzene and toluene at the reactor outlet decreasing with time under hydrogen.

8.3.2 Characterization

The specific area of the fresh catalyst is 0.2 m^2g^{-1}. After experiment H and P, these values respectively increase to 1.8 m^2g^{-1} and 1.3 m^2g^{-1}. The main XRD peaks for the fresh sample are typical of Mo_8O_{23} (JCPDS n°5-0339).

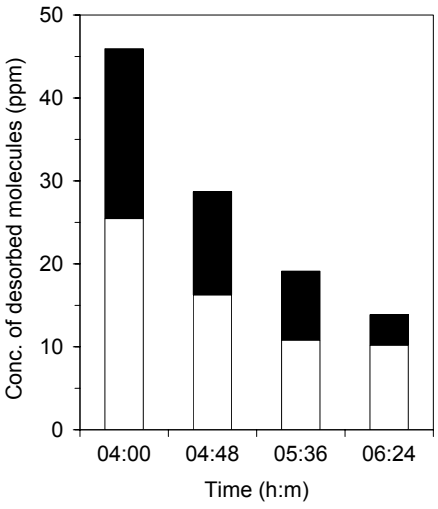

Figure 8.3: Concentration of toluene (black) and benzene (white) measured during the desorption procedure.

The presence of Mo_9O_{26} (JCPDS n°12-0753) is also revealed. After catalytic tests (both experiments H and P), characteristic peaks of MoO_2 were found in addition to the phases detected in the fresh sample (figure 8.4). XPS analyses reveal that after catalytic test, the carbon content at the surface of the catalyst increases significantly (figure 8.5). Whereas there was only 24% of carbon in the fresh material, for the test run in presence of hydrogen, the C 1s contribution increases to 70%. With propylene as the reducing agent, the carbon content is 42% ; a small peak is detected at about 291eV, corresponding to the shake up of an aromatic molecule (figure 8.6). The analysis of Mo 3d region (figure 8.7) shows that the fresh catalyst has only Mo^{6+} (88%) and Mo^{5+} species (12%). The catalysts used in experiments H and P are more reduced than the fresh one since Mo^{4+} species is detected in considerable amount (22 and 26% respectively).

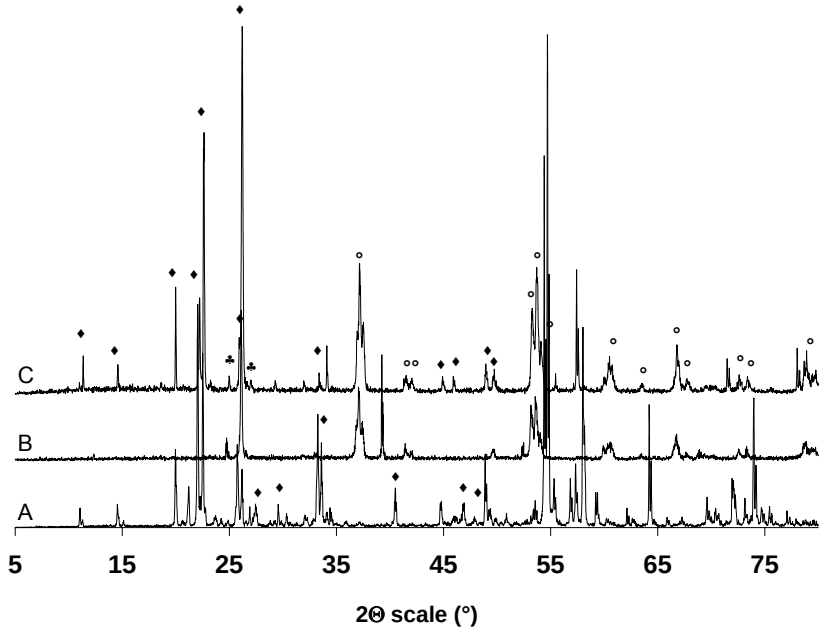

Figure 8.4: XRD spectra of fresh catalyst (A), catalyst after experiment H (B) and catalyst after experiment P (C). Symbols ♦ indicate Mo_8O_{23} peaks, symbols ◯ indicate MoO_2 peaks and symbols ♣ indicate Mo_9O_{26} peaks. Peaks not marked are not identified or not reported in the database beyond 2θ=49°

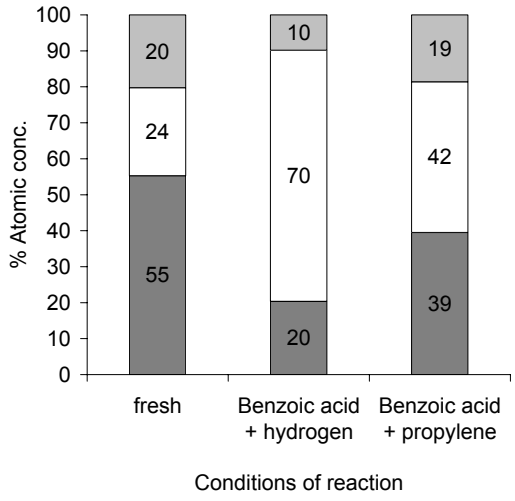

Figure 8.5: C (white), O (black) and Mo (grey) atomic percentage measured by XPS on the fresh, after experiment H and P catalysts.

8.4 Discussion

The comparison of experiments P and H shows that : (i) in the absence of molecular hydrogen in the feed (experiment P), a part of benzoic acid remains irreversibly adsorbed at the surface of the catalyst, (ii) the benzene and toluene synthesis is only possible in the presence of molecular hydrogen in the gas feed (experiment H). Without any doubt, the mechanism of the products formation (benzaldehyde, toluene and benzene) is dictated by the reducing agent used during the catalytic test.

XPS measurements highlight a large amount of carbon at the surface of the samples recovered after the tests. After experiment P, this could be explained by the presence of a large amount of aromatic molecules adsorbed on the surface of the catalyst. This was confirmed by the detection of the aromatic shake up in the XPS measurements (figure 8.6). Concerning the sample corresponding to the experiment H, the high carbonaceous content is

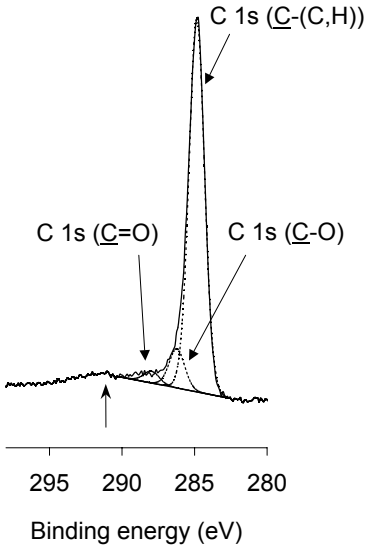

Figure 8.6: Spectra of C 1s obtained by X-ray photoelectron spectroscopy on Mo_8O_{23} recovered after experiment P. Aromatic shake up is at 291 eV.

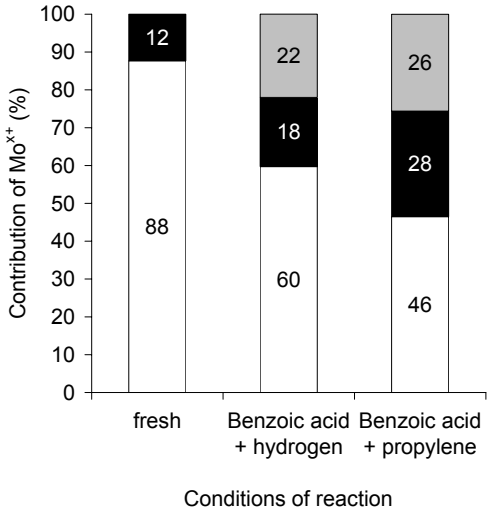

Figure 8.7: Importance of the Mo^{6+}(white), Mo^{5+}(black) and Mo^{4+} (grey) contributions measured by XPS on fresh catalyst, after experiment H and P.

more surprising since no aromatic molecules remains adsorbed on the surface. However, from the comparison of the experiments H and P, we know that when molecular hydrogen is used, the conversion is higher and leads to the formation of a large amount of benzene. Remembering the proposed mechanism for the benzene formation (figure 2.6 on page 34), we know that the acidic function of the benzoic acid is removed and probably remains adsorbed on the catalyst, contributing to a higher carbon content. This is perfectly illustrated in figure 8.8 : the C=O contribution increases after experiment H.

The different carbon contents could influence the reactivity in experiments H and P but two other hypotheses must be envisaged to explain the observed differences : (i) a modification of the main crystallographic phase in relation with the reducing agent used could induce a major difference in the nature of the catalytic sites available at the surface of the catalyst, (ii) the nature and the reactivity of hydrogen atoms introduced either by molecular hydrogen

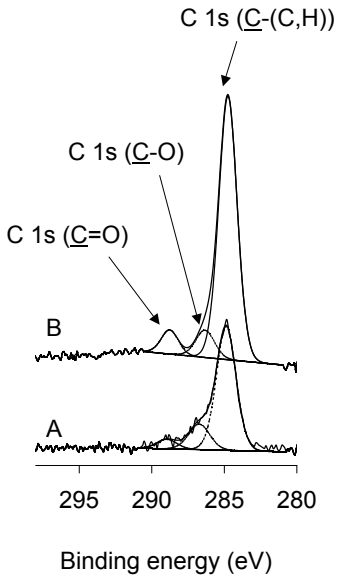

Figure 8.8: Spectra of C 1s obtained by X-ray photoelectron spectroscopy on fresh Mo_8O_{23} (A) and recovered after experiment H (B).

(experiment H) or by propylene and benzoic acid (experiment P) could be the determining factor in the formation of the deoxygenation products. The first hypothesis can be rejected because, in both experiments H and P, the catalyst undergoes a similar reduction to MoO_2 (surface and bulk). Moreover, we know from present and previous sets of catalytic tests that, in presence of hydrogen, Mo_9O_{26} is inactive, Mo_8O_{23} mainly produces toluene and MoO_2 is mainly responsible for the production of benzaldehyde [87]. In the present situation, catalytic activities are different but the catalysts used in experiments H and P undergo the same reduction towards MoO_2. As a consequence, the difference of performances cannot be only attributed to the nature of the catalyst itself.

The other hypothesis is related to the nature of the reactants. The mobility and the nature of hydrogen atoms coming from the dissociation of molecular hydrogen are likely different from those resulting from the acidic function of benzoic acid or from the total oxidation of propylene. Our results suggest that the first species would be needed for the formation of benzene and toluene, whereas the second and third ones could only take part in the formation of benzaldehyde, allowing its desorption. A piece of answer is that on one side the activation of molecular hydrogen is easier than the activation of several C-C and C-H bonds. This is related to the very low conversion of propylene (experiment P) with as a consequence, the fact that small quantities of hydrogen atoms[2] are available to transform the benzoic acid molecules or to desorb the benzene and the toluene. On the other side, dissociative adsorption of molecular hydrogen could occur on catalytic sites different from those responsible for the propylene transformation. Indeed, in our system, hydrogen (whatever its origin) can be fixed by molybdenum atoms or by oxygen atoms. These two species are thus quite different since the first one is richer in electrons than the second one. So, in the presence of propylene, one can assume that one of the two hydrogen species, i.e. the hydrogen species similar to those formed in the presence of molecular hydrogen, is missing

[2]The hydrogen provided by propylene would not come from its dehydrogenation to propyne (no propyne detected in the test) but it would rather come from the abstraction of the α-hydrogen atom of the olefin.

(or present in too small quantities) implying the non-formation of toluene and benzene.

8.5 Conclusion

This chapter highlights the specificity of the deoxygenation reaction pathway according to the source of hydrogen. Indeed, the comparison of the catalytic tests performed in presence of molecular hydrogen or propylene as the co-reagent of benzoic acid indicated that the hydrogen atoms involved during the reaction can have very different properties according to their origin. Thus, hydrogen atoms coming from the transformation of propylene do not have the required properties to allow the transformation and/or desorption of toluene and benzene whereas the hydrogen atoms coming from the molecular hydrogen do. More generally, data can contribute to the understanding of the role of hydrogen in the Mo (sub)oxides behaviour at work in the deoxygenation of acids.

Chapter 9

Coupling on metal molybdates

Abstract

Several metal molybdates were tested in two different catalytic reactions, namely the deoxygenation of benzoic acid in the presence of hydrogen or propylene (coupling reaction) as the reducing gas and the oxidation of propylene in the presence of molecular oxygen. The systematic comparison of the measured activity under the three conditions of reaction allowed us to precise (i) the formation and the characteristics of hydrogen species involved in the deoxygenation of benzoic acid, (ii) the oxidizing properties of benzoic acid compared to the molecular oxygen. Moreover, the results obtained in the coupling reaction, namely the deoxygenation of benzoic acid with the oxidation of propylene, reveals that such a reaction is possible and can provide some interesting information both on the catalytic sites responsible for the reactivity towards the acid and propylene side.

9.1 Introduction

The preliminary results exposed in chapter 8 revealed an unexpected phenomenon when tempting to implement the coupling between the

deoxygenation of benzoic acid and the oxidation of propylene on molybdenum suboxides. It appeared that the desorption of benzene and toluene was not possible when using propylene as reducing gas instead of molecular hydrogen. It is suspected that the low amount of propylene activated could be the main cause of the poor quantity of hydrogen atoms available for the synthesis of both benzene and toluene.

We have thus planned to use metal molybdates in replacement of molybdenum (sub)oxides. Indeed, it is well-known that metal molybdates are intrinsically more active than simple molybdenum oxides. It could thus be expected that a higher propylene conversion will provide more hydrogen atoms for the formation of toluene and benzene, allowing their desorption of the catalyst. Moreover, metal molybdates are more stable against reduction which could help to avoid the phase transformation observed with most of the molybdenum (sub)oxides. Finally, molybdates can be considered "closer" to the industrial catalysts (see section 1.2) and can thus better mimic their catalytic performances.

The present chapter confronts the results obtained in the coupling reaction with those obtained in the course of the two independent reactions, namely the oxidation of propylene and the deoxygenation of benzoic acid in their respective classical configurations, i.e. in the presence of molecular oxygen or hydrogen.

9.2 Experiments

9.2.1 Preparation of the catalysts

$Fe_2(MoO_4)_3$ was prepared by a co-precipitation method whereas $NiMoO_4$, $CoMoO_4$, $Bi_2(MoO_4)_3$, $Bi_2Mo_2O_9$ and Bi_2MoO_6 were synthesized by the complexation of metal precursors using the "citrate" method. The detailed protocol of preparation is available at page 42.

9.2.2 Catalytic activity measurements

The catalytic tests were realized at atmospheric pressure in a stainless steel fixed bed micro-reactor in isothermal conditions. Three different catalytic experiments were realized : (i) in experiment BAC3, the reaction feed contained 635 ppm of benzoic acid (Aldrich, 99% pure) and 318 ppm of propylene (Indugas, 2.01% Vol. in He). Helium (Indugas, 99.996% pure) was the gas balance. (ii) In experiment BAH2, the reaction feed contained 635 ppm of benzoic acid (Aldrich, 99% pure) and 50000 ppm of hydrogen (Indugas, 99.95% pure) diluted in helium (Indugas, 99.996% pure) as the gas balance. (iii) In experiment C3O2, the reaction feed contained only 318 ppm of propylene (Indugas, 2.01% Vol. in He) and 630 ppm of oxygen (Indugas, 99.995% pure) in helium (Indugas, 99.996% pure) as the gas balance. In the experiments involving the propylene, the oxidant/reducing gas concentration ratio is kept constant to 2 to allow an easy comparison.

In all the cases, the total flow was adjusted to 100 ml $min^{-1}$and 300 mg of catalyst with a granulometry of 100-315 μm were used except for experiment BAH2 (100 mg, same granulometry). For all the catalytic conditions, the performances were measured at 723K for 16 or 9 hours.

9.2.3 Characterization

The catalysts were characterized before and after the catalytic reactions by specific area measurement, X-ray diffraction and X-ray photoelectron spectroscopy. Specifications and detailed information are given elsewhere (section 5 on page 49).

9.3 Results

To facilitate the reading and for the sake of clarity, the results are grouped by catalysts. Moreover, the catalytic tests corresponding to the different experimental conditions are presented in a single figure to allow an easy

comparison between the benzoic acid side of the experiment BAC3 and the experiment BAH2, the propylene side of the experiment BAC3 and the experiment C3O2. Finally, as the different catalysts have very different specific areas and the amount of catalyst being the same, the number of active catalytic site can be different among the catalysts. Consequently, the benzoic acid conversion is standardized according to the total area developed by the amount of catalyst in the reactor. Thus, standardized conversion can exceed 100% m^{-2}. The conversion to standardized transformation rate expressed in μmole $(m^2.h)^{-1}$ can be done by multiplying the standardized conversion in % m^{-2} by $6{,}4.10^{-2}$ (benzoic acid conversion) or by $3{,}2.10^{-2}$ (propylene conversion).

9.3.1 $Fe_2(MoO_4)_3$

9.3.1.1 Catalytic activity measurements

The catalytic activity measured on $Fe_2(MoO_4)_3$ is presented in figure 9.1.

Comparing the benzoic acid conversion in BAC3 and BAH2 experiments, one noticed very different activities. In BAC3, conversion is about 40% m^{-2} after 48 minutes and decreases to 10% m^{-2} at the end of the catalytic test. In BAH2, the conversion starts at 90% m^{-2} and increases to 180% m^{-2} after 2 hours only. In experiment BAC3, benzaldehyde (from 4 to 30% selectivity) and benzene (60% selectivity on average) are the main products. A small amount of toluene is also produced episodically. Whereas the conversion is stable, the total selectivity fluctuates from 28% to 100%. Sometimes, a big gap is thus observed but an unknown product is also detected. Many attempts to identify the molecule were conducted in particular by mass spectrometry but without success. We can nevertheless discard the formation of benzyl alcohol or benzophenone which are calibrated in our chromatographic system. In fact, it is suspected that the unknown molecule could be the reaction product of benzoic acid with acrolein. This unknown product is detected in the similar conditions for all the metal molybdates; we will thus call it product UKN1.

Selectivities in experiment BAH2 are more regular : benzene and

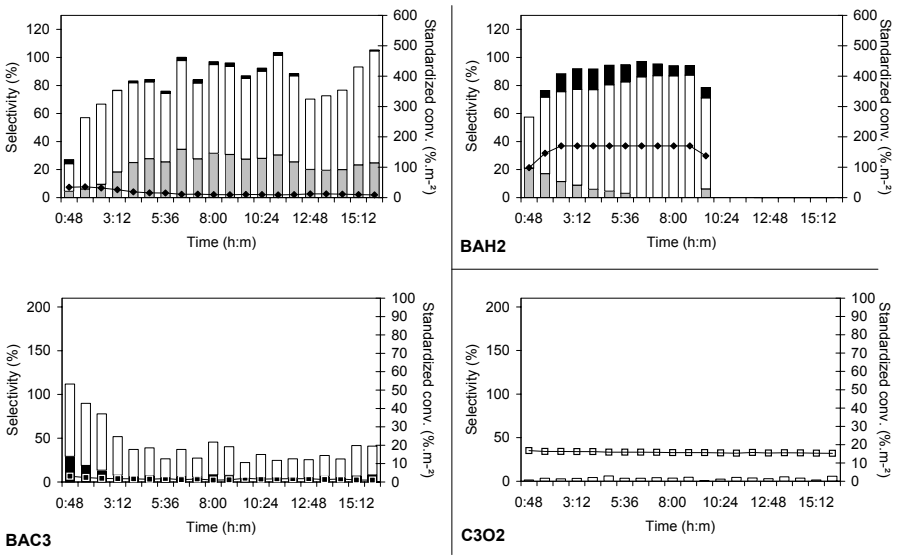

Figure 9.1: Catalytic activity measured on $Fe_2(MoO_4)_3$ during experiment BAC3: conversion of benzoic acid (♦) and selectivities in benzaldehyde (grey), benzene (white) and toluene (black) with time on stream at 723K (upper graphic), conversion of propylene (□) and selectivities in CO (black) and CO_2 (white) with time on stream at 723K (bottom graphic). Experiment BAH2: conversion of benzoic acid and selectivities in benzaldehyde and benzene with time on stream at 723K. Experiment C3O2: conversion of propylene and selectivities in CO and CO_2 with time on stream at 723K.

benzaldehyde are the main products at the beginning of the catalytic test (respectively 20% and 35% selectivities). With time on stream, benzaldehyde vanishes and toluene appears with a selectivity of about 10%. The benzene selectivity grows up to 85%. A gap in the selectivity is observed at the initial time but once more a new product is detected. It is different from the product detected in BAC3 experiment and is also unidentified.

On the propylene side, the comparison of the BAC3 experiment with the C3O2 experiment highlights some differences: (i) like the benzoic acid side, the propylene conversion is lower in BAC3 than in C3O2 (respectively 4% m^{-2} and 16% m^{-2}). (ii) While CO_2 and CO are produced in BAC3, only CO_2 is detected in C3O2. In both experiments, the carbon balance is by far less than 100% except for BAC3 at the beginning of the catalytic test where the total selectivity reaches 115%. Such a result is not astonishing since the conversion level is very low making the error on the selectivity higher.

9.3.1.2 Characterization

Specific area of fresh iron molybdate is 5.86 m^2 g^{-1}. After BAC3, BAH2 and C3O2, it is respectively 7.90 m^2 g^{-1}, 9.18 m^2 g^{-1}, 2.84 m^2 g^{-1}.

The presence of crystallographic phases was analysed by X-ray diffraction. Fresh sample and sample recovered after C3O2 test correspond to $Fe_2(MoO_4)_3$ (JCPDS n°35-0183). After the BAC3 and BAH2 experiments , the catalyst is partially reduced to $Fe_2Mo_3O_8$ (JCPDS n°36-0526) and MoO_2 (JCPDS n° 32-0671), the phase corresponding to the fresh sample is still present.

Table 9.1 presents the atomic percentages measured by XPS at the surface of the fresh and used samples. It reveals that the amount of carbon increases after all the catalytic tests following the growing order : fresh<C3O2<BAH2<BAC3. The highest Fe/Mo atomic ratio is observed for the fresh catalyst and corresponds to the theoretical value. It decreases to 0.53 after BAC3, 0.44 after BAH2 and 0.38 after C3O2. The carbon content not being identical for the different samples and due to its possible participation in the oxygen content, it is not adequate to comment the O/Mo atomic ratio

Table 9.1: Atomic percentage at the surface of $Fe_2(MoO_4)_3$ measured by XPS.

	Sample			
	Fresh	***After BAC3 test***	***After BAH2 test***	***After C3O2 test***
%O	51.1	20.9	35.7	48.0
%C	23.5	69.5	43.1	29.0
%Mo	15.3	6.3	14.7	16.7
%Fe	10.1	3.3	6.5	6.3
O/C	2.18	0.30	0.83	1.65
O/Mo	3.33	3.34	2.42	2.88
Fe/Mo	0.66	0.53	0.44	0.38

to evaluate the oxidation state of the catalyst. For this purpose, we report the detailed analysis of Mo 3d in figure 9.2. Surfaces of the fresh catalyst and of the catalyst recovered after C3O2 test are fully oxidized while after BAC3 and after BAH2, the surfaces are reduced. Indeed, we detect respectively 66% and 48% of Mo^{6+} in the samples BAC3 and BAH2. The distribution of the reduced molybdenum species between these two samples is different. In the presence of hydrogen, the surface of the catalyst contents more Mo^{5+} while in the presence of propylene, the amount of Mo^{4+} is higher.

No differences, i.e. no chemical shift, was observed concerning the oxidation state of Fe between the fresh and the used catalyst after BAC3, BAH2 an C3O2.

9.3.2 $NiMoO_4$

9.3.2.1 Catalytic activity measurements

The catalytic activities measured on $NiMoO_4$ are represented in figure 9.3.

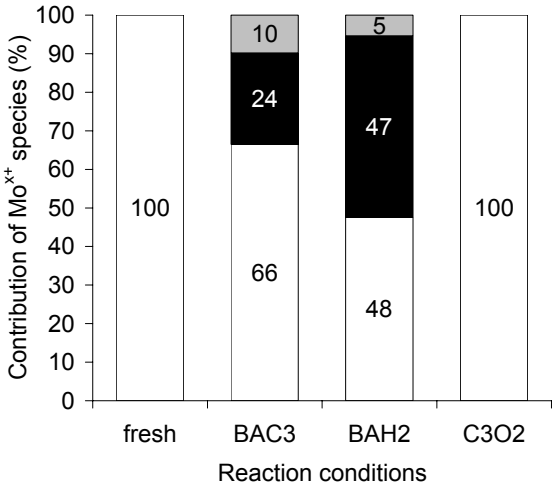

Figure 9.2: Importance of the Mo^{6+}(white), Mo^{5+}(black) and Mo^{4+} (grey) contributions measured by XPS on fresh $Fe_2(MoO_4)_3$, after experiment BAC3, BAH2 and C3O2.

Like for $Fe_2(MoO_4)_3$, the benzoic acid conversion is lower in BAC3 than in BAH2 with a constant conversion rate of 10% m^{-2} for BAC3 against 27% m^{-2} for BAH2. In the presence of propylene in the gas feed, the deoxygenation of benzoic acid produces only benzaldehyde and benzene. Except at the first hour of reaction, a rather constant ratio of 0.48 between benzene and benzaldehyde is obtained along the test. The total selectivity reaches 90%. Small amount of the UKN1 product detected in the corresponding catalytic test on $Fe_2(MoO_4)_3$ is also detected.

Results collected in the course of BAH2 experiment are more particular. Indeed, no known products are detected during the whole duration of the test. However, an intense peak in the chromatogram indicates the formation of a new product (UKN2). According to its retention time we can identify this product as molecule similar to benzene and heavier than propylene. Despite references [64] and [88] state it, cyclohexane and phenol could thus not be

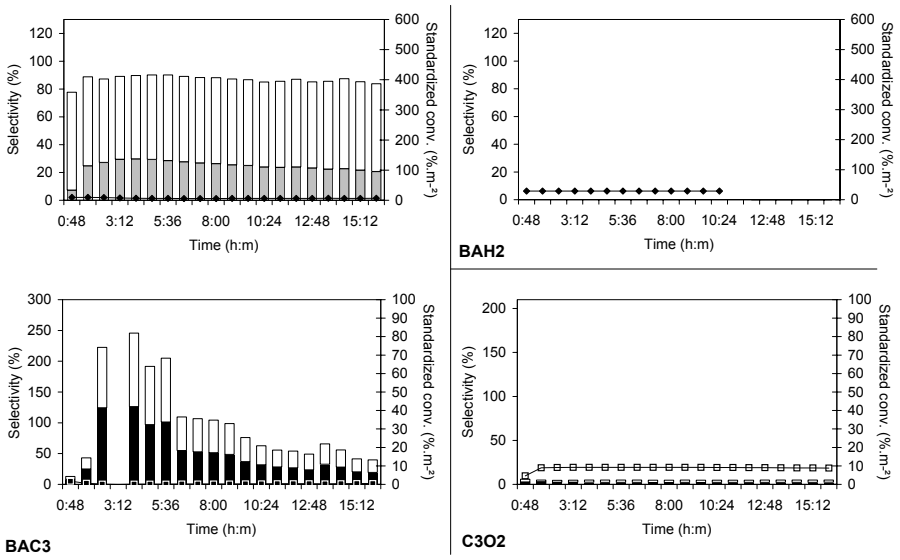

Figure 9.3: Catalytic activity measured on $NiMoO_4$ during experiment BAC3: conversion of benzoic acid (⧫) and selectivities in benzaldehyde (grey), benzene (white) and toluene (black) with time on stream at 723K (upper graphic), conversion of propylene (□) and selectivities in CO (black) and CO_2 (white) with time on stream at 723K (bottom graphic). Experiment BAH2: conversion of benzoic acid and selectivities in benzaldehyde and benzene with time on stream at 723K. Experiment C3O2: conversion of propylene and selectivities in CO and CO_2 with time on stream at 723K.

formed on Ni based catalysts. Nevertheless, we can guess that UKN2 could be an aliphatic molecule containing six carbon atoms resulting from the selective hydrogenation of benzene, benzaldehyde, toluene or benzoic acid.

The comparison of the propylene side in BAC3 experiment with the C3O2 experiment indicates once again that the conversion is higher in the presence of oxygen (9% m^{-2} against $\sim$1% m^{-2}). In both cases, the products detected are CO and CO_2. One notices that the selectivities in BAC3 vary strongly with time on stream. Sometimes, their sum exceeds 100%. This is never the case in C3O2 test for which, a large gap (about 80%) in the total selectivity indicates an important defect in the carbon balance. Since the acrolein threshold of the GC apparatus is about 2000 ppm, this important selectivity gap could be due to some undetected acrolein.

9.3.2.2 Characterization

Fresh catalyst has a specific area of 34.33 m^2 g^{-1}. After the catalytic tests, it respectively decreases to 30.33 m^2 g^{-1} and 32.62 m^2 g^{-1} for the tests BAC3 and C3O2. Concerning the sample recovered after the experiment BAH2, the specific area increases to 65.53 m^2 g^{-1}.

The crystallographic phase of the fresh catalyst corresponds to $NiMoO_4$ (JCPDS n°33-0948) as the main phase. Two peaks at 2θ value of 26° and 34° are attributed to another $NiMoO_4$ (JCPDS n°45-0142) with a different crystal cell. After BAC3 and C3O2 experiments, only $NiMoO_4$ (JCPDS n°33-0948) is detected, the peaks corresponding to $NiMoO_4$ (JCPDS n°45-0142) have vanished. A deep recrystallization of the catalyst occurs in BAH2 test since no more $NiMoO_4$ phases are detected. Instead of the nickel molybdates, we found NiO (JCPDS n°44-1159). One peak of the diffractogram (2θ =51°) remains unattributed. It could be the signature of a molybdenum based phase that we did not succeed to identify with the available diffractograms database.

XPS results are presented in table 9.2 and figure 9.4. The carbon content at the surface of the fresh sample is 20.5%. After use, it increases to 71.8% for BAC3 (highest value), 45.8% for BAH2 and 65.9% for C3O2. The

Table 9.2: Atomic percentage at the surface of $NiMoO_4$ measured by XPS.

	Sample			
	Fresh	***After BAC3 test***	***After BAH2 test***	***After C3O2 test***
%O	49.3	18.0	33.9	22.4
%C	20.5	71.8	45.8	65.9
%Mo	13.3	6.8	8.2	8.2
%Ni	17.0	3.3	4.2	3.5
O/C	2.41	0.25	0.74	0.34
O/Mo	3.69	2.66	4.14	2.74
Ni/Mo	1.27	0.49	0.51	0.43

experimental Ni/Mo ratio in the fresh catalyst is 27% higher than the expected theoretical value and dramatically decreases after the catalytic tests to about 0.5. The results presented in figure 9.4 show that there is only fully oxidized molybdenum species present at the surface of the fresh $NiMoO_4$. After all the catalytic tests, both +4 and +5 molybdenum species are detected. The most reduced catalyst is recovered after BAH2 test with 38% of Mo^{4+} and 16% of Mo^{5+}. The catalyst recovered after BAC3 contains 5% of Mo^{4+} and 11% of Mo^{5+} on its surface. The catalyst used in the presence of oxygen is also reduced but with only 1% of Mo^{4+} and 14% of Mo^{5+}.

Nickel in the fresh sample and in the catalysts used in the C3O2 and BAC3 experiments corresponds to Ni^{2+} inserted in a molybdate structure. After BAH2, in addition to Ni^{2+} inserted in a molybdate structure, some nickel corresponds to Ni^{2+} included in NiO.

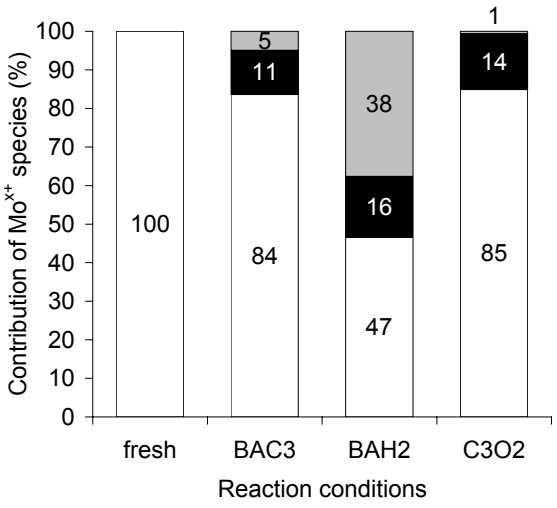

Figure 9.4: Importance of the Mo^{6+}(white), Mo^{5+}(black) and Mo^{4+} (grey) contributions measured by XPS on fresh $NiMoO_4$, after experiment BAC3, BAH2 and C3O2.

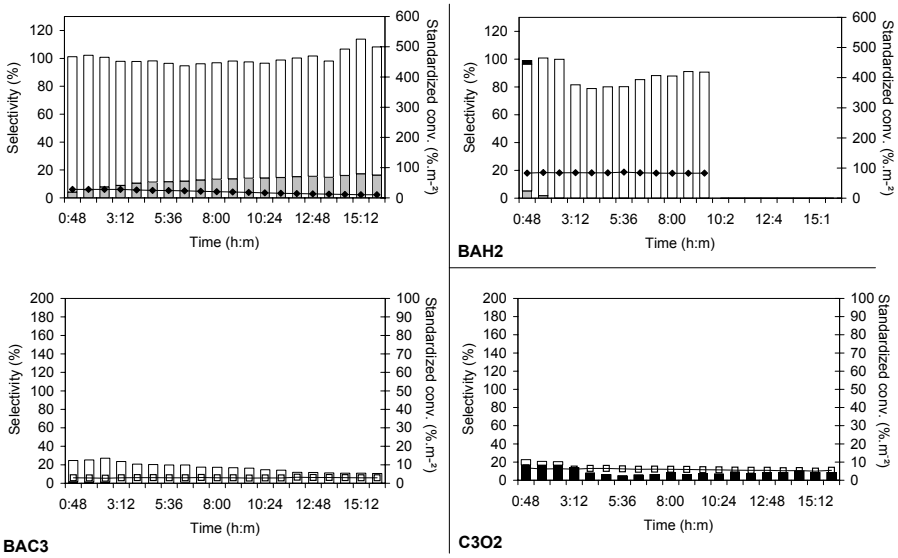

Figure 9.5: Catalytic activity measured on $CoMoO_4$ during experiment BAC3: conversion of benzoic acid (♦) and selectivities in benzaldehyde (grey), benzene (white) and toluene (black) with time on stream at 723K (upper graphic), conversion of propylene (□) and selectivities in CO (black) and CO_2 (white) with time on stream at 723K (bottom graphic). Experiment BAH2: conversion of benzoic acid and selectivities in benzaldehyde and benzene with time on stream at 723K. Experiment C3O2: conversion of propylene and selectivities in CO and CO_2 with time on stream at 723K.

9.3.3 $CoMoO_4$

9.3.3.1 Catalytic activity measurements

The results are described in figure 9.5. First, let us compare the results of the tests where benzoic acid is involved. The benzoic acid conversions are respectively 27% m^{-2} and 100% m^{-2} for BAC3 and BAH2 experiments. In the first test, benzoic acid is converted to benzaldehyde and benzene while in BAH2, toluene, benzaldehyde and benzene are produced in the very first minutes of the catalytic test then only benzene is produced. The carbon balance

is completed in BAC3 (benzoic acid side). On the contrary, in the BAH2 experiment, about 20% of the converted benzoic acid is missing among the known products. Once more, the peak corresponding to the UKN1 product is detected.

The conversion of propylene in BAC3 and C3O2 is rather similar, respectively 4% m^{-2} and 6% m^{-2}. But, the profile of selectivities is totally inverted : while the selectivity to carbon dioxide is the highest one in BAC3, the highest selectivity value in C3O2 is attributed to carbon monoxide. In both tests, a gap of about 75% selectivity is observed.

9.3.3.2 Characterization

Fresh catalyst is 11.30 m^2 g^{-1}. The specific area increases after catalytic test to 13.83 m^2 g^{-1} (BAC3), 17.67 m^2 g^{-1} (BAH2) and 13.42 m^2 g^{-1} (C3O2).

The freshly synthesized and calcined catalyst is composed of two crystalline phases : $CoMoO_4$ (JCPDS n°25-1434) and $CoMoO_4$ (JCPDS n°21-0868). These two phases differ by the unit cell parameters. After the test in the presence of hydrogen, the catalyst appears to be fully recrystallised to CoO (JCPDS n°48-1719) and $CoMoO_3$ (JCPDS n°21-0869). This does not happen when the catalyst is used with propylene and benzoic acid in the feed : $CoMoO_4$ (JCPDS n°21-0868) and $CoMoO_3$ (JCPDS n°21-0869) are the only phases detected. After experiment C3O2, only peaks corresponding to $CoMoO_4$ (JCPDS n°21-0868) are detected.

The analysis of the surface composition by XPS is reported in table 9.3. It indicates that the fresh sample and the one recovered after test C3O2 have the same composition in carbon (30.7%) and a similar Co/Mo ratio close to the theoretical value. Like the previous molybdates, when the test is run with benzoic acid in the gas feed, the carbon content increases drastically : respectively 63.4% and 56.9% for BAC3 and BAH2. The oxidation state of molybdenum at the surface of the catalyst is presented in figure 9.6. Fresh catalyst and the catalyst used in C3O2 experiment exhibit only Mo^{6+} while samples related to BAC3 and BAH2 are reduced. One should remark that the

Table 9.3: Atomic percentage at the surface of $CoMoO_4$ measured by XPS.

	Sample			
	Fresh	***After BAC3 test***	***After BAH2 test***	***After C3O2 test***
%O	42.2	23.6	26.8	42.9
%C	30.7	63.4	56.9	30.7
%Mo	14.3	6.9	10.4	13.2
%Co	12.8	6.1	5.9	13.2
O/C	1.37	0.37	0.47	1.40
O/Mo	2.96	3.44	2.59	3.26
Co/Mo	0.90	0.89	0.57	1.01

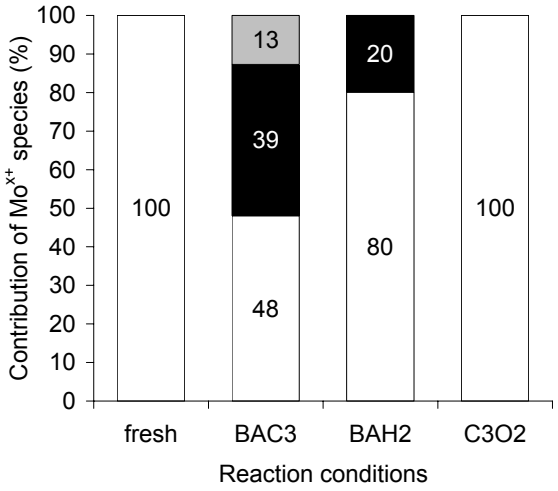

Figure 9.6: Importance of the Mo^{6+}(white), Mo^{5+}(black) and Mo^{4+} (grey) contributions measured by XPS on fresh $CoMoO_4$, after experiment BAC3, BAH2 and C3O2.

BAC3 sample is more reduced than the BAH2 since the Mo^{6+} content is only 48% in BAC3 and 80% in BAH2. Moreover, we detect only Mo^{5+} when the catalyst is used in the presence of hydrogen while Mo^{4+} is additionally detected in the BAC3 sample.

Oxidation state of Co was the same before and after all the catalytic tests.

9.3.4 $Bi_2(MoO_4)_3$

9.3.4.1 Catalytic activity measurements

The catalytic activity measured on $Bi_2(MoO_4)_3$ according to the three experimental conditions are summarized in figure 9.7. The catalytic activity on the benzoic acid side shows very different behaviours in BAC3 and in BAH2 experiments. The benzoic acid conversion is much higher in the presence of hydrogen than in the presence of propylene. Moreover, the presence of hydrogen induces the formation of toluene while propylene not.

More precisely, in BAC3, the conversion of BA is 111% m^{-2} in the very first moments of the catalytic test, then it decreases to almost 0% m^{-2}. In BAH2, the conversion is about 450% m^{-2} during the first two hours of the catalytic test. It then increases to 500% m^{-2} after three hours before going down to 100% m^{-2} after 10 hours.

When the deoxygenation is performed with the propylene as the reducing gas, the main product of the reaction is benzene (from 60 to 30% selectivity with time on stream). Some benzaldehyde is also produced until the twelfth hour (from 16 to 24% selectivity). One observes a major gap in the carbon balance corresponding to about 20% in the total selectivity and even 70% at the end of the test. It can be linked to the production of UKN1 product detected along the test. On the contrary, the deoxygenation of benzoic acid with hydrogen as the reducing agent leads to a major production of benzaldehyde (from 22 to 60% selectivity with time on stream). Benzene and toluene are also produced in the course of the reaction respectively with 20% and 30% on average. Two things must be highlighted : (i) no toluene is produced

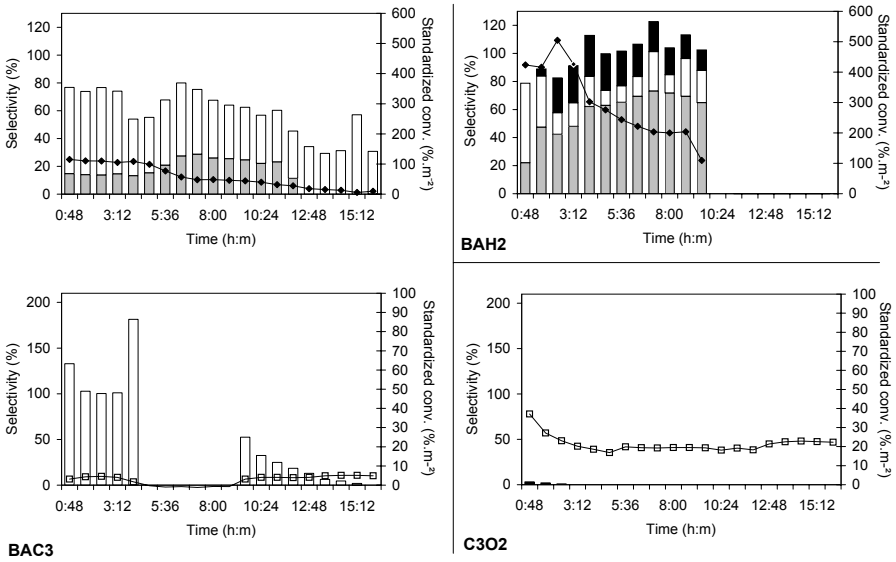

Figure 9.7: Catalytic activity measured on $Bi_2(MoO_4)_3$ during experiment BAC3: conversion of benzoic acid (♦) and selectivities in benzaldehyde (grey), benzene (white) and toluene (black) with time on stream at 723K (upper graphic), conversion of propylene (□) and selectivities in CO (black) and CO_2 (white) with time on stream at 723K (bottom graphic). Experiment BAH2: conversion of benzoic acid and selectivities in benzaldehyde and benzene with time on stream at 723K. Experiment C3O2: conversion of propylene and selectivities in CO and CO_2 with time on stream at 723K.

in the first hour of reaction and (ii) the selectivities to the different products are fluctuating thus making the total selectivity sometimes higher, sometimes lower than 100%.

The comparison of the tests BAC3 (propylene side) and C3O2 shows that : (i) the conversion is about 20% m^{-2} in C3O2 whereas it is only 5% m^{-2} in BAC3, (ii) no activity is observed between the fourth and the ninth hour in BAC3, (iii) CO is the only product in C3O2 and CO_2 is the only product in BAC3, (iv) both in BAC3 and C3O2, an important gap in the carbon balance is observed.

9.3.4.2 Characterization

The BET measurements reveal that the fresh catalyst is 1.97 m^2 g^{-1}. In the reducing conditions, the specific area increases to 4.09 m^2 g^{-1} (BAC3) or 2.76 m^2 g^{-1} (BAH2) whereas in the presence of oxygen (C3O2), this value decreases to 1.08 m^2 g^{-1}.

According to the X-ray diffraction, the fresh catalyst and the catalyst used in the C3O2 experiment correspond to pure $Bi_2(MoO_4)_3$ (JCPDS n°21-0103). After uses in both the BAC3 and BAH2 conditions, the catalysts are reduced to metallic bismuth (JCPDS n°44-1246) and MoO_2 (JCPDS n°32-0671).

XPS analyses are described in table 9.4. Concerning the carbon content, the same observations as those made for the previous molybdates can be done : for the fresh catalyst, the carbon content is about 25%, this value increases to 33.4% after C3O2 but is much higher when the catalyst has been used in the presence of benzoic acid, i.e. 59.1% after BAH2 and 71.6% after BAC3. The Bi/Mo ratio increases according to the following order : fresh<BAH2<C3O2<BAC3. The oxidation level of the molybdenum in each sample is represented in figure 9.8. The surface of the fresh catalyst contains 99% of Mo^{6+} and 1% of Mo^{5+} whereas the catalyst used in C3O2 is fully oxidized. The surface of the catalysts used in the BAC3 and BAH2 tests are reduced since the first one contains 45% of Mo^{6+}, 29% of Mo^{5+}, 26% of Mo^{4+} and the second one is 54% of Mo^{6+}, 18% of Mo^{5+}, 28% of Mo^{4+}.

Table 9.4: Atomic percentage at the surface of $Bi_2(MoO_4)_3$ measured by XPS.

	Sample			
	Fresh	***After BAC3 test***	***After BAH2 test***	***After C3O2 test***
%O	50.4	17.6	27.4	41.2
%C	25.3	71.6	59.1	33.4
%Mo	13.6	5.6	7.2	13.6
%Bi	10.7	5.3	6.1	11.8
O/C	1.99	0.25	0.46	1.23
O/Mo	3.71	3.17	3.81	3.02
Bi/Mo	0.79	0.94	0.84	0.86

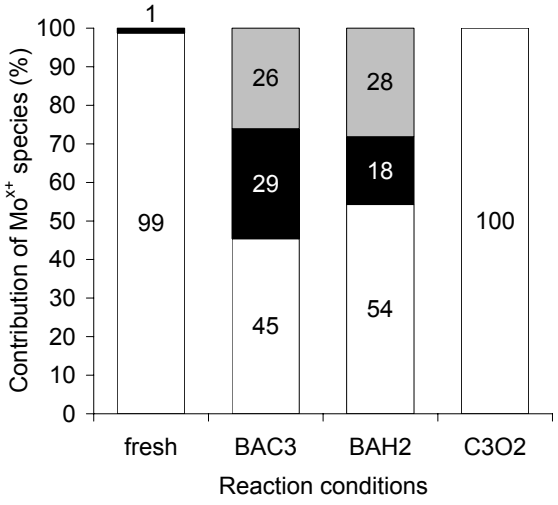

Figure 9.8: Importance of the Mo^{6+}(white), Mo^{5+}(black) and Mo^{4+} (grey) contributions measured by XPS on fresh $Bi_2(MoO_4)_3$, after experiment BAC3, BAH2 and C3O2.

Like $CoMoO_4$, the BAC3 experimental conditions reduces the catalyst more deeply than the BAH2 conditions.

No changes were observed in the oxidation state of Bi before and after all the catalytic experiments.

9.3.5 $Bi_2Mo_2O_9$

9.3.5.1 Catalytic activity measurements

In a general manner, this catalyst behaves like the $Bi_2(MoO_4)_3$ catalyst (figure 9.9), but several observations must be commented. (i) The difference between the benzoic acid conversion obtained in BAC3 and in BAH2 experiments is even more marked for $Bi_2Mo_2O_9$. Whereas the conversion drops in both cases at the end of the reaction, the initial conversion rate is 25% m^{-2} in BAC3 and more than 600% m^{-2} in BAH2. (ii) Like $Bi_2(MoO_4)_3$, the catalyst mainly produces benzene in the presence of propylene and benzaldehyde in the presence of hydrogen but the toluene production (test BAH2) stops after 6 hours while it did not stop in the case of $Bi_2(MoO_4)_3$. (iii) Product UKN1 is also detected in BAC3 experiment but its production is higher at the beginning and the end of the catalytic test while on $Bi_2(MoO_4)_3$, the UKN1 production is rather constant with time on stream and increases after 12 hours of reaction. (iv) Like $Bi_2(MoO_4)_3$, the conversion in the propylene side (BAC3) is very low. Only CO_2 is produced. In C3O2 experiment, the propylene conversion is higher (50% m^{-2}) and CO is main product. CO_2 is produced in trace at the beginning of the catalytic test.

9.3.5.2 Characterization

The specific area of the fresh catalyst is 1.22 m^2 g^{-1}. Once more, after BAC3 and BAH2, it respectively increases to 2.22 m^2 g^{-1} and 1.50 m^2 g^{-1}. The sample recovered after C3O2 experiment has a 1.02 m^2 g^{-1} specific area. Fresh catalyst exhibits typical peaks of the $Bi_2Mo_2O_9$ crystalline phase (JCPDS n° 33-0209) whereas the catalyst corresponding to the C3O2 test is modified to a mixture

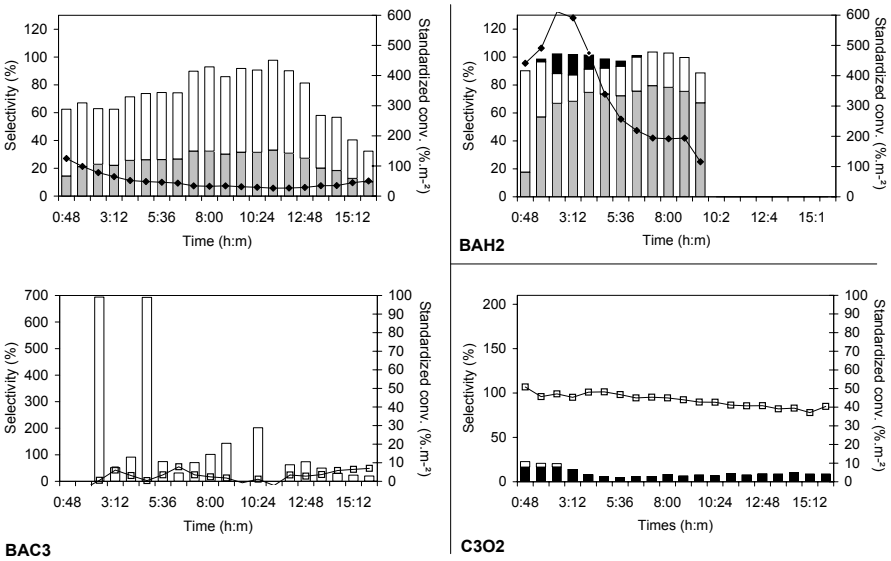

Figure 9.9: Catalytic activity measured on $Bi_2Mo_2O_9$ during experiment BAC3: conversion of benzoic acid (♦) and selectivities in benzaldehyde (grey), benzene (white) and toluene (black) with time on stream at 723K (upper graphic), conversion of propylene (□) and selectivities in CO (black) and CO_2 (white) with time on stream at 723K (bottom graphic). Experiment BAH2: conversion of benzoic acid and selectivities in benzaldehyde and benzene with time on stream at 723K. Experiment C3O2: conversion of propylene and selectivities in CO and CO_2 with time on stream at 723K.

Table 9.5: Atomic percentage at the surface of $Bi_2(MoO_4)_3$ measured by XPS.

	Sample			
	Fresh	***After BAC3 test***	***After BAH2 test***	***After C3O2 test***
%O	50.4	17.6	27.4	41.2
%C	25.3	71.6	59.1	33.4
%Mo	13.6	5.6	7.2	13.6
%Bi	10.7	5.3	6.1	11.8
O/C	1.99	0.25	0.46	1.23
O/Mo	3.71	3.17	3.81	3.02
Bi/Mo	0.79	0.94	0.84	0.86

of $Bi_2(MoO_4)_3$ (JCPDS n° 21-0103) and Bi_2MoO_6 (JCPDS n°21-0102). The catalysts tested in the deoxygenation of benzoic acid reaction, whatever the used reducing agent, are recrystallized to metallic bismuth (JCPDS n°44-1246) and MoO_2 (JCPDS n°32-0671).

The surface composition obtained by XPS is summarized in table 9.5. The carbon content and the Bi/Mo ratio both increase according to the following order : fresh<C3O2<BAH2<BAC3, the experimental Bi/Mo ratio of the fresh catalyst being higher than the theoretical value. The molybdenum at the surface of the fresh sample (figure 9.10) are mainly at the Mo^{6+} oxidation state. Only 1% of Mo^{5+} is found. The catalyst used in C3O2 is fully oxidized while those corresponding to BAC3 and BAH2 are reduced. Indeed, their Mo^{6+} content falls respectively to 63% and 47%. The most reduced catalyst is BAH2 with 29% of Mo^{4+} and 24% of Mo^{5+}. The BAC3 catalyst is less reduced with only 23% of Mo^{4+} and 14% of Mo^{5+}.

No changes were observed in the oxidation state of Bi before and after all

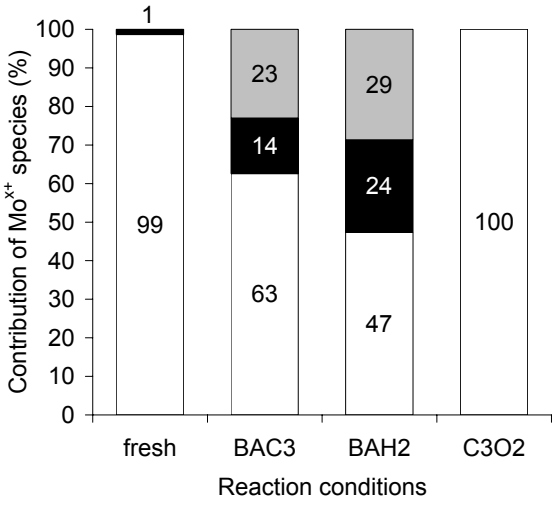

Figure 9.10: Importance of the Mo^{6+}(white), Mo^{5+}(black) and Mo^{4+} (grey) contributions measured by XPS on fresh $Bi_2Mo_2O_9$, after experiment BAC3, BAH2 and C3O2.

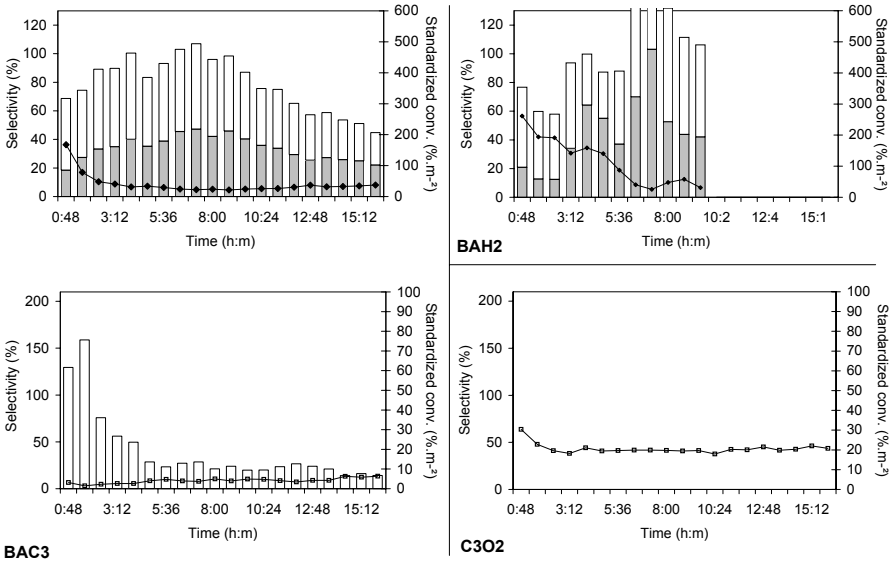

Figure 9.11: Catalytic activity measured on Bi_2MoO_6 during experiment BAC3: conversion of benzoic acid (♦) and selectivities in benzaldehyde (grey), benzene (white) and toluene (black) with time on stream at 723K (upper graphic), conversion of propylene (□) and selectivities in CO (black) and CO_2 (white) with time on stream at 723K (bottom graphic). Experiment BAH2: conversion of benzoic acid and selectivities in benzaldehyde and benzene with time on stream at 723K. Experiment C3O2: conversion of propylene and selectivities in CO and CO_2 with time on stream at 723K.

the catalytic experiments.

9.3.6 Bi_2MoO_6

9.3.6.1 Catalytic activity measurements

Figure 9.11 presents the catalytic performances measured on Bi_2MoO_6 in the experiments BAC3, BAH2 and C3O2. The profiles of activity are quite similar to those measured on $Bi_2Mo_2O_9$ and $Bi_2(MoO_4)_3$. It is noticed that the conversion of benzoic acid is higher in BAH2 test than in BAC3 although in

BAH2 it drops dramatically with time on stream. In both tests, only benzene and benzaldehyde are produced. In BAC3 experiment, the initial conversion of the acid is 166% m^{-2} and is rapidly stabilised to 33% m^{-2}. The ratio between the benzene and benzaldehyde selectivities is rather constant. The carbon balance is uncompleted but one remarks the formation of the UKN1 product. In BAH2 experiment, the production of benzene and benzaldehyde is unstable and fluctuates with time on stream.

On the propylene side in BAC3 experiment, a constant conversion level of about 6% m^{-2} is observed. CO_2 is only detected with a selectivity exceeding 100% at the beginning of the catalytic test but rapidly decreasing to about 25%, leading to a gap of 75% in the total selectivity. In C3O2, the conversion is 30% m^{-2} at initial time then decreases to 22% m^{-2}. No products are detected. A gap of 100% is thus observed in the carbon balance.

9.3.6.2 Characterization

Fresh catalyst exhibits a specific area of 1.32 m^2g^{-1}. After the catalytic tests, it is 1.47 m^2g^{-1} (C3O2), 1.11 m^2g^{-1}(BAH2) and 1.71 m^2g^{-1} (BAC3). The fresh catalyst and that recovered after C3O2 test exhibit the presence of crystalline Bi_2MoO_6 (JCPDS n°21-0102). After the BAC3 test, this phase remains present but some reduced phases appear : namely metallic bismuth (JCPDS n°44-1246) and MoO_2 (JCPDS n°32-0671). Bi_2MoO_6 totally disappears after test BAH2 and recrystallises to metallic bismuth (JCPDS n°44-1246) and MoO_2 (JCPDS n°32-0671).

XPS analyses are described in table 9.6. Concerning the carbon content, the fresh catalyst is about 36.5%. This value decreases to 34.1% after C3O2 but is much higher when the catalyst has been used in the presence of benzoic acid, precisely 61.0% after BAC3 and 75.6% after BAH2. The Bi/Mo ratio increases according to the following order : fresh=C3O2<BAC3<BAH2 and is always higher than the expected value (2). The oxidation level of the molybdenum at the surface of each sample is presented in figure 9.12. The fresh catalyst and that recovered after C3O2 have 99% of Mo^{6+} and 1% of

Table 9.6: Atomic percentage at the surface of Bi_2MoO_6 measured by XPS.

	Sample			
	Fresh	***After BAC3 test***	***After BAH2 test***	***After C3O2 test***
%O	37.3	23.0	16.6	38.4
%C	36.5	61.0	75.6	34.1
%Mo	7.9	4.3	1.6	8.3
%Bi	18.3	11.8	6.2	19.2
O/C	1.02	0.38	0.22	1.13
O/Mo	4.74	5.33	10.12	4.63
Bi/Mo	2.32	2.73	3.79	2.32

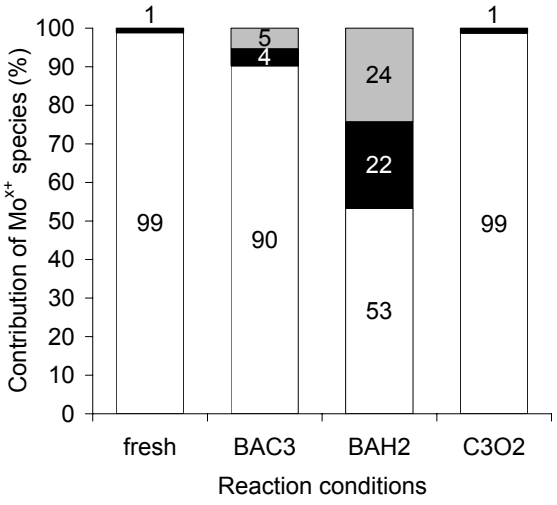

Figure 9.12: Importance of the Mo^{6+}(white), Mo^{5+}(black) and Mo^{4+} (grey) contributions measured by XPS on fresh Bi_2MoO_6 , after experiment BAC3, BAH2 and C3O2.

Mo^{5+}. The surface of the catalysts used in BAC3 and BAH2 is reduced since the first one contains 90% of Mo^{6+}, 4% of Mo^{5+}, 5% of Mo^{4+} and the second one contains 53% of Mo^{6+}, 22% of Mo^{5+}, 24% of Mo^{4+}. Among the three bismuth molybdates prepared and tested, Bi_2MoO_6 is the only one which is not dramatically reduced after BAC3 experiment.

No changes were observed in the oxidation state of Bi before and after all the catalytic experiments.

9.4 Discussion

Due to the big amount of data described in this chapter and in order to facilitate the discussion, the key results are summarized in table 9.7. The reading of such a table allows to directly compare the catalytic activities under the different experimental conditions obtained for the different catalysts. In a first approach, we will thus discuss the effect of the formulation of the molybdates on their catalytic performances in reactions.

Then, in an independent manner, the same results will allow us to compare and to discuss two points relative to, on the one hand, the use of metal molybdates instead of molybdenum suboxides in the coupling reaction, on the other hand, the replacement of molecular oxygen in an oxidation reaction by a more complex oxygen donating molecule, namely the benzoic acid.

9.4.1 Comparison of the catalytic activity

As it is clearly illustrated by the table 9.7, no strong and straightforward tendencies through the different catalysts or the catalytic conditions are visible. However, one can highlight some experimental facts : (i) all the products derived from the benzoic acid, namely benzaldehyde, toluene and benzene are detected at the outlet of the reactor in the presence of propylene as the reducing gas, (ii) the conversion of the acid and the propylene is always lower in the BAC3 experiment than in the corresponding reactions BAH2 and C3O2, (iii) the specific area increases in the presence of hydrogen (experiments BAH2) or

Table 9.7: Main catalytic and characterization results of the BAH2, BAC3 and C3O2 experiments run on metal molybdates.

	Catalytic tests				*Characterizations*											
					BET (m^2g^{-1})				*XRD (main phases detected)*				*XPS (Mo^{6+}, Mo^{5+}, Mo^{4+}) in %*			
						After test			*fresh*	*After test*			*fresh*	*After test*		
	BAH2	*BA*	*BAC3*	*C3*	*C3O2*	*fresh*	*BAH2*	*BAC3*	*C3O2*		*BAH2*	*BAC3*	*C3O2*		*BAH2*	*BAC3*	*C3O2*
$Fe_2(MoO_4)_3$	90↑180	40↓10	benzaldehyde↓	4→	16→												
	benzaldehyde↑	benzaldehyde↑	CO	CO	--					$Fe_2(MoO_4)_3$	$Fe_2Mo_3O_8$	$Fe_2Mo_3O_8$	$Fe_2(MoO_4)_3$	100	48	66	100
	benzene→	benzene→	CO_2	CO_2	CO_2	5.86	9.18	7.90	2.84		MoO_2	MoO_2		0	47	24	0
	toluene↓	**toluene↓**												0	5	10	0
$NiMoO_4$	27→	10→	benzaldehyde→	1→	9→												
	no products	benzene→	CO_2	CO	CO									100	47	84	85
		--		CO_2	CO_2	34.33	65.53	30.33	32.62	$NiMoO_4$	NiO	$NiMoO_4$	$NiMoO_4$	0	16	11	14
														0	38	5	1
$CoMoO_4$	100→	27↓5	benzaldehyde↓	4→	6→												
	benzaldehyde↑	benzaldehyde↑	CO	CO	CO									100	48	80	100
	benzene→	benzene→	CO_2	CO_2	CO_2	11.30	17.67	13.83	13.42	$CoMoO_4$	Co	$CoMoO_4$	$CoMoO_4$	0	39	20	0
	toluene↓	--									$CoMoO_3$	$CoMoO_3$		0	13	0	0
$Bi_2(MoO_4)_3$	450↓100	111↓2	benzaldehyde↓	5→	20→												
	benzaldehyde↑	benzaldehyde↓	--	CO	CO									99	54	45	100
	benzene→	benzene↓	CO_2	CO_2	--	1.97	2.76	4.09	1.08	$Bi_2(MoO_4)_3$	Bi	Bi	$Bi_2(MoO_4)_3$	1	18	29	0
	toluene→	--									MoO_2	MoO_2		0	28	26	0
$Bi_2Mo_2O_9$	600↓120	100↓50	benzaldehyde↓	5→	45→												
	benzaldehyde↑	benzaldehyde↓	--	CO	CO									99	47	63	100
	benzene↓	benzene↓	CO_2	CO_2	CO_2	1.22	1.5	2.22	1.02	$Bi_2Mo_2O_9$	Bi	Bi	$Bi_2(MoO_4)_3$	1	24	14	0
	toluene↓	--									MoO_2	MoO_2	Bi_2MoO_6	0	29	23	0
Bi_2MoO_6	280↓40	166↓33	benzaldehyde↓	6→	30↓22												
	benzaldehyde↑	benzaldehyde↓	--	--	no									99	53	90	99
	benzene↑	benzene↓	CO_2	CO_2	products	1.32	1.11	1.71	1.47	Bi_2MoO_6	Bi	Bi	Bi_2MoO_6	1	22	4	1
	--	--									MoO_2	MoO_2		0	24	5	0

1. BA or C3 conv. (% m^2)
2. Products and tendencies

propylene (experiments BAC3) while it decreases in the presence of oxygen after experiment C3O2 (excepted for $CoMoO_4$ and Bi_2MoO_6), (iv) XPS and XRD analyses indicates that C3O2 conditions do not modify the phase and the oxidation state of the catalysts, (v) the combination of any reducing gas in the deoxygenation of the benzoic acid involves a reduction of both the bulk and the surface of the catalysts.

The first and the last observations will be discussed in detail respectively in the sections 9.4.2 and 9.4.3.

The conversion of benzoic acid and the selectivity to the relative products are not constant with time on stream whatever the catalysts and the reaction conditions. Such a behaviour could be correlated to the reduction undergone by the catalysts and the increase of their specific area with time on stream. In many cases, the reduction of the catalysts involves a decrease of the benzoic acid conversion. But, this is not true for the FeMo catalyst whose conversion increases (BAH2) and for NiMo and CoMo catalysts whose acid conversion remains constant both in the BAH2 and BAC3 experimental conditions. Concerning the selectivities in BAH2 experiment, one notices that the increase of the benzoic acid conversion induces a decrease of the selectivity in benzaldehyde. This is not verified in the BAC3 conditions. No clear tendencies can be found concerning the selectivities in toluene and benzene.

The comparison of the propylene side indicates that the propylene conversion is higher in the presence of oxygen but remains constant in BAC3 and C3O2. Such a stable conversion is in agreement with the stability exhibited by the catalysts used in the presence of oxygen but seems contradictory with the reduction and the increase of specific area undergone by the catalysts used in the presence of benzoic acid (BAC3 experiment). Indeed, in BAC3, the conversion of the benzoic acid and the production of the related products is affected by the reduction of the catalysts whereas the conversion of the propylene in the same reaction seems to be constant. Such a dual behaviour could indicate the presence of two types of catalytic sites. The first one related to the deoxygenation of the benzoic acid would undergo a deactivation

mechanism by the way of a reduction process whereas the second type of active site related to the oxidation of propylene does not seem to be affected by the reduction of the catalysts. If we take into account that the two reactions are linked through a MVK mechanism, this observation involves an unbalance between the oxidation and the reduction part of the cycle. Since the benzene formation is not dependent on the presence of oxygen vacancies at the surface of the catalyst, it must be a critical parameter. We could suggest that the production of benzene is responsible for the high conversion of the benzoic acid but also contributes to the deactivation of the site active in the deoxygenation reaction. Indeed, it is suspected that the benzene formation contributes to the carbon deposit at the surface of the catalyst. As this deactivation does not affect the conversion of propylene in a perceptible way, the oxidation of propylene would contribute to reduce the catalyst.

It is thus difficult to discuss more deeply the raw data relative to the coupling reaction on the molybdate catalysts. However, some new information are revealed concerning the role of the hydrogen species in the coupling reaction and the role of the benzoic acid as an oxidant.

9.4.2 Hydrogen species

Contrary to what was observed on the molybdenum (sub)oxides, the coupling reaction between the deoxygenation of benzoic acid and the oxidation of propylene is possible on the metal molybdates. Indeed, all the products from the benzoic acid, namely benzaldehyde, benzene and toluene, do not remain adsorbed at the surface of the catalysts and are desorbed in the gas phase when the propylene is used as the reducing gas.

In the previous chapter, our first attempts to develop the coupling on Mo_8O_{23} revealed that without the presence of molecular hydrogen in the gas feed, only benzaldehyde was detected at the outlet of the reactor. Whereas a major gap in the total selectivity was observed, we have demonstrated that a large amount of benzoic acid and/or toluene and/or benzene remained irreversibly adsorbed on the catalyst. The only way to release the adsorbed

molecules was to add molecular hydrogen to the feed. Basing our conclusion on this result, we deduced that the hydrogen species coming from the propylene and the benzoic acid were different in reactivity and mobility from the atoms provided by the dissociation of the molecular hydrogen. A clue to explain such a difference was based on the specific electronic properties of molybdenum and oxygen. The present results allow us to deepen the previous discussion.

Many intrinsic characteristics of the catalyst can be responsible for an improved activity depending on the catalytic operating conditions. We will thus compare the specific area and the crystalline phases of the molybdate catalysts used in the presence of hydrogen or propylene in the deoxygenation of benzoic acid. This approach could help to determine why metal molybdates do not need molecular hydrogen to desorb the products coming from the acid.

All the catalysts undergo a modification of their specific area. In a general way, this value increases after BAH2 and BAC3 experiments except for the particular case of the NiMo catalyst after BAC3 which undergoes a significant decrease of the specific area. Comparing the specific area of the samples recovered after BAH2 and BAC3, the tendency is that the increase is larger when the catalyst is used in the presence of hydrogen. Such an increase could be related to the recrystallization of the existing material, in a similar way as demonstrated in chapter 7. It is precisely what happens in these catalytic tests, particularly in the BAH2 tests. Indeed, as shown by XRD, when the deoxygenation of benzoic acid is performed in the presence of hydrogen, all the catalysts are totally transformed to a new crystalline phase without any exception. When the reaction is performed with propylene in the feed, the reduction is much less marked. However, how the extend of these reduction phenomena does affect the selectivity to benzaldehyde, benzene and toluene is unclear. In some cases, the reduction induces an increase or a decrease of the benzaldehyde, toluene and benzene selectivities. But the acid conversion is affected by the very deep reduction state. More precisely, the presence of metallic species seems to induce a dramatic loss of acid conversion both in

BAH2 and BAC3 experiment. This is observed with the three Bi molybdates and the CoMo catalyst. Such a deep reduction appears to be responsible for the loss of 80% of the acid conversion with time on stream. Whatever the reducing conditions, one notices that the reduction is very deep to metallic bismuth and molybdenum dioxide. But, when the reduction is weaker, i.e. when hydrogen is replaced by propylene, the activity is lower but constant with time on stream. This behaviour is normal since to remove one or two oxygen atoms from one benzoic acid molecule, the catalyst must have some oxygen vacancies at its surface. In the case of Bi and MoO_2 phases, it appears that they do not have such oxygen vacancies and are thus inactive to form toluene and benzaldehyde. The reduction of the catalyst and the newly formed crystalline phases are thus not responsible for the removal of the toluene and benzene in the absence of molecular hydrogen since in many cases, a similar reduction and the same crystalline phases appear whatever the reducing gas without inhibiting the desorption of toluene and benzene. We can thus discard any hypothesis involving the reduction state and the crystalline phases as determining factors in the production and desorption of toluene and benzene on metal molybdates.

Since the recrystallization of the active phases is not a determining factor to allow the desorption of toluene and benzene into the gas phase, an alternative way must be explored. A major difference between metal molybdates and molybdenum (sub)oxides is the presence of another metallic element (Fe, Bi, Co, Ni) in the molybdate catalysts. On the one hand, it is reported in the literature that in molybdate catalysts, the second metallic element (Fe, Bi, Co, Ni) is the main actor in the activation of alkenes. Indeed, it allows the removal of the α -hydrogen in the rate-limiting step of the reaction by the activation of the weakest C-H bond [89, 29]. Moreover, it is also well-known that MoO_3 is very selective to acrolein but poorly active because the active centers for activating the propylene, i.e. those able to abstract the α -hydrogen, are scarce [89]. On the other hand, we observed : (i) the toluene and the benzene (or their precursors) remain adsorbed at the surface of Mo_8O_{23} during

the coupling reaction but are desorbed when the propylene is replaced by molecular hydrogen, (ii) benzene and toluene are detected at the outlet of the reactor when the deoxygenation of benzoic acid is performed in the presence of propylene or hydrogen on metal molybdate catalysts.

In the light of these experimental facts, it becomes evident that the molybdates can generate the same hydrogen species in the coupling reaction as the dissociation of molecular hydrogen did both on molybdenum suboxides and metal molybdates. Our results also strongly confirm that the hydrogen atoms allowing the formation of benzaldehyde are different from those allowing the formation of toluene and benzene. We know from the BAC3 catalytic tests (benzoic acid and propylene) on Mo_8O_{23} that the only active hydrogen species is the proton (H^+) coming from the acid function of the benzoic acid. H^+ only participates in the formation of benzaldehyde since, in these experimental conditions, no toluene or benzene are detected. Of course, in the same experimental conditions on molybdates catalysts, the same H^+ species is present since benzaldehyde is also formed. In addition, we observe the formation of toluene and benzene. Thus, an additional hydrogen species is simultaneously formed on metal molybdates. Our hypothesis suggests that this hydrogen species is the α -hydrogen resulting from the activation of the propylene and fixed by the cation (Fe, Bi, Ni, Co). This α -hydrogen is thus missing when the coupling reaction is performed on the molybdenum suboxides : no adequate cations are present to significantly activate the molecules of propylene. A discovery brought by our experiments is the existence of similarities between the intrinsic properties of the α -hydrogen and the hydrogen species formed by the dissociative chemisorption of the molecular hydrogen. Such an affirmation is supported by the fact that in the presence of both hydrogen species, the same products of reaction requiring several hydrogen atom to be formed, namely toluene and benzene, are produced on the molybdate catalysts used in BAC3 and BAH2 experiments. The figure 9.13 illustrates our hypothesis. Two hydrogen species are presented, one coming from the acid function of benzoic acid, the other coming from the

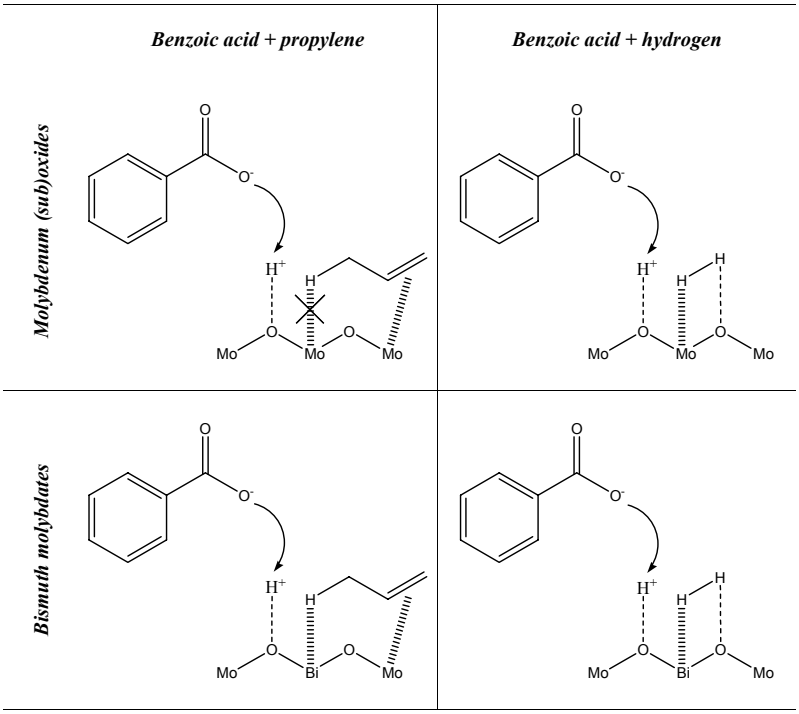

Figure 9.13: Schematic representation of the hydrogen species formed in the presence of molecular hydrogen or propylene on molybdenum (sub)oxides or bismuth molybdates. Hashed lines suggest a stabilisation function while dashed lines indicate a bond in formation.

α -hydrogen of propylene (BAC3) or from the molecular hydrogen (BAH2). Our hypothesis is supported in the literature by Haber et al. [89], Bruckman et al. [90] or Grasselli et al. [12] who claimed that the abstraction of the first α -hydrogen takes place on Bi^{3+}, Co^{2+} or Ni^{2+} leading to the formation of an allylic species [50, 90] whereas the molybdenum atoms allow (i) the stabilisation of the hydrocarbons and (ii) the abstraction of the second hydrogen atoms from the propylene (see 1.1 on page 16). The molybdenum atoms are thus essential to allow the insertion of oxygen atoms and to produce the partially oxygenated compounds but are poorly efficient to activate the propylene. The determining factor to explain the difference in the activation of propylene between the molybdenum (sub)oxides and the metal molybdates could be, according to our hypothesis, a steric effect. Indeed, the dissociation of a small molecule like the molecular hydrogen occurs on the Bi, Ni and Co atoms but also on the Mo atoms. But, when the molecule is longer (propylene), its activation seems only possible on Bi, Ni and Co cations. Our suspicion is that if the molybdenum site is not at an adequate distance from the cationic site, i.e. Bi^{3+}, Co^{2+} or Ni^{2+}, there is no stabilisation [12] and thus no activation of the propylene. Such an inadequate distance can be the cause of the absence of activation of α -hydrogen when there is only molybdenum atoms at the surface of the catalyst. To check the validity of such a hypothesis, we have built a model to measure the inter-atomic distance between the molybdenum and the oxygen atoms in the molybdates and molybdenum oxides. According to this model, the Mo-O distances in bismuth molybdate ($Bi_2(MoO_4)_3$) are 1.89 $\dot{A}$ and 2.32 $\dot{A}$ whereas the corresponding distances in MoO_3 are respectively 1.89 $\dot{A}$ and 2.08 $\dot{A}$. Thus, a weak difference exists and could be responsible for the absence of activation of the α -hydrogen on molybdenum (sub)oxides with the consequence that no hydrogen species is present to allow the formation of the toluene and the benzene.

If this theory is acceptable considering the molybdates containing Bi^{3+}, Co^{2+} or Ni^{2+} cations, the particular case of $Fe_2(MoO_4)_3$ is slightly different. Indeed, Fe^{3+} cation does not play the same role as Bi^{3+}, Co^{2+} or Ni^{2+} [50, 90].

Fe^{3+} does not extract itself the α -hydrogen like Bi^{3+} in $Bi_2(MoO_4)_3$ does but, it indirectly contributes to its activation. In fact, when some Fe^{3+} are added in the structure of MoO_3 by impregnation, the lattice parameters are modified in such a way that the mobility of oxygen lattice is improved [90, 91]. This improvement is related to the modification of the inter-atomic distance between two neighbour molybdenum atoms. This inter-atomic distance allows the activation of propylene by a molybdenum atom while another molybdenum site stabilizes the newly formed allylic species. This reinforces our hypothesis based on some structural considerations to explain the formation of benzene and toluene in the absence of molecular hydrogen on the molybdate catalysts.

9.4.3 Benzoic acid as an oxidant

The comparison of all the catalysts used both in the deoxygenation of benzoic acid in the presence of propylene (BAC3) and the oxidation of propylene with oxygen (C3O2) highlights some major differences in the propylene side : (i) the conversion of propylene is always lower in the BAC3 experiment, (ii) the ratio CO/CO_2 is always very different between the two experiments, (iii) a particular case of this is on bismuth and cobalt molybdates, no CO is produced in BAC3 experiment whereas a large quantity is detected in C3O2 tests, (iv) total selectivity in the coupling reaction often exceeds 100% at the beginning of the test then it falls down with time on stream. But some similar catalytic behaviours are noticed on the propylene side : (i) the conversion of propylene is constant with time in both experiments, (ii) only CO and CO_2 are detected, (iii) there is a gap in the total selectivity.

The corresponding characterizations also reveal some interesting information which could help to compare the behaviour of the catalysts in the two sets of reaction conditions. Some differences are noticed : (i) the carbon content is always higher in the samples corresponding to BAC3 than in those corresponding to C3O2, (ii) the specific area of the catalysts recovered after BAC3 increases whereas for those recovered after C3O2 it decreases in most of the cases, (iii) the crystalline phase is modified after test BAC3, not after

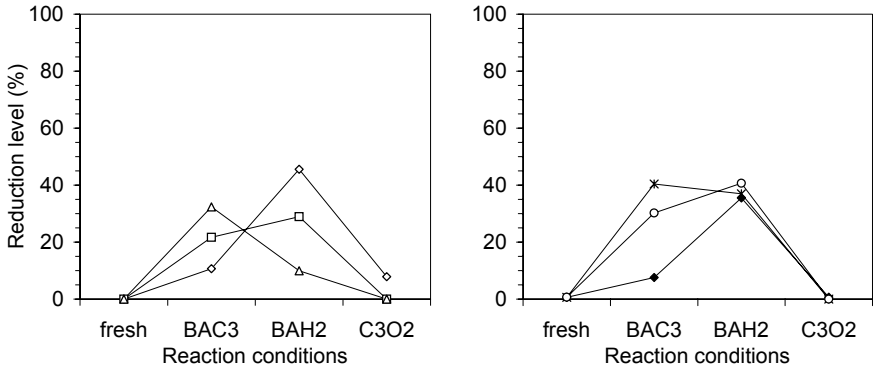

Figure 9.14: Reduction level of the molybdate catalysts, $NiMoO_4$ (◊), $Fe_2(MoO_3)_4$ (□), $CoMoO_4$ (△), $Bi_2(MoO_4)_3$ (×), $Bi_2Mo_2O_9$ (○) and Bi_2MoO_6 (♦) fresh sample and recovered after BAC3, BAH2 and C3O2 experiments.

C3O2, (iv) the surface of the catalysts is more reduced after BAC3 than after C3O2 experiments. Thanks to these data, we will discuss the benzoic acid efficiency as an oxidant agent in the oxidation of propylene. Next, we will discuss the carbonaceous content and the catalytic activity.

The oxidant properties of the benzoic acid are crucial if we remember the aim of the coupling, namely to probe the oxygen vacancies formed during the oxidation of propylene by the deoxygenation of benzoic acid. To evaluate the oxidation strength of the benzoic acid, we calculated the reduction level according to the equation 9.1 applied to the XPS results.

$$\text{Reduction level } (RL) = \frac{Y}{2} + Z \tag{9.1}$$

Where Y and Z respectively represent the atomic percentage of Mo^{5+} and Mo^{4+} detected at the surface of the samples by XPS.

A fully oxidized MoO_3 exhibiting only Mo^{6+} at the surface will have a reduction level of 0 while a pure MoO_2 only presenting Mo^{4+} at the surface will have a RL of 1. Results are presented in figure 9.14. It is clear that the

surface of all the catalysts is reduced after the coupling reaction and remains fully oxidized after C3O2 experiment. The exception is $NiMoO_4$ for which the molybdenum reduction level is still the same after BAC3 and C3O2 catalytic tests. If we consider that the coupling reaction follows a classical Mars & Van Krevelen cycle, the global observation of the occurrence of a reduction in BAC3 (but not in C3O2) suggests that the re-oxidation step by the benzoic acid is less efficient than the re-oxidation by the molecular oxygen. This could also be reinforced by the fact that the conversion level of propylene in BAC3 experiment is lower than in C3O2 experiment. But this could be easily explained. Indeed, both in BAC3 and C3O2, the oxygen and benzoic acid concentration are about 600 ppm. When oxygen is the oxidant gas, the totality of the converted oxygen is used to oxidize the catalysts and thus participates in the MVK cycle. In the BAC3 conditions, the concentration of benzoic acid is about 600 ppm but half of this amount is, in most of the cases, converted into benzene and thus does not participate in the oxidation step of the catalyst. Moreover, a quantity of benzoic acid (although small and in several cases null) is converted into benzaldehyde and thus provides only one oxygen atom per benzoic acid molecule while molecular oxygen always gives two oxygen atoms. Moreover, a rough thermodynamic estimation of the transformation of the molecular oxygen or the benzoic acid by the HSC software [92] reveals very different reaction enthalpies (equations 9.3 and 9.2).

$$\begin{gathered} O_{2\,ads} + 2e^- \rightleftharpoons 2O^-_{ads} \\ \Delta H_{723K} = -862.07kJ \end{gathered} \tag{9.2}$$

$$\begin{gathered} C_6H_5COOH + e^- \rightleftharpoons C_6H_5COH + O^-_{ads} \\ \Delta H_{723K} = 49.00kJ \end{gathered} \tag{9.3}$$

The dissociation reaction at 723K of the molecular oxygen adsorbed on a solid surface[1] is clearly exothermic and thus favoured while the removal of only

[1] we have considered O^- because this oxygen species is often considered to be the species responsible for the total oxidation. In our system, we only detect CO and CO_2.

an oxygen atom from the benzoic acid is slightly endothermic. Thus, the dissociation enthalpy is not in favour of the use of benzoic acid as a efficient oxidant because it requires higher energy to be activated at the surface of the catalysts and whereas it contains two oxygen atoms, only one is used most of the time. These two factors contribute to lower the reaction rate by limiting the re-oxidation step of the MVK mechanism leading to a low level of propylene conversion. If the conversion of propylene is low, then the benzoic acid conversion must be low too. Indeed, a lower conversion of propylene induces a scarce formation of oxygen vacancies. The entire Mars & Van Krevelen cycle is thus running slowly.

In addition to the oxidant properties and the conversion level of the propylene, a noticeable difference was highlighted by XPS between BAC3 and C3O2 experiments . Indeed, the comparison of the carbon content after the two catalytic tests reveals a high level of carbon when the catalysts are tested in the presence of benzoic acid whereas in the presence of oxygen, the carbon level is still in the range commonly observed. Several experimental facts can explain this observation. (i) Since the benzoic acid is less oxidant than the molecular oxygen, some coke formation from the conversion of propylene cannot be avoided. Indeed, in the conventional system, i.e. propylene and oxygen, the coke can be burned by the oxygen leading to a lower carbon content at the surface of the molybdate catalysts. (ii) When the catalysts are tested in the coupling reaction, the benzoic acid can contribute to the carbon deposit at the surface of the catalyst.

The atomic percentage of carbon at the surface of the catalysts recovered after BAH2 clearly indicates that the deoxygenation of benzoic acid in the presence of hydrogen largely contributes to the deposit of carbon. This carbon deposit could not result from the presence of benzaldehyde, toluene and benzene adsorbed at the surface of the molybdate catalysts since it was already demonstrated that the presence of a second cation in the catalysts allows their desorption in absence of molecular hydrogen. Even if we cannot totally exclude this irreversible adsorption, the contribution of the benzaldehyde,

toluene and benzene in the carbon content is surely negligible because, in most of the cases, the totality of the converted acid is recovered at the outlet of the reactor since the total selectivity in the acid side (BAC3 and BAH2 experiments) is near of 100%. So, where does the carbon come from? One solution remains unexplored : the formation of benzene from the benzoic acid involves the loss of one carbon atom. What does this carbon become? According to the proposed mechanism describing the formation of benzene, a radical-like breaking of the bond between the aromatic cycle and the acid function occurs without the participation of any oxygen vacancy [59]. Nothing is described in the literature on what happens to the acid function adsorbed on the catalyst. Our XPS results strongly suggest that the acid function remains adsorbed in the catalyst contributing to increase the carbon content. Whereas this hypothesis could seem evident, it will be discussed more deeply in the chapter 10 thanks to some further observations. However, it is evident that the carbon deposit at the surface of the catalyst contributes to the deactivation of the active sites. It would be quite fast since we generally observed a drop in the conversion of benzoic acid after one or two hours of reaction.

9.5 Conclusion

This chapter gives some clues on the behaviour of the molybdate catalysts in the coupling between the deoxygenation of benzoic acid and the oxidation of propylene. We demonstrate that on the metal molybdates, the molecular hydrogen is not necessary to allow the desorption of the products coming from the benzoic acid. On the contrary to what was observed on molybdenum suboxides, the hydrogen species needed for the desorption of the product is produced on the molybdate catalysts thanks to the presence of a second cation (Bi^{3+}, Co^{2+}, Ni^{2+} and Fe^{3+}). This hydrogen species would have similar properties as the atomic species coming from the dissociative chemisorption of molecular hydrogen.

Globally, the activity in the coupling reaction is lower in terms of both

benzoic acid and propylene conversions than in the respective reactions in the presence of hydrogen or oxygen. Indeed, benzoic acid has a lower oxidative capacity than molecular oxygen in the oxidation of propylene and, similarly, propylene is less reducer than molecular hydrogen for the deoxygenation of benzoic acid. Moreover a deposition of carbonaceous material on the catalyst could lead to some selective deactivation phenomena. Nevertheless, the coupling reaction, as designed, seems to be possible on metal molybdate catalysts although with a lower rate.

Further investigations are needed to demonstrate that a MVK cycle occurs in the coupling between the deoxygenation of benzoic acid and the oxidation of propylene.

Chapter 10

Evidence in favour of the coupling[1]

Abstract

An innovating coupling between the deoxygenation of benzoic acid and the oxidation of propylene was set up and gave new information about the mechanism involved in the oxidation of propylene on a Co-Mo based oxide catalyst. The production of CO_2 during the catalytic reaction is bound to the formation of benzene and benzaldehyde. The first case corresponds to the removal of the carboxyl function of the benzoic acid. The second case is the evidence that benzaldehyde and products coming from the oxidation of propylene are formed on the same catalytic sites during the Mars and van Krevelen cycle. In this cycle, the oxygen atoms used for the oxidation come from the benzoic acid by the intermediate of the oxide lattice. In particular, it has been demonstrated that the oxidation of propylene involves lattice oxygen atoms far from each other in such a way that the reaction leaves single oxygen vacancies at the surface of the catalyst.

[1] results published in Journal of Molecular Catalysis A : Chemical, 237 (2005) 9-16.

10.1 Introduction

The previous chapter demonstrated that the coupling between the deoxygenation of benzoic acid and the oxidation of propylene was possible on the molybdate catalysts without irreversible adsorption of the benzoic acid based products. However, this did not provide any real evidence that the coupling reaction is dictated by a MVK mechanism. This chapter is devoted to demonstrate that, like the conventional oxidation of propylene in the presence of oxygen, the coupling reaction follows the MVK mechanism. Some evidences are brought thanks to a detailed study performed on the cobalt molybdate.

The well-known cobalt molybdate catalysts are very active and exhibit high resistance to poisoning and deactivation. Some authors have studied cobalt molybdates in other processes like selective oxidation reactions [29], especially in the selective oxidation of propane [93, 94, 95], isobutene [96, 97], propylene or acrolein [29, 98]. Like Ni-Mo, Bi-Mo or Fe-Mo oxide catalysts, the good activity shown by these phases is not well understood yet. Several explanations are based on the oxidation state of the surface and/or of the bulk [99, 42], some crystallographic considerations [100, 101] or some complex mechanisms involving atom vacancies [50, 98, 102].

Our work contributes to highlight some molecular aspects involved in the good activity exhibited by the cobalt molybdate catalysts.

10.2 Experiments

10.2.1 Preparation of the catalysts

Co molybdate was prepared by the "citrate" method following the protocol described in section 3.2. The ratio between Co and Mo precursors was determined in such a way to obtain $CoMoO_4$ as the final phase.

10.2.2 Catalytic activity measurements

Three different catalytic experiments were realized at atmospheric pressure in a fixed bed micro-reactor. (i) In experiment BAC3, the reaction feed contained 635 ppm of benzoic acid (Aldrich, 99%) and 318 ppm of propylene (Indugas, 2.01% Vol. in He). Helium (Indugas, 99.996%) was the gas balance. (ii) In experiment BA, the reaction feed contained 635 ppm of benzoic acid (Aldrich, 99%) diluted in helium (Indugas, 99.996%) as the gas balance. (iii) In experiment C3, the reaction feed contained only 318 ppm of propylene (Indugas, 2.01% Vol. in He) in helium (Indugas, 99.996%) as the gas balance.

The total flow was adjusted to 100 ml min^{-1}. 300 mg of catalyst with a granulometry of 100-315 μm were used. For all the catalytic conditions, the performances were measured at 723K for 16 hours.

Raw data were analysed by statistical methods using Pearson product-moment correlation coefficient (eq. 10.1) and a commercial software (STATISTICA).

$$r = \frac{(X - \overline{X}).(Y - \overline{Y})}{N.\sigma_X.\sigma_Y} \tag{10.1}$$

where $\overline{X}, \overline{Y}$ are the mean, σ_X, σ_Y are the standard deviations and N the number of considered samples.

According to this mathematical definition (eq. 10.1), r will be equal to zero if no relation can be found between two variables X and Y. A negative value means that when X or Y increases, Y or X decreases at the same time. On the contrary, a positive value means that when X or Y increases, Y or X also increases.

10.2.3 Characterization

The catalysts were systematically characterized before and after catalytic tests by BET, X-ray diffraction (XRD) and photoelectron spectroscopy (XPS) techniques. Mo 3d, Co 2p, O 1s and C 1s bands and survey spectra were

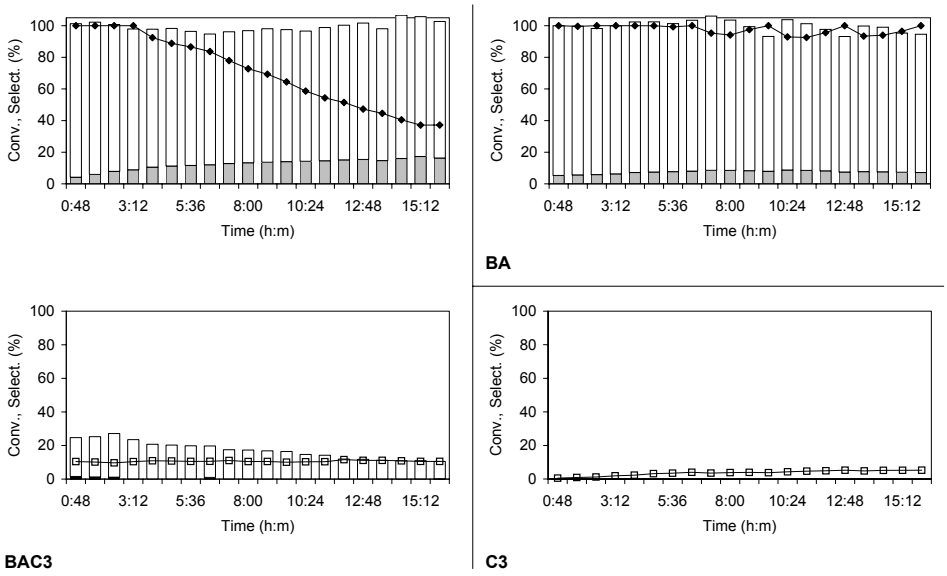

Figure 10.1: Experiment BAC3: Conversion of benzoic acid (♦) and selectivities in benzaldehyde (grey) and benzene (white) with time on stream at 723K (upper graphic), conversion of propylene (□) and selectivities in CO (black) and CO_2 (white) with time on stream at 723K (bottom graphic), Experiment BA: conversion of benzoic acid and selectivities in benzaldehyde and benzene with time on stream at 723K, Experiment C3: conversion of propylene and selectivities in CO and CO_2 with time on stream at 723K (experiment C3).

recorded by XPS following the procedure described in section 5.

10.3 Results

10.3.1 Catalytic activity measurements

Figure 10.1 describes the performances measured for the deoxygenation of benzoic acid and the oxidation of propylene in the experiment BAC3. Concerning the benzoic acid side, initial conversion is 100% and decreases

with time on stream to stabilize at 40% after 15 hours of reaction. Two products of reaction are identified : benzaldehyde and benzene, corresponding respectively to 3% and 97% of selectivity in the first hour of reaction. The selectivity to benzaldehyde increases with time on stream to the detriment of the benzene production and reaches 18% in the last hour of reaction. Toluene was not detected during the whole duration of the catalytic test. The total selectivity in aromatic compounds is thus complete considering the error due to the GC apparatus.

The evolution of the activity measured at the same time for the oxidation of propylene is totally different : a conversion of 10% is observed and remains constant during the whole reaction. Concerning the selectivities, some important modifications between the different products are observed. After the first hour of reaction, selectivity to CO_2 decreases from 23% to 10% in 16 hours. CO is only detected in traces. For the propylene side, the carbon balance could not be reached but no additional products are detected.

The catalytic results of experiment BA are described in Figure 10.1. This catalytic test is performed only with benzoic acid in the gaseous feed. Until the sixth hour of reaction, the conversion is maximum. After that, some oscillations between 100 and 95% of conversion are observed. Three products of reaction are formed : benzaldehyde and benzene, respectively with 8 and 92% of selectivity (on average) and CO_2 with a rather constant concentration of 35 ppm. No other products are detected.

Figure 10.1 also shows the results obtained in the conditions of experiment C3, i.e. with propylene in the feed but without benzoic acid. The conversion of propylene is low (less than 10%) and increases slightly with time on stream. No acrolein, CO, CO_2 nor any unknown product are detected with the direct consequence that carbon balance is not reached. But, remembering that the detection threshold of acrolein is 2000 ppm and as our GC apparatus is able to detect concentrations of CO_x as low as 35 ppm, one could assume that the selective product is formed with a selectivity near 100%.

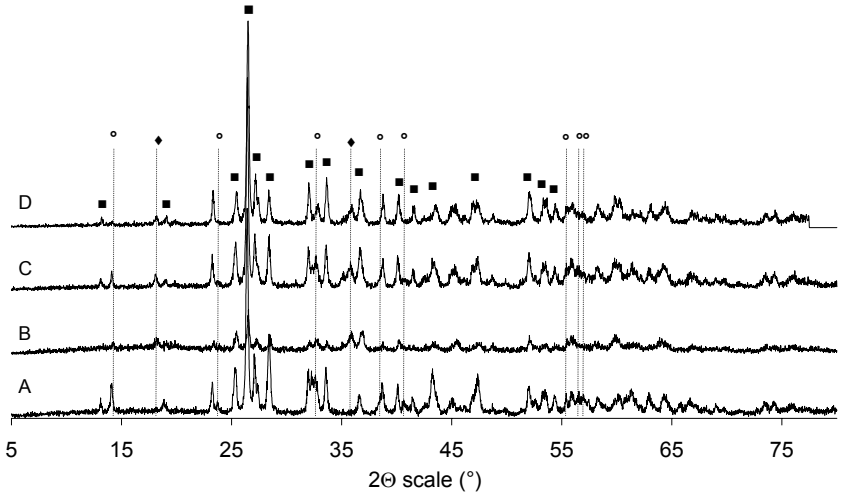

Figure 10.2: X-ray diffractograms of (A) fresh Co-Mo oxide, (B) Co-Mo oxide used in experiment BAC3, (C) Co-Mo oxide used in experiment BA, (D) Co-Mo oxide used in experiment C3. ■ indicates X-ray peaks attibuted to $CoMoO_4$ (JCPDS n°21-0868). ◯ indicates X-ray peaks attributed to $CoMoO_4$ (JCPDS n°25-1434). ♦ indicates X-ray peaks attributed to $CoMoO_3$ (JCPDS n°21-0869). Peaks not marked are not identified or not reported in the database beyond 2θ=62°.

10.3.2 Characterization

The specific area of the fresh catalyst is 11.3 m^2g^{-1}. After experiments BAC3, BA and C3, these values respectively increase to 13.8 m^2g^{-1}, 13.1 m^2g^{-1} and 12.1 m^2g^{-1}.

X-ray diffraction analysis (Figure 10.2) performed on fresh Co-Mo oxide catalyst reveals the presence of two crystallographic phases corresponding to $CoMoO_4$ (JCPDS n°25-1434) and $CoMoO_4$ (JCPDS n°21-0868). These two phases only differ by the cell sizes. In addition to those phases, two peaks attributed to $CoMoO_3$ (JCPDS n°21-0869) are detected in the three samples recovered after experiments BAC3, BA and C3.

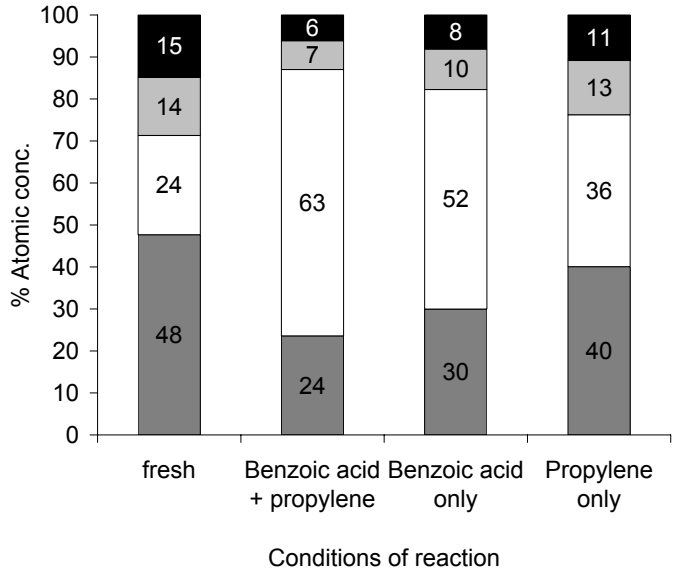

Figure 10.3: Atomic concentrations measured by XPS in fresh and samples corresponding to BAC3, BA and C3 experiments. O is dark grey, C is white, Mo is light grey and Co is black.

Atomic concentrations measured by XPS are reported in Figure 10.3. The histogram shows an important increase in the carbon content at the surface of the used catalysts which makes inconsistent the calculation of any elemental ratio relative to carbon or oxygen. Co/Mo atomic ratios are in slight diminution in all the samples recovered after catalytic test : 0.85 (BAC3), 0.80 (BA), 0.85 (C3) against 1.07 in the fresh catalyst. Figure 10.4 gives the importance of the different Mo^{n+} detected for the fresh catalyst and after the different tests. Compared to the fresh material, the catalyst recovered after the test with propylene only (experiment C3) is the most reduced one. The sample recovered after the test with benzoic acid only (experiment BA) is the most oxidized one after the fresh catalyst. The sample recovered after the test in presence of both benzoic acid and propylene (experiment BAC3) presents an

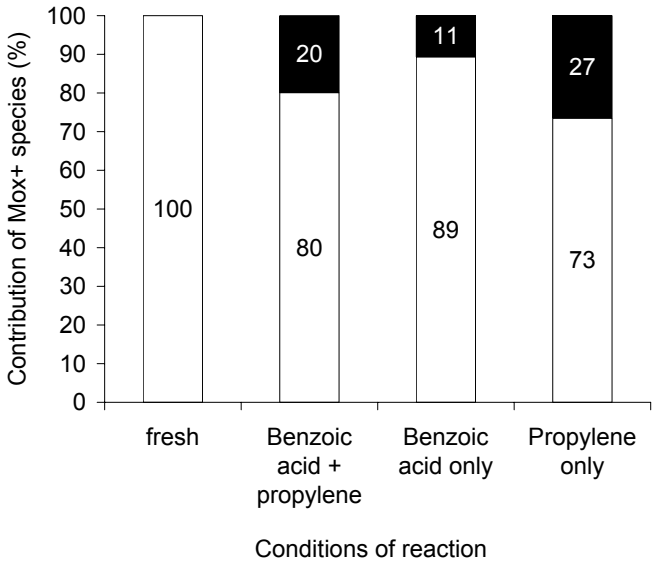

Figure 10.4: Importance of the Mo^{6+}(white), Mo^{5+}(black) and Mo^{4+} (grey) contributions measured by XPS in fresh material and samples corresponding to BAC3, BA and C3 experiments.

intermediate reduction degree between the BA and C3 samples.

10.4 Discussion

Let us discuss the primary available results. Thanks to the probe reaction mechanism, the detection of benzaldehyde formed during the deoxygenation of benzoic acid on Co molybdate catalyst and the absence of toluene (both observed in both tests BA and BAC3) reveal that only single oxygen vacancies are present at the surface of the catalyst. However, the large amount of benzene also indicates that these single oxygen vacancies are scarce at the surface of the Co molybdate.

Besides, the BA experiment highlights a small and constant production of CO_2, namely 35 ppm. In a first approach, one could discuss the relevance of assigning the origin of this carbon dioxide to the total oxidation of benzoic acid. This hypothesis would be supported by the fact that a slight reduction of the catalyst corresponding to the experiment BA is detected by XPS. This reduction would be due to the fact that the envisaged total oxidation of benzoic acid proceeds without oxygen in the feed, i.e. by using the O_L (lattice oxygen) of the catalyst only. If a total oxidation reaction occurs, one should observe : (i) a diminution of the total concentration in aromatic compounds in the outlet flow, i.e. a total selectivity in aromatic compounds of less than 100%, (ii) a concentration of CO_2 at the outlet of the reactor corresponding to the generation of 7 molecules of CO_2 per molecule of benzoic acid burned, (iii) the probable presence of other products from (almost) total oxidation, namely CO. None of these three expectations were validated by our experiments. Therefore, although it cannot be absolutely discarded, one must admit that the total oxidation of benzoic acid, if it occurs, is marginal compared to the formation of benzaldehyde and benzene. This view matches well with the observations concerning the formation of benzaldehyde. Namely, starting from a fully oxidized surface of Co molybdate (see XPS), the catalyst is not able to produce benzaldehyde as it misses O_V (oxygen vacancy). The total oxidation

of benzoic acid would be responsible for the creation of some scarce single oxygen vacancies, which are detected by the probe reaction accordingly to the observed selectivity to benzaldehyde in experiment BA.

Focusing on the second side of the coupling reaction, namely the propylene oxidation, the available literature reports Co molybdate as an active and very selective catalyst in the selective oxidation of propylene [29, 91, 98]. In the experiment BAC3 and C3, whereas a significant conversion of propylene is measured, no selective products are detected and an important lack of selectivity is observed. There are two possible reasons to explain such a major lack in the carbon balance : (i) the technical limitation exposed above makes impossible the detection of the formed acrolein and (ii) a part of the propylene and/or acrolein contributes to form a coke deposit at the surface of the catalyst. The first cause is unfortunately a certainty verified by the measurement of the GC detection threshold of the acrolein. The second reason cannot be discarded either : acrolein and/or propylene can be precursors of coke. Indeed, XPS results show that the carbon content increases in both BAC3 and C3 tests, to 63% and 36% respectively whereas the carbon content at the surface of the fresh catalyst is only 24%. However, one cannot conclude that no acrolein is formed in our catalytic conditions since the carbon increase observed in the case of the C3 experiment is acceptable for a catalyst used in a selective oxidation reaction and releasing the oxidation products. Moreover, the noticeable difference of the carbon contribution between C3 and BAC3 indicates that the benzoic acid, when it is present, is involved in the coke formation. The arguments to discuss this point will be provided later in the text.

The raw data discussed until now do not show any direct and concluding information to reach our objectives. But, by refining these results, major new evidences for the feasibility of the coupling through a MVK mechanism are highlighted.

Refined data are summarized in Figures 10.5 to 10.7. Yield to CO_2 is plotted as a function of the benzoic acid conversion. By applying a linear

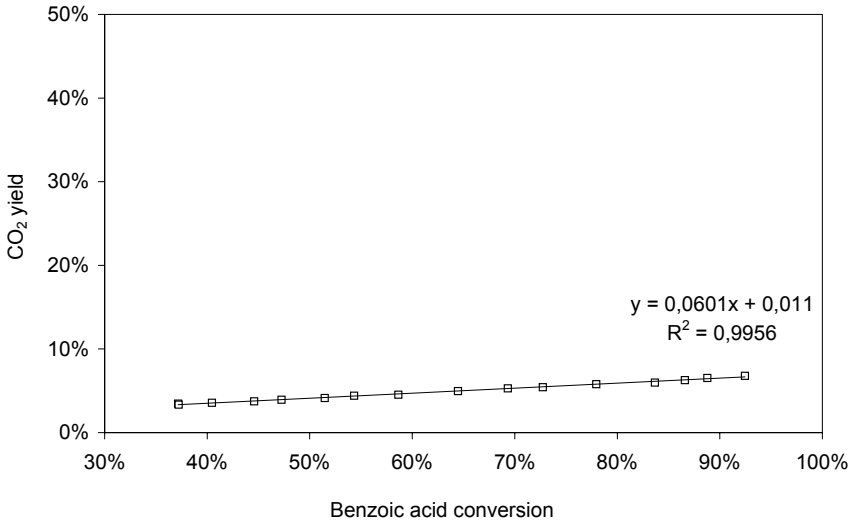

Figure 10.5: CO_2 yield as a function of benzoic acid conversion.

regression to the available points (R^2=0.99), it appears that a correlation binds the benzoic acid conversion with the formation of CO_2. A previous part of this discussion established that benzoic acid is only marginally burned, whereas Figure 10.1 shows that benzoic acid is mainly converted to benzene and benzaldehyde. Taking this into account, the correlation between benzoic acid and carbon dioxide thus suggests that at least one relation must exist between benzene and CO_2 and/or between benzaldehyde and CO_2. Four relations are evaluated by the Pearson product-moment correlation coefficient method (Table 10.1). According to the p-level, all are significant. Among these, we notice that two positive correlations exist between the CO_2 concentration and the benzaldehyde or benzene concentrations. A more surprising negative but however significant correlation is found between CO_2 and propylene. To visualize the relations, data are plotted in Figure 10.6 which presents the benzene and benzaldehyde concentrations in the outlet feed as a function of the CO_2 concentration. The linear correlations obtained between CO_2 and

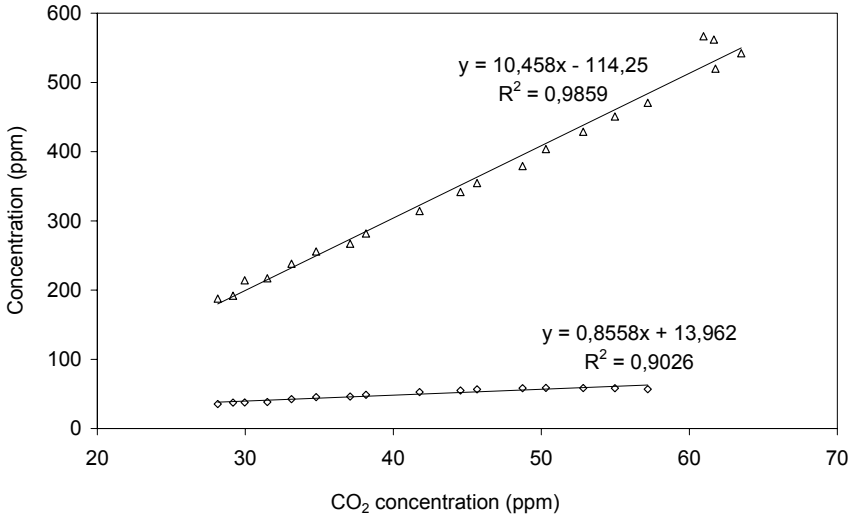

Figure 10.6: Concentration of benzene (△) and benzaldehyde (◇) as a function of the CO_2 concentration.

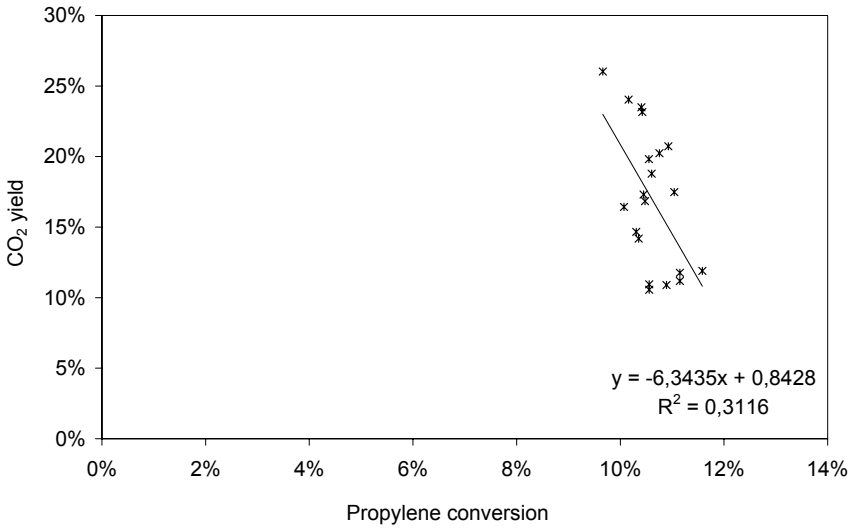

Figure 10.7: CO_2 yield as a function of propylene conversion.

Table 10.1: Pearson product-moment correlation coefficients at p-level < 0.05 (N=21) between the CO_2 concentration and the benzoic acid, propylene, benzaldehyde and benzene concentrations. Bold and Italic values mark the significant coefficients according to the p-level.

Pearson product-moment correlation coefficients (**r**)	**CO_2 concentration**
Benzoic acid conc.	***-0.99***
Propylene conc.	***-0.57***
Benzaldehyde conc.	***0.59***
Benzene conc.	***0.99***

benzene/benzaldehyde are both very strong (R^2=0.98 and 0.90 respectively) and can then be considered. The R^2 of the respective correlation function indicates that the dependence between CO_2 and benzene or benzaldehyde is clearly the reflect of a specific mechanism of reaction. However, the fact that the corresponding angular coefficient for the two correlations is different indicates that the mechanism of reaction describing the formation of the two products are different. In order to elucidate the nature of these different mechanisms, it is crucial to discuss the origin of the CO_2.

After a previous part of this discussion has established that CO_2 is only marginally coming from the total oxidation of benzoic acid, two hypotheses must be examined : (i) CO_2 could be the product formed by the removal of the carboxylic function from the benzoic acid when benzene is generated, (ii) CO_2 could be the total oxidation product from propylene. Further correlations shown in Figure 10.6 and 10.7 permit us to elaborate an answer.

Concerning the relation between the benzene and the CO_2, a dependence is clearly significant regarding the angular coefficient of the linear regression (10.28). It can be assumed that carbon dioxide is formed co-linearly with the benzene. CO_2 would be the result of the carboxylic group removed from the

benzoic acid. Such a hypothesis is not in contradiction with the literature. Indeed, it is proposed that benzene is formed by a radical-like rupture of the bond between the aromatic cycle and the acidic function of the benzoic acid molecule [22]. Nevertheless, this proposed mechanism is subjected to one condition : benzoic acid may lose its acidic proton and may be adsorbed on the catalyst in its benzoate form. No information are available on what happened to the acidic function but our results suggest that the acidic function is transformed into one CO_2 molecule. That transformation is stoichiometric but the desorption of CO_2 would not be quantitative as shown by Figure 10.6 : there is only about one CO_2 molecule released for ten molecules of benzene whereas it could be expected that one CO_2 molecule would be released for each molecule of benzoic acid transformed to benzene. Experiment BA demonstrates that fact. Whereas a constant benzene concentration of about 570 ppm is measured, we only detect 35 ppm of CO_2 at the same time. It means that more than 90% of the CO_2 coming from the benzene formation remains at the surface of the catalyst and contributes mainly to the carbonaceous deposit detected by XPS.

The second hypothesis for the CO_2 formation is the total oxidation of propylene. Figure 10.7 presents the yield to CO_2 as a function of propylene conversion. Although no strong correlation could be found, it is sure that a relation exists between the two compounds as demonstrated in Table 10.1. The poor correlation can be explained by the small range of propylene conversion which induces an important inaccuracy on the chromatogram integration. The surprising negative coefficient of that linear relation (-6.34) is a mathematical artifact which suggests that CO_2 is mainly coming from the benzene formation and only to a lower extent from the propylene reaction. The part of CO_2 coming from the decarboxylation of benzoic acid cannot be differentiated of the CO_2 coming from the total oxidation of propylene. Since the negative correlation calculated between the propylene and the benzene concentrations (r=-0.45) is significant, it fully explains why the coefficient in the linear relation between propylene and CO_2 is negative.

At this point of the discussion, it could be interesting to summarize the data: (i) a marginal part of CO_2 comes from the total oxidation of benzoic acid, (ii) CO_2 formation is bound to the benzaldehyde and benzene synthesis, (iii) a part of the produced CO_2 comes from the transformation of benzoic acid to benzene, (iv) 90% of the CO_2 co-linearly produced with the benzene contribute to the carbonaceous species at the surface of the catalysts, (v) a small part of carbon dioxide comes from the total oxidation of propylene. One fact remains unexplained : why is the benzaldehyde formation strongly correlated with the CO_2?

Our hypothesis is totally innovative and based on the mechanism of the deoxygenation of benzoic acid. Remembering that deoxygenation occurs on oxygen vacancies at the surface of the catalyst, it can be suggested that the oxidation of propylene and the formation of benzaldehyde occurs consecutively on the same catalytic site (Figure 10.8). In that scheme, benzoic acid gives one oxygen atom to one oxygen vacancy, forming benzaldehyde and a filled oxygen vacancy at the surface of the catalyst. In a second step, one propylene molecule is oxidized to acrolein or an intermediate molecule[2] on that filled oxygen vacancy (or another equivalent one[3]). Afterward, the intermediate molecules could react on other lattice oxygen to give CO_2. Taking into account a stoichiometric reaction (eq. 10.2), 9 benzoic acid molecules are thus necessary to oxidize one propylene molecule and to produce 3 CO_2 molecules.

$$C_3H_6 + 9\,C_6H_5COOH \rightarrow 3\,CO_2 + 9\,C_6H_5COH + 3\,H_2O \qquad (10.2)$$

The comparison of the molybdenum oxidation state at the surface of the cobalt molybdate used in different reaction conditions supports our hypothesis.

[2]By intermediate molecule, we consider a molecule in which an oxygen atom has been added.

[3]One can imagine that the oxidation and the reduction steps of the catalyst are dissociated in the time and thus occur on different catalytic sites. These view is still compatible with our hypothesis since the benzoic acid gives its oxygen atoms to the surface of the catalyst.

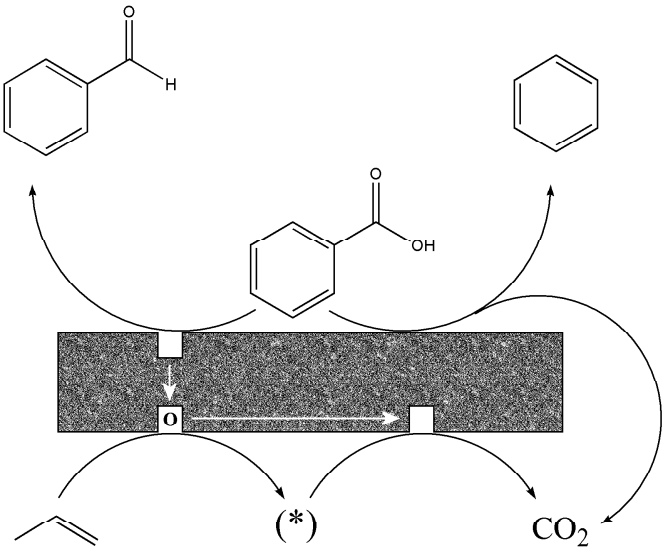

Figure 10.8: Proposed mechanism for the coupling between the probe reaction and the total oxidation of propylene. ($\star$) represents the possible intermediate molecules formed during the total oxidation of propylene.

While fresh catalyst has only Mo^{6+} species at its surface, used catalysts also exhibit Mo^{5+} species. Mo^{4+} or Mo^{0} were never detected in any sample. Moreover, it appears that the catalyst used in presence of both benzoic acid and propylene is less reduced than the one used in presence of only propylene. Indeed, the Mo^{5+} content at the surface of the catalyst is lower when benzoic acid is used. This observation is in agreement with the mechanism of reaction described before. The lower reduction level of the catalyst when benzoic acid is present means that oxidation of the surface occurs during the coupling reaction. If an oxidation of the molybdenum atoms is possible, we must admit that an oxygen source is available for the oxidation. In our case, there is only one possibility : the oxygen atoms coming from the benzoic acid.

By admitting that the benzoic acid provides oxygen atoms to the catalyst, we can conclude that the coupling reaction between propylene and benzoic acid occurs according to a MVK mechanism. So, propylene oxidation and benzaldehyde formation can be linked only if they occur on the same catalytic site. In other words, benzaldehyde is formed on a specific catalytic site presenting isolated oxygen vacancies whereas the products of the propylene oxidation, acrolein and CO_2, are generated on any equivalent catalytic sites in their oxidized form i.e. with filled oxygen vacancies.

10.5 Conclusions

The imagined coupling between the deoxygenation of benzoic acid and the oxidation of propylene according to a Mars & van Krevelen mechanism fits well with the results described above. Such a model can give some new precisions about the working mechanism of oxides. In particular, the potential coupling reaction points out that the oxidation of propylene occurs in such a way that the reaction leaves single oxygen vacancies at the surface of the catalyst. Moreover, our results suggest that the total oxidation of propylene, i.e. the formation of carbon dioxide would be a multi-step mechanism involving several lattice oxygen atoms far from each other.

Chapter 11

Characterization of the oxygen vacancies[1]

Abstract

The systematic correlation of the superficial oxidation state of all the catalysts measured by X-ray photoelectron spectroscopy with the information provided by the probe reaction allow us to precise, at the atomic scale, the architecture of the selective and total oxidation sites at work. Thanks to the deoxygenation of the benzoic acid, we succeed in demonstrating that a chemical shift of the O 1s is related to the oxidation state and the coordination of the molybdenum atoms. We suggest that the presence of scarce single oxygen vacancies does not affect in a detectable way the oxidation state of the catalyst. On the contrary, a large amount of oxygen vacancies at the surface of the catalyst modifies the electronic behaviour of the remaining oxygen atoms.

[1] presented as an oral contribution in the 5th WCOC (World Congress On Oxidation Catalysis) Sapporo (Japan), September 2005

11.1 Introduction

Many authors have reported that alkane/alkene selective and total oxidation reactions take place on different catalytic sites [103, 104]. Among the numerous proposed hypotheses, it has been suggested that oxygen atoms and their corresponding vacancies play a crucial role in the reactivity and selectivity of the oxide catalysts.

Our new probe reaction allows to characterize the catalysts "at work" in terms of oxygen vacancies. Such a coupling between the deoxygenation of benzoic acid and the oxidation of propylene was demonstrated in the previous chapter to occur on a $CoMoO_4$ catalyst according to the MVK mechanism. We have established that CO_2 formation is closely positively correlated with the benzene and benzaldehyde productions [105]. Although a part of carbon dioxide directly comes from the transformation of the acidic function of benzoic acid leading to the formation of benzene, there is another origin for a small amount of CO_2. Our hypothesis is that such a small amount is formed on the same catalytic sites as those where benzaldehyde is formed, making the coupling between the oxidation of propylene and the deoxygenation of benzoic acid an attractive tool for the characterization of the Mo-based oxide catalysts.

In the present chapter, the systematic characterization of about 100 samples by X-ray photoelectron spectroscopy allows us to use some statistical tools in order to correlate several surface properties, like oxidation states of the active elements, with the catalytic activity in the deoxygenation of benzoic acid and the oxidation of propylene. This gives us the opportunity to describe the active sites responsible for the activity in the selective and total oxidation reactions.

11.2 Experiments

11.2.1 Preparation of the catalysts

Several Mo based oxide catalysts were synthesized : molybdenum (sub)oxides (MoO_3, Mo_8O_{23}, Mo_9O_{26}, Mo_4O_{11} and MoO_2) and metal molybdates

($NiMoO_4$, $Bi_2Mo_2O_9$, Bi_2MoO_6, $Bi_2Mo_3O_{12}$, $Fe_2Mo_3O_{12}$ and $CoMoO_4$).

MoO_2 (Aldrich, 99%) was pre-treated under a 60 ml min^{-1} flow of 5% H_2 in nitrogen (Indugas, 99.95% pure) at 723K during 1h to reduce the potential oxidized species at the surface of the powder. Similarly, MoO_3 (Aldrich, 99.5%) was oxidized in a 60 ml min^{-1} flow of pure oxygen (Indugas, 99.995% pure) at 623K during 2h. Molybdenum suboxides were prepared according to the "solid state method" described in section 3.1.

Metal molybdates were prepared by the "citrate method". Complete protocol is available in section 3.2.

11.2.2 Catalytic activity measurements

Deoxygenation of benzoic acid was performed at atmospheric pressure in a stainless steel fixed bed micro-reactor. The reaction mixture contained either 574 ppm of benzoic acid and 50000 ppm of hydrogen (Indugas, 99.95 pure) either 574ppm of benzoic acid and 167000 ppm of propylene (Indugas, 99.8% pure) or 635 ppm of benzoic acid and 318 ppm of propylene (Indugas, 2.01% Vol. in He) while helium (Indugas, 99.996% pure) was the gas balance. Total flow was adjusted to 100ml min^{-1}. All catalytic tests were performed at 723K for 10 hours. Reactants and products were analysed by gaseous chromatography.

11.2.3 Characterization

The catalysts were characterized before and after the catalytic tests by X-ray photoelectron spectroscopy (XPS). They were analyzed according to the specifications described in section 5. C 1s, O 1s, Mo 3d, Ni 2p, Co 2p, Bi 4f and Fe 2p were thus measured according to the sample. Decomposition of the Mo 3d doublets to Mo^{n+} species was done by fixing an energy gap of 3.13 eV, and an area ratio of 2/3 between the Mo 3d3/2 and the Mo 3d5/2 bands. FWHM of Mo 3d doublet were linked together. Solutions of the decomposition were afterwards validated by checking that the binding energies

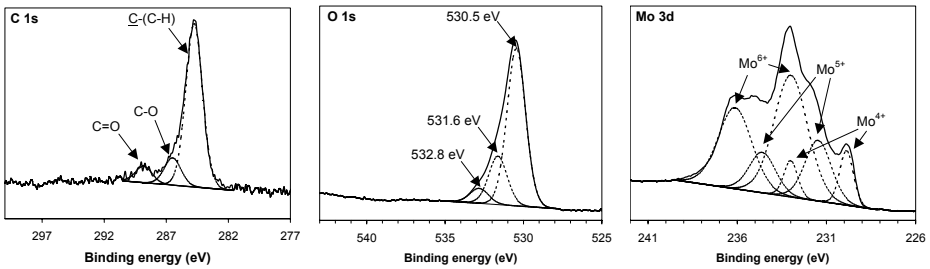

Figure 11.1: Typical X-ray photoelectron spectroscopy results obtained on molybdenum based oxide catalysts.

for the different Mo^{n+} eventually found fitted with those commonly accepted and that an energy gap around 1.2 eV existed between corresponding bands of two successive Mo^{n+} species. Oxygen (O 1s) and carbon (C 1s) contributions were also decomposed into several species by imposing the same FWHM between the different contributions of a same element.

11.3 Results

In four years, more than 100 catalytic tests were realized with molybdenum based oxide catalysts. Some of them were performed in the presence of hydrogen, others in the presence of propylene as the reducing gas. It is impossible to report all the catalytic results and their corresponding characterizations generated during these tests since the amount of data is very big. However, some catalytic tests were previously presented in this thesis and published [105, 87].

Hereafter, we present some basic statistics based on all the XPS and catalytic results collected when performing the reaction on molybdenum based oxides catalysts.

To illustrate the basis of our work, we report typical X-ray photoelectron spectroscopy results in figure 11.1. C 1s, O 1s and Mo 3d contributions are

decomposed with respect to the rules fixed in the experimental section. Other elements like Fe, Co, Ni and Bi are not reported since no significant changes in their binding energy after catalytic tests are observed.

Three components are found in the carbon contribution. The main peak is centered at 284.8 eV and corresponds to the C-(C, H) contribution of the carbon content. The second peak is centered at 286.5 eV and is generally attributed to carbon atoms simply bonded to oxygen atoms (C-O). The last component is located at 288.8 eV and can be attributed to carbon atoms doubly bonded with an oxygen atom (C=O) [106, 107]. We also reproduce the oxygen spectrum of the same sample. The oxygen shape seems asymmetrical as we only succeed in fitting the peak with three components. Precisely, a good solution is only validated when three components with the same FWHM is used to fit the oxygen spectrum. The components are centered at 530.5 eV (O_I), 531.6 eV (O_{II}) and 532.8 eV (O_{III}). The last XPS spectrum reported in figure 11.1 concerns the molybdenum contribution. The complex shape observed for this element is due to two factors : (i) Mo 3d is a doublet and (ii) the molybdenum atoms are present at the surface of the sample in three oxidation states (Mo^{6+}, Mo^{5+} and Mo $^{4+}$). The solution shown here fits quite well with the experimental shape. The 3d5/2 contribution of each oxidation stage has respectively a binding energy of 233.0 eV, 231.5 eV and 299.9 eV. This kind of results is found in almost all the molybdenum based catalysts analysed after catalytic tests.

Benefiting from the large number of data, we have sought correlations between the different variables like the molybdenum oxidation state, the concentration of products derived from the benzoic acid or the three oxygen "species" detected by XPS. Hereafter, we report three tables providing interesting insights towards the atomic description of the active oxidation site on molybdenum based catalysts.

As the C 1s shift observed in figure 11.1 could be the consequence of the presence of an oxygenated carbonaceous content at the surface of the samples, we have first checked the existence of some correlations between

Table 11.1: Pearson product-moment correlation coefficients at p-level<0.05 (N=104) between the different components of C 1s and O 1s. Bold and italic values mark the significant coefficients according to the p-level.

Pearson product-moment correlation coefficients (**r**)	**C 1s (C=O)**	**C 1s (C-O)**	**C 1s (C-(C,H))**
O1s (532.8eV) – O_{III}	***-0.23***	***-0.25***	***0.28***
O1s (531.6eV) – O_{II}	0.06	0.06	-0.06
O1s (530.5eV) – O_{I}	0.04	0.06	-0.06

Table 11.2: Pearson product-moment correlation coefficients at p-level<0.05 (N=104) between the different components of Mo 3d and O 1s. Bold and italic values mark the significant coefficients according to the p-level.

Pearson product-moment correlation coefficients (**r**)	**O1s (532.8eV) O_{III}**	**O1s (531.6eV) O_{II}**	**O1s (530.5eV) O_{I}**
Mo^{6+}	***-0.75***	***-0.64***	***0.72***
Mo^{5+}	***0.59***	***0.41***	***-0.50***
Mo^{4+}	***0.75***	***0.69***	***-0.76***

the C 1s and O 1s (table 11.1). Three coefficients are significant according to the p-level<0.05. A positive linear dependence is found between the C-(C,H) component and O_{III}. Two negative linear dependences exist respectively between the O_{III} and the C=O or C-O components. All the other combinations indicate that no dependence exists between these variables. In a similar way, we have tested the correlations between the Mo 3d and O 1s components (table 11.2). It appears that the oxygen peak found at 530.5 eV (O_I) is positively correlated with the presence of Mo^{6+} and negatively correlated with the other molybdenum species. On the contrary, O_{II} and O_{III} are positively correlated with the reduced molybdenum species (Mo^{5+} and Mo^{4+}) while a negative correlation is highlighted with the fully oxidized Mo^{6+} molybdenum atoms.

Table 11.3: Pearson product-moment correlation coefficients at p-level<0.05 (N=57) between the different components of Mo 3d, O 1s and the concentrations in benzaldehyde, toluene and benzene . Bold and italic values mark the significant coefficients according to the p-level.

Pearson product-moment correlation coefficients (**r**)	**Benzaldehyde conc.**	**Toluene conc.**	**Benzene conc.**
Mo^{6+}	0.15	***-0.30***	***0.28***
Mo^{5+}	-0.01	-0.17	-0.26
Mo^{4+}	-0.17	***0.46***	***-0.27***
O1s (532.8eV) – O_{III}	-0.07	***0.26***	-0.08
O1s (531.6eV) – O_{II}	-0.20	***0.45***	-0.18
O1s (530.5eV) – O_{I}	0.16	***-0.43***	0.16

In a third step, we tried to check the existence of correlations between the products formed during the catalytic tests, namely benzaldehyde, toluene and benzene, and the oxidation state at the surface of the molybdenum based oxide catalysts (table 11.3). Several important facts are observed : (i) the benzene concentration is positively linked with the atomic percentage of $Mo^{6+}$and negatively linked with the reduced molybdenum species, (ii) the toluene concentration is positively correlated with the Mo^{4+} and negatively correlated with the Mo^{6+}, (iii) a poor dependence is suspected between the benzaldehyde concentration and the atomic percentage of Mo^{6+}, (iv) weak negative correlation is also suggested between the benzaldehyde concentration and the atomic percentage of Mo^{4+}, (v) no correlation exists between the benzaldehyde concentration and the atomic percentage of Mo^{5+} as suggested by r=-0.01.

11.4 Discussion

The statistics highlight several negative or positive correlations between spectroscopic and catalytic data. But another interesting point is the asymmetry of the oxygen peak on the high binding energy side and its relation with the different molybdenum oxidation levels. After repeating the analyses and checking that all the precautions were taken (charge effects, contaminations by undesired elements,...), we have validated these results. Without any doubt, such an observation is possible thanks to the excellent resolution in the binding energy scale (about 0.2eV) and sensitivity of the available XPS apparatus.

Whereas it is possible to link instinctively the presence of three oxygen components to the different molybdenum states, a more quantitative analysis of these XPS data is needed. First, we have checked the independence between the carbon contributions and the oxygen. Indeed, the presence of oxygenated coke or some organic molecules could explain the oxygen chemical shift. This is commonly observed on several biological and synthetic organic compounds like glucose 6-phosphate [107] or polycarbonate [106]. In the present case, one correlation exists between the most shifted oxygen component (O_{III}, binding energy of 532.8eV) and each component of the C 1s. Whereas these are significant, they are not reflecting some direct chemical relationships : the best demonstration is provided by the positive correlation between O_{III} and C 1s (C-(C,H)). Such a positive correlation has no significance since the C 1s contribution at 284.8 eV is the well-known binding energy of a carbon atom bonded with another carbon atom or a hydrogen atom but not with an oxygen atom [106, 107]. So, this relation is indirect and means that both C 1s (C-(C,H)) and O_{III} are both correlated, but in an independent manner, with a third identical parameter. We provided the corresponding plots for better supporting our statements (figures 11.2 to 11.4).

Now that we have discarded the link between the oxygen and the carbon content, the alternative way that we have suggested in table 11.2, i.e. the

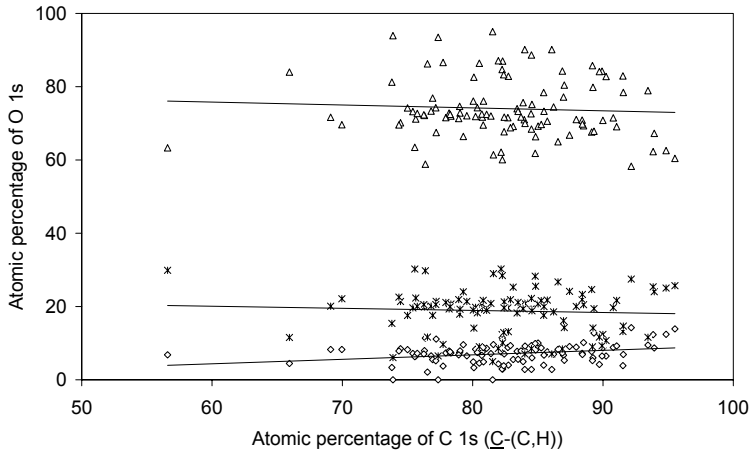

Figure 11.2: Variation of the O 1s atomic concentration as a function of the C 1s (C-(C,H)) atomic concentration. $\triangle, \star$ and $\diamondsuit$ represents respectively the data relative to O 1s components centered at 530.5 eV (O_I), 531.6 eV (O_{II}) and 532.8 eV (O_{III}).

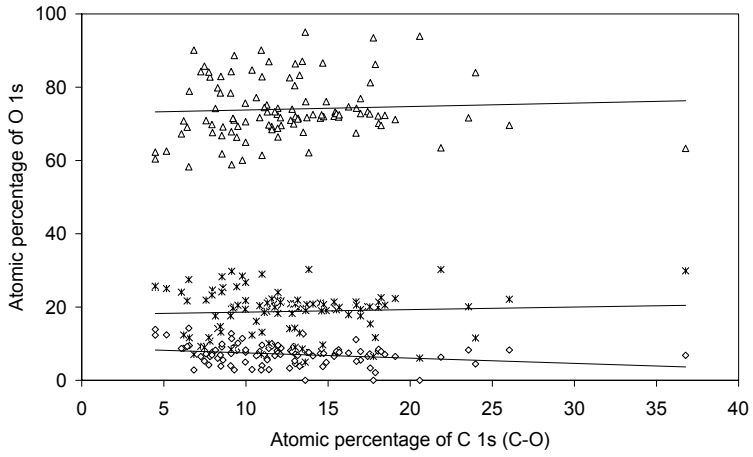

Figure 11.3: Variation of the O 1s atomic concentration as a function of the C 1s (C-O) atomic concentration. $\triangle$, $\star$ and $\diamondsuit$ represents respectively the data relative to O 1s components centered at 530.5 eV (O_I), 531.6 eV (O_{II}) and 532.8 eV (O_{III}).

correlations between the oxidation levels of molybdenum and the chemical shifts of oxygen, can be considered as a real property of the molybdenum based oxide catalysts and not as an artifact. It is clearly suggested that the most oxidized molybdenum species (Mo^{6+}) are only bonded with the "normal" oxygen components found at 530.5 eV (O_I) while the Mo^{5+} and Mo^{4+} are both linked with the presence of the O 1s components at 531.6 eV (O_{II}) and 532.8 eV (O_{III}).

According to Dupin et al [108], O_I can be considered as an oxygen with a strong ionic character, namely O^{2-} bonded with a metal atom fully coordinated. Moreover, the work of Jimenez et al [109] suggests that O_{II} and O_{III} could be the signature of some oxygen atoms bonded with metal atoms whose coordination is lower. Thanks to the new probe reaction that we have developed, we are able to confirm this hypothesis. Indeed, the correlations provided in table 11.3 reveals that the O_{II} and O_{III} are both significantly

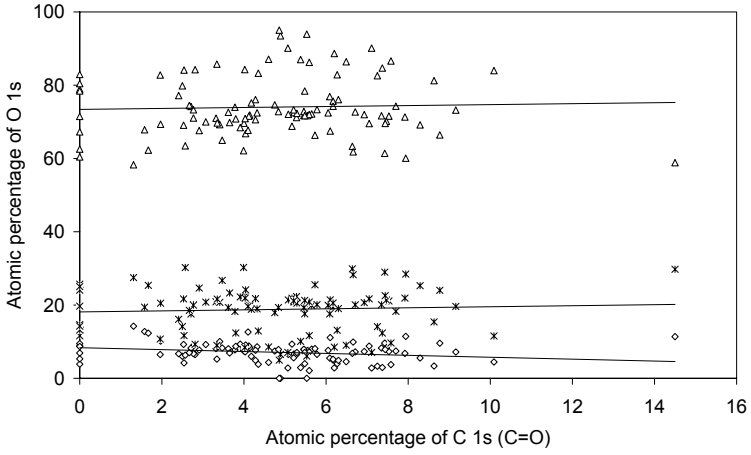

Figure 11.4: Variation of the O 1s atomic concentration as a function of the C 1s (C=O) atomic concentration. $\triangle, \star$ and $\diamondsuit$ represents respectively the data relative to O 1s components centered at 530.5 eV (O_I), 531.6 eV (O_{II}) and 532.8 eV (O_{III}).

linked with the toluene concentration. According to the principle of our probe reaction, the production of toluene occurs at the surface of the oxide catalysts presenting twin oxygen vacancies, namely two oxygen vacancies close to each other ($\pm\, 2\dot{A}$). Thus, the transformation of benzoic acid to toluene occurs by filling two superficial oxygen vacancies with the two oxygen atoms coming from a single benzoic acid molecule. The obvious corollary to this mechanism is that the molybdenum atoms near of the oxygen vacancies have two oxygen atoms missing in their surrounding. It is thus under-coordinated compared to the molybdenum atoms related to a fully oxidized surface whose characteristics are : (i) the +6 oxidation level, (ii) the correlated O_I component and (iii) the correlated concentration of benzene whose formation does not necessitate the presence of oxygen vacancies. Our work clearly confirms that such an under-coordinated molybdenum atom induces a chemical shift of the O 1s (XPS). In that precise case, the chemical shift towards the higher binding

energy reflects the impoverishment of the core electron density around the oxygen atoms. It is related to the lower coordination state detected by the formation of toluene and characterized by the molybdenum atoms in the +4 and +5 oxidation levels (figure 11.5). This correlation suggests that when a

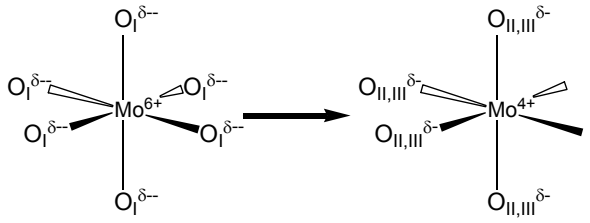

Figure 11.5: Idealized octahedral coordination of Mo atoms in the fully oxidized state and after the removal of two oxygen atoms.

+6 molybdenum atom loses two oxygen atoms in its coordination sphere, it consequently attracts more core electrons of the four remaining oxygen atoms. As a result of this phenomena, the molybdenum atom will switch to a lower oxidation state. The remaining oxygen atoms in the coordination sphere have thus less electrons. The remaining core electrons are more retained by the atom nucleus, so explaining that the core electrons appear at a higher binding energy. This mechanism involves two consequences : (i) the Mo-O bond is thus less polarised, i.e. the charge of the oxygen atom is less negative when the charge of the molybdenum atom is less positive. (ii) The concerned molybdenum atoms are in a more reduced state and are detected as Mo^{5+} or Mo^{4+} in the XPS analysis thanks to the chemical shift.

On the contrary to the twin oxygen vacancies, the single oxygen vacancies do not seem modify the polarisation of the Mo-O bond as revealed by the negative correlation between the benzaldehyde concentration and the Mo^{4+}/O_{II} components [2]. This is reinforced by the weak but nevertheless positive

[2]This hypothesis must be considered with precautions since the correlations between benzaldehyde and Mo^{4+}/O_{II} are not significant at p-level<0.05 but these could provide some clues.

correlation between the benzaldehyde formation and the presence of Mo^{6+}. These observations in addition to our previous work could lead to a better description of the active site in the oxidation of propylene. Indeed, we have suggested that the oxidation of propylene to acrolein and/or CO_2 occurs in such a way that single oxygen vacancies are formed at the surface of the catalyst [105]. Whereas the article was devoted to $CoMoO_4$ catalyst, we have checked under identical conditions that the same hypothesis is verified for all the catalytic phases mentioned above. Thus, it is now possible to reject the twin oxygen vacancies and its related under-coordinated molybdenum structure as a potential candidate in the participation of the propylene oxidation. This is definitively validated since we never detected any correlation between any oxidation product and the formation of toluene.

Single oxygen vacancies are the key. As a reminder, (i) these are formed after the oxidation of a propylene molecule, (ii) they are rather surrounded by fully oxidized molybdenum atoms and (iii) they do not modify (in a detectable way) the polarisation of the Mo-O bond. Such a hypothesis is in phase with the results claimed by Bertinchamps et al. These authors argue that a slight reduction of MoO_3, namely the presence of a small quantity of Mo^{5+} at the surface of the catalyst induces an improved catalytic activity towards the oxidation of 2-butanol [24]. According to this probe reaction, a better reactivity in oxidation instead of dehydration means that a few +5 molybdenum increases the exchangeability of surface lattice oxygen atoms. Our work thus highlights that the deep reduction of the surface, through the presence of large quantities of Mo^{5+} and Mo^{4+}, leads to a strong modification of the catalyst, especially in the electronic properties of oxygen and the activity of the catalyst. A slight reduction seems to be necessary for the oxidation reaction since it is less disturbing in the electronic behaviour of both the molybdenum and oxygen atoms.

11.5 Conclusions

Important correlations between Mo oxidation state, O chemical shift, number and mutual disposition of oxygen vacancies have been revealed on molybdenum based oxide catalysts by the way of the deoxygenation of benzoic acid used as a probe reaction. These correlations indicate that twin oxygen vacancies are involved in a deep molybdenum-reduced environment and that single vacancies are found on a more oxidized surface. Further investigation on the three O contributions detected by XPS and their relation with Mo oxidation level gives us a better understanding on the mutual disposition of Mo and O atoms in the catalytic site responsible for total or selective oxidation. This allows us to discard the twin oxygen vacancies, i.e. oxygen vacancies separated by about $2\dot{A}$ and related to an under-coordinated molybdenum atom as actresses in the oxidation of propylene. On the contrary, single vacancies seems not to induce such an electronic perturbation in the Mo and O vicinity, being thus the correct reduced site catalyzing the propylene oxidation.

Part V

General conclusions and perspectives

General conclusions

This work aimed to develop in a two-step strategy the deoxygenation of benzoic acid as a new probe reaction of the oxidation catalysts "at work". This choice was based on the experimental fact that the distribution of the potential main products, namely benzaldehyde, toluene and benzene depends on the presence and the mutual disposition of oxygen vacancies at the surface of the oxide catalysts. Indeed, it is claimed in the literature that single oxygen vacancies selectively produces benzaldehyde, twin oxygen vacancies (i.e. two oxygen vacancies separated by about $2\dot{A}$) induce the formation of toluene while the benzene production does not need the presence of any oxygen vacancies. Two molybdenum based catalytic systems were chosen to test the new probe reaction : the molybdenum (sub)oxides and the metal molybdates.

By the way of a new and original coupling between the probe reaction and the oxidation of propylene, we planned to correlate *in real time* the formation of the superficial oxygen vacancies monitored by the deoxygenation of benzoic acid and the activity in an oxidation reaction. Such an experimental coupling is a promising and a powerful tool which allows the fine characterization of the active catalytic site at work in an oxidation reaction.

First step

The scientific strategy adopted to meet these goals was, first, to evaluate the potentialities of the deoxygenation of benzoic acid used as described in the literature, i.e. in the presence of an excess of hydrogen (part III). Some molybdenum (sub)oxides were thus tested in these catalytic conditions. Chapter 6 was dedicated to the H_2-TPR study of the molybdenum (sub)oxides in order to evaluate their stability in a very reducing gaseous atmosphere. Thus, Mo_9O_{26} was found to be the most stable suboxide while Mo_8O_{23}, a rather similar catalyst in term of crystalline structure, underwent a deep reduction. These information were used in chapter 7 to support the justification of a hysteresis of conversion and selectivities detected when increasing the

temperature of reaction. The modifications of the acid conversion and the related selectivities were due to several temperature dependent reduction and recrystallization phenomena. Thanks to the illustration of the different molybdenum (sub)oxides specificity toward a deoxygenation product and the systematic characterization of the catalysts at different moments of the reaction, we succeeded to show the deoxygenation of benzoic acid as a suited probe reaction of the catalyst oxidation state. This encouraged us to switch the catalytic system for a more stable and more realistic one by substituting the hydrogen by the propylene.

Second step

The second step (part IV) thus consisted in implementing and optimizing the coupling between the probe reaction and the oxidation of propylene on some selected molybdenum based oxide catalysts. Our first attempts on the molybdenum (sub)oxides (chapter 8) have highlighted some differences between the use of the molecular hydrogen or propylene as the reducing agent. The propylene does not allow the desorption of toluene and benzene when the deoxygenation of the benzoic acid is performed on molybdenum (sub)oxides. This experimental fact suggested that the hydrogen species involved in the formation of toluene and benzene are different according to whether it comes from the dissociation of molecular hydrogen or the transformation of propylene. Our main hypothesis was the difference of nature of the active site responsible for the activation of molecular hydrogen or propylene respectively induces such a difference in the catalytic activity. This hypothesis was improved in chapter 9 thanks to the comparison of the catalytic activity measured on the molybdenum (sub)oxides and the metal molybdates. Indeed, when performed on metal molybdates, the formation of toluene and benzene is possible in the presence of propylene. This fact strongly underlined the importance of the second cation present in the molybdates. Roughly, Ni, Co, Bi and Fe cations increase the distance between the adsorption and the dissociation sites so that the activation of the α-hydrogen from a

propylene molecule by a close oxygen atom of the catalyst is possible. The α-hydrogen having some similar properties to the hydrogen atoms generated by the dissociative chemisorption of molecular hydrogen, the transformation of the benzoic acid to toluene and benzene occurs on the molybdate catalysts.

In chapter 10, by the way of the positive correlation between the formation of benzaldehyde and CO_2, we have suggested that the coupling reaction follows a Mars & Van Krevelen mechanism. In parallel to this hypothesis, we also showed that the total and selective oxidation of propylene involves the creation of single oxygen vacancies only. This constituted the first results of the probe reaction in the characterization of the oxidation sites at work. The investigation towards the description of the oxidation site was further engaged in chapter 11. Thus, the Mo 3d and O 1s XPS results together with the results provided by the probe reaction allowed us to propose a mechanism explaining the observed chemical shift of the O 1s according to the coordination of the molybdenum atoms. We claimed that twin oxygen vacancies, detected thanks to the production of toluene are not involved in the oxidation of propylene because the absence of two oxygen atoms in the vicinity of a molybdenum atom induces a modification of the electronic properties of both the molybdenum and the remaining oxygen atoms. These oxygen atoms could not thus be used to oxidize a propylene molecule. The important corollary is that single oxygen vacancies are the key in the oxidation reactions and do not involve a systematic deep reduction of the catalytic surface.

In this last step, we succeeded in precising the architecture of the active catalytic site in the oxidation of the propylene thanks to the probe reaction. This definitively confirms the deoxygenation of benzoic acid as an efficient tool to characterize the oxidation catalytic site “at work” in terms of superficial oxygen vacancies.

Perspectives

The coupling reaction between the deoxygenation of benzoic acid and the oxidation of propylene being now quite well understood, two categories of perspectives can be considered : fundamental and industrial.

In the fundamental point of view, at least another complementary use of this new tool is still possible. Indeed, this work has developed the deoxygenation of benzoic acid as a real and complete oxidant agent, i.e. in total replacement of the molecular oxygen in the coupling reaction with the oxidation of propylene. This use of the probe reaction has highlighted several problems despite the positive results obtained and described in this thesis : catalysts reduction, products adsorption, high level of carbon deposition, etc.

These drawbacks may be avoided or attenuated in a particular use of the probe reaction. One can imagine to inject simultaneously in the reactor about 600ppm of benzoic acid with the molecular oxygen and the propylene. Such an approach would allow to characterize “in real time”, by the way of the deoxygenation of the benzoic acid, the oxygen vacancies formed at the surface of the catalyst during the oxidation of propylene in some more real oxidative conditions, i.e. in the presence of molecular oxygen. This further work would be a true probe reaction approach of an oxidation reaction in order to determine the architecture of the oxide catalysts “at work”. Nevertheless, to be a success and to allow the correct interpretation of the catalytic results, one must check the reactivity of the benzoic acid and the aromatic products with the molecular oxygen. Indeed, a total oxidation of these molecules could occur since (i) the amount of molecular oxygen will be much higher than the amount of benzoic acid, (ii) the reaction temperature is above 673K and (iii) the catalysts content some transition metals known to be active in the total oxidation of the aromatic compounds.

This step in the use of our new tool would open the way to the study of some other molybdenum oxide based catalysts and more generally some other oxide catalysts used in the oxidation of propylene. By using a

similar methodology exposed in this work and the proposed perspectives, i.e. by correlating the information provided by the probe reaction with the oxidation state, it should be possible to precise the architecture of the active sites in terms of atoms coordination and of oxygen vacancies (number and mutual disposition) involved in the oxidation of propylene on several oxide catalysts. On this late point, two kind of experimentations can be envisaged to definitively confirm the correlations revealed in the chapter 10 : (i) a systematic correlation of the XPS and Raman measurements of the molybdenum based oxides catalysts and (ii) some isotopic oxygen exchanges. Both approaches should provide some new data about the Mo-O bonds involved in the oxygen vacancies formation.

Another interesting and promising use of this new tool is certainly to couple the deoxygenation of benzoic acid with the oxidation of an alkane. Such a coupling could be very useful to characterize the nature of the active site in the oxidation of propane to propylene or in the oxidation of propane to acrolein. This would allow to meet the wish of the petrochemical industries in the development of a single step oxidation process for the production of some more added value molecules like acrolein or acrylic acid.

In the industrial point of view, the coupling reaction between the oxidation of propylene and the deoxygenation of benzoic acid could be developed for the production of some raw material like acrolein, benzaldehyde or benzene. Although such a coupling is not in agreement with the market demands, one can imagine that the coupling between the oxidation of a paraffin or of an olefin longer than propylene with the deoxygenation of benzoic acid could be of great interest. We would be able to produce benzene and/or benzaldehyde together with selective oxidation product by the way of a cleaner and environment friendly process.

Last but not least, academics and petrochemical industries would profit of the results generated by this new characterization tool, the deoxygenation of benzoic acid, in the improvement of the catalytic phases developed in the field of heterogeneous catalysis.

Appendix

Appendix A

Molybdenum (sub)oxides

The first set of catalysts, namely the molybdenum (sub)oxides, possess intrinsically some oxygen deficiencies and are thus good candidates as catalysts with oxygen vacancies at their surface. Indeed, as illustrated below, the molybdenum (sub)oxides are constituted of different molybdenum coordinations which made their average oxidation level intermediate between MoO_3 (+6) and MoO_2 (+4).

- Mo_4O_{11} (+5.5)
- $Mo_{17}O_{47}$ (+5.53)
- Mo_5O_{14} (+5.6)
- Mo_8O_{23} (+5.75)
- Mo_9O_{26} (+5.78)
- $Mo_{13}O_{38}$ (+5.84)

Among these crystallographic phases, we have focused our attention on Mo_4O_{11}, Mo_8O_{23} and Mo_9O_{26} because they have been reported in the literature to be responsible for an improved catalytic activity [22, 24, 110].

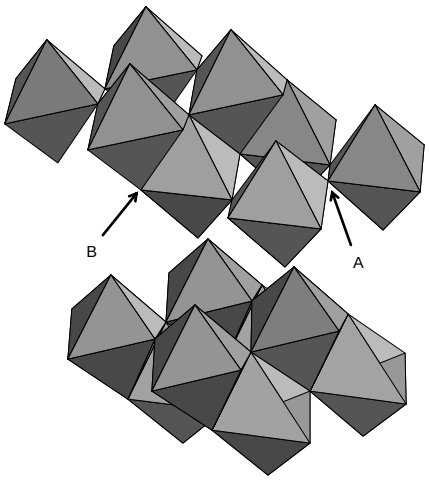

Figure A.1: 3D-structure of MoO_3. A and B respectively indicates the corner sharing and the edge sharing arrangement between two adjacent octahedra.

To support our explanations, we provide a short review of the molybdenum (sub)oxides used in this work.

In order to highlight the specificity of molybdenum suboxides, let us remind first the structure of MoO_3. This molybdenum oxide may be regarded as a layer structure in which each layer is built up of distorted MoO_6 octahedra at two levels as shown in figure A.1. Edge sharing occurs between octahedra at different levels. Each octahedron has one corner not shared with other octahedra, corresponding to an oxygen atom bonded to only one molybdenum atom [69, 111]. The crystallographic cell of MoO_3 is orthorhombic.

Mo_8O_{23} and Mo_9O_{26} (figure A.2) are quite close from MoO_3 since they also adopt exclusively an octahedral coordination between molybdenum and oxygen atoms. But, due to their suboxide character, i.e. the presence of some "bulk oxygen vacancies", the mutual disposition of the octahedra are somewhat different of MoO_3 [67, 75, 18]. Arrows in figure A.2 indicates some missing octahedra in Mo_9O_{26} compared to the structure of MoO_3.

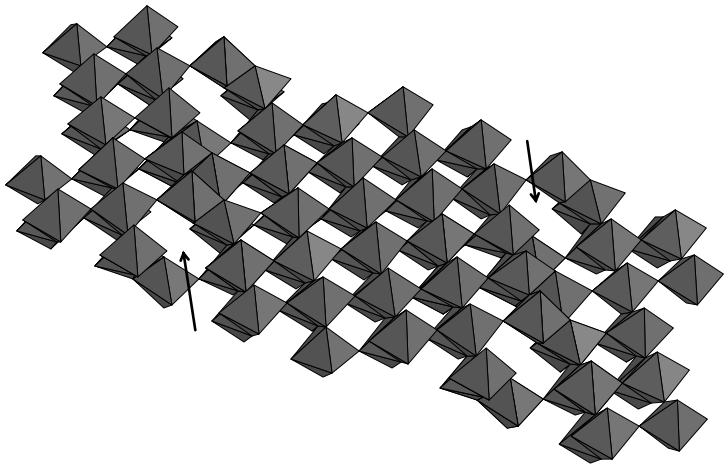

Figure A.2: 3D-structure of Mo_9O_{26}.

Consequently, the crystalline cells are respectively monoclinic and triclinic for Mo_8O_{23} and Mo_9O_{26}.

Mo_4O_{11} , sometimes named γ-molybdenum oxide [112, 67, 74], is constructed of MoO_6 octahedra and MoO_4 tetrahedra coupled together by sharing corners (figure A.3).

The structure of MoO_2 [113, 114] consists in slightly distorted MoO_6 octahedra joined by corners and edges as shown in figure A.4. Compared to the structure of MoO_3, one must see a difference in the mutual disposition of the octahedra which induces a higher number of molybdenum atoms sharing two oxygen atoms with their neighbours. The crystallographic cell of MoO_2 is monoclinic.

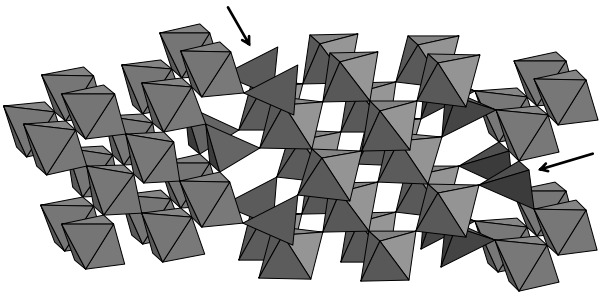

Figure A.3: 3D-structure of Mo_4O_{11}. Arrows indicates the MoO_4 tetrahedra.

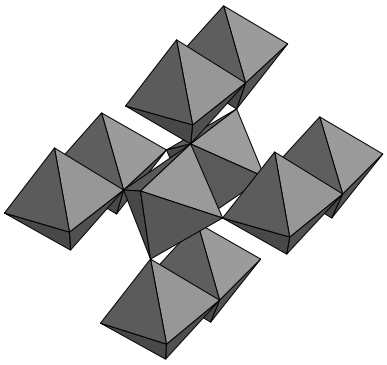

Figure A.4: 3D-structure of MoO_2.

Appendix B

Metal molybdates

Metal molybdates are catalysts widely used in oxidation reactions. Moreover, they constitute the basis of industrial multicomponent catalysts. Metal molybdates are thus good aspirants to mimic the oxide catalysts used in "real" conditions. Several molybdates were selected after an extended bibliographic research because : (i) they are studied in the field of some oxidation reactions, especially the oxidation of propylene, (ii) they exhibit a significant activity when they are used in an oxidation reaction in presence of oxygen. This can allow to confront our results with the data available in the literature. We have thus selected the following catalysts : α-$NiMoO_4$, $CoMoO_4$, $Fe_2(MoO_4)_3$, α-$Bi_2(MoO_4)_3$, β-$Bi_2Mo_2O_9$ and γ-Bi_2MoO_6.

The cell of α-$NiMoO_4$ is monoclinic. Nickel and molybdenum ions are localized in oxygen octahedra building chains [115, 100].

$CoMoO_4$ crystallizes in a monoclinic cell and possesses raws of octahedral molybdenum to oxygen coordination stacked according to one direction by sharing one edge. Some Mo^{6+} ions are in a tetrahedral coordination which makes this crystalline structure specific [116, 117].

$Fe_2(MoO_4)_3$ is monoclinic and consists in an open framework of octahedral FeO_6 and tetrahedral MoO_4 building blocks which are fused together by Fe-O-Mo bonds [118, 100].

The three bismuth molybdates are quite similar concerning the coordination relative to the oxygen atoms : they present twin molybdenum tetrahedra structure. α-$Bi_2(MoO_4)_3$ has a monoclinic cell and is composed of distorted tetrahedra of oxygen ions surrounding the molybdenum ions. They occur in pairs. Each bismuth ion has eight oxygen neighbours [119, 120, 121]. β-$Bi_2Mo_2O_9$ (monoclinic cell) has four configurations of molybdenum tetrahedric coordination with the surrounding oxygen atoms and four kinds of bismuth cations. Four sets of twin molybdenum tetrahedra and four bismuth +3 ions without oxygen ions characterize this phase [119]. The γ-Bi_2MoO_6 also possesses four molybdenum tetrahedra structures arranged according to three twin tetrahedra. Its cell is orthorhombic [119].

List of Figures

List of Tables

Bibliography

[1] Centi, G., Ciambelli, P., Perathoner, S., and Russo, P., Catalysis Today **75** (2002) 3 .

[2] Global energy and Environmental catalyst market to reach nearly $13 billion by 2009, http://www.the-infoshop.com/press/bc21724_en.shtml, 2004.

[3] Catalysts and Specialty Chemicals, http://www.catalystgrp.com/catalystsandchemicals.html, 2003.

[4] Yunoki, H. and Tanimoto, M., US Patent **US20050215818** (2005).

[5] Borgmeier, F., Hibst, H., Tenten, A., Mattmann, W., and Machhammer, O., US Patent **US20040092768** (2004).

[6] Jachow, H., Tenten, A., Unverricht, S., and Arnold, H., US Patent **US6541664** (2003).

[7] Arpentinier, P., Cavani, F., and Trifirò, F., *The Technology of Catalytic Oxidations. 1. Chemical, catalytic & engineering aspects*, Editions TECHNIP, 2001.

[8] Chauvel, A. and Lefebvre, G., *Petrochemical Processes*, Institut Français du Pétrole Publications, 1989.

[9] DUBOIS, J.-L., DESDEVISES, F., SERREAU, S., VITRY, D., and UEDA, W., Patent Application **WO2004024665** (2003).

[10] Tanimoto, M., US Patent **US6545178** (2003).

[11] Yada, S., Ogawa, Y., Suzuki, Y., Hosaka, H., and Jinno, K., US Patent **US20040249000** (2004).

[12] Grasselli, R. and Burrington, J., Ind. Eng. Chem. Res. Dev. **23** (1984) 393 .

[13] Ueda, W., Vitry, D., and Katou, T., Catalysis Today **96** (2004) 235.

[14] Katou, T., Vitry, D., and Ueda, W., Catalysis Today **9192** (2004) 237.

[15] Ueda, W., Vitry, D., and Katou, T., Catalysis Today **99** (2005) 43.

[16] Grasselli, R. K. et al., Catalysis Today **9192** (2004) 251.

[17] Wagner, J. B. et al., Journal of Catalysis **224** (2004) 28.

[18] Wang, D., Su, D., and Schlogl, R., Crystal Research and Technology **38** (2003) 153.

[19] Bruckman, K. et al., J. Catal. **104** (1987) 71.

[20] Volta, J. C. and Moraweck, B., J. Chem. Soc., Chem. Commun. (1980) 338.

[21] Vedrine, J., Millet, J., and Volta, J., Catalysis Today **32** (1996) 115 .

[22] Volta, J. C., Bertrand, O., and Floquet, N., J. Chem. Soc., Chem. Commun. (1985) 1283.

[23] Haber, J. and Lalik, E., Catalysis Today **33** (1997) 119.

[24] Bertinchamps, F. and Gaigneaux, E., Catalysis Today **91-92** (2004) 105 .

[25] Gaigneaux, E., Genet, M., Ruiz, P., and Delmon, B., Journal of Physical Chemistry B **104** (2000) 5724 .

[26] Roget's II: The New Thesaurus, Third Edition., Answers.com GuruNet Corp. http://www.answers.com/topic/catalyst, 1995.

[27] Prather, K., *Integrated Chemical Engineering (ICE) Topics: Biocatalysis.*, MIT Chemical Engineering Department, 2004.

[28] Arora, N., Deo, G., Wachs, I., and Hirt, A., Journal of Catalysis **159** (1996) 1 .

[29] Bettahar, M., Costentin, G., Savary, L., and Lavalley, J., Applied Catalysis A-General **145** (1996) 1 .

[30] Haber, J., Janas, J., Schiavello, M., and Tilley, R. J. D., J. Catal. **82** (1983) 395.

[31] Valente, N. G., Cadus, L. E., Gorriz, O. F., Arrua, L. A., and Rivarola, J. B., Appl. Catal., A **153** (1997) 119.

[32] Matsuda, T., Hirata, Y., Suga, S., Sakagami, H., and Takahashi, N., Applied Catalysis A: General **193** (2000) 185.

[33] Matsuda, T., Hirata, Y., Sakagami, H., and Takahashi, N., Microporous and Mesoporous Materials **42** (2001) 345.

[34] Volta, J. C., Forissier, M., Theobald, F., and Pham, T. P., Faraday Discussions (1981) 225.

[35] Matsuda, T., Hanai, A., Uchijima, F., Sakagami, H., and Takahashi, N., Microporous and Mesoporous Materials **51** (2002) 155.

[36] Demoulin, O. et al., Catalysis Today **99** (2005) 217 .

[37] Weng, L. and Delmon, B., Applied Catalysis A-General **81** (1992) 141 .

[38] Dury, F., Centeno, M., Gaigneaux, E., and Ruiz, P., Applied Catalysis A-General **247** (2003) 231 .

[39] Dury, F., Centeno, M., Gaigneaux, E., and Ruiz, P., Catalysis Today **81** (2003) 95 .

[40] Dury, F., Gaigneaux, E., and Ruiz, P., Applied Catalysis A-General **242** (2003) 187 .

[41] Gaigneaux, E., Ruiz, P., and Delmon, B., Catalysis Today **32** (1996) 37 .

[42] Godard, E., Gaigneaux, E., Ruiz, P., and Delmon, B., Catalysis Today **61** (2000) 279 .

[43] Weng, L., Yasse, B., Ladriere, J., Ruiz, P., and Delmon, B., Journal of Catalysis **132** (1991) 343 .

[44] Weng, L. et al., Journal of Catalysis **132** (1991) 319 .

[45] Weng, L., Ruiz, P., Delmon, B., and Duprez, D., Journal of Molecular Catalysis **52** (1989) 349 .

[46] Weng, L., Patrono, P., Sham, E., Ruiz, P., and Delmon, B., Journal of Catalysis **132** (1991) 360 .

[47] Weng, L., Ma, S., Ruiz, P., and Delmon, B., Journal of Molecular Catalysis **61** (1990) 99 .

[48] Wiesmann, M. et al., Journal of Magnetism and Magnetic Materials **150** (1995) L1 .

[49] Delporte, P. et al., Catalysis Today **23** (1995) 251.

[50] Brazdil, J. F., Glaeser, L. C., and Grasselli, R. K., Journal of Catalysis **81** (1983) 142.

[51] Bordes, E., Comptes Rendus De L'AcadÃ©mie Des Sciences Serie II Fascicule C-Chimie **3** (2000) 725 .

[52] Ressler, T., Wienold, J., Jentoft, R. E., and Girgsdies, F., European Journal of Inorganic Chemistry (2003) 301.

[53] Mars, P. and van Krevelen, D. W., Chemical Engineering Science **3** (1954) 41.

[54] Doornkamp, C. and Ponec, V., Journal of Molecular Catalysis A: Chemical **162** (2000) 19.

[55] Rohrer, G. S., Lu, W., Smith, R. L., and Hutchinson, A., Surf. Sci. **292** (1993) 261.

[56] Smith, R. L. and Rohrer, G. S., J. Solid State Chem. **124** (1996) 104.

[57] Smith, R. L. and Rohrer, G. S., J. Catal. **173** (1998) 219.

[58] Smith, R. L. and Rohrer, G. S., J. Catal. **163** (1996) 12.

[59] Sakata, Y., Tol-Koutstaal, C. A. V., and Ponec, V., J. Catal. **169** (1997) 13.

[60] de Lange, M. W., van Ommen, J. G., and Lefferts, L., Applied Catalysis A: General **220** (2001) 41.

[61] de Lange, M. W., van Ommen, J. G., and Lefferts, L., Applied Catalysis A: General **231** (2002) 17.

[62] Tatibouet, J., Applied Catalysis A-General **148** (1997) 213 .

[63] Holderich, W. F. and Tjoe, J., Applied Catalysis A: General **184** (1999) 257.

[64] Koutstaal, C. A. and Ponec, V., Stud. Surf. Sci. Catal. **92** (1995) 105.

[65] Sakata, Y. and Ponec, V., Appl. Catal., A **166** (1998) 173.

[66] Andersson, G. and Magneli, A., Acta Chem. Scand. **4** (1950) 793.

[67] Kihlborg, L., Acta Chem. Scand. **13** (1959) 954.

[68] Kihlborg, L., Acta Chem. Scand. **23** (1969) 1834.

[69] Kihlborg, L., Arkiv Kemi **21** (1963) 443.

[70] Kihlborg, L., Arkiv Kemi **21** (1963) 427.

[71] Kihlborg, L., Advan. Chem. Ser. **39** (1963) 37.

[72] Kihlborg, L., Acta Chem. Scand. **14** (1960) 1612.

[73] Kihlborg, L. and Magneli, A., Acta Chem. Scand. **9** (1955) 471.

[74] Magneli, A., Acta Chem. Scand. **2** (1948) 861.

[75] Magneli, A., Acta Chem. Scand. **2** (1948) 501.

[76] Soares, A. P. V., Portela, M. F., Kiennemann, A., Hilaire, L., and Millet, J. M. M., Applied Catalysis A: General **206** (2001) 221.

[77] Firment, L. E. and Ferretti, A., Surface Science **129** (1983) 155.

[78] Moro-oka, Y., Ueda, W., and Lee, K., Journal of Molecular Catalysis A-Chemical **199** (2003) 139 .

[79] Ressler, T., Wienold, J., Jentoft, R. E., and Neisius, T., Journal of Catalysis **210** (2002) 67.

[80] Arnoldy, P., De Jonge, J., and Moulijn, J., Journal of Physical Chemistry **89** (1985) 4517.

[81] Gaigneaux, E. M., Ruiz, P., Wolf, E. E., and Delmon, B., Applied Surface Science **121** (1997) 552.

[82] Choi, J. G. and Thompson, L. T., Applied Surface Science **93** (1996) 143.

[83] Kim, D. S. et al., Applied Catalysis A: General **150** (1997) 21.

[84] Laurent, E. and Delmon, B., Applied Catalysis a-General **109** (1994) 97.

[85] Ressler, T., Jentoft, R. E., Wienold, J., Gunter, M. M., and Timpe, O., Journal of Physical Chemistry B **104** (2000) 6360.

[86] Bielanski, A. and Haber, J., Catal. Rev.-Sci. Eng. **19** (1979) 1.

[87] Dury, F., Misplon, V., and Gaigneaux, E., Catalysis Today **91-92** (2004) 111 .

[88] Duma, V. et al., Chemical Engineering Journal **99** (2004) 227 .

[89] Haber, J. and Grzybowska, B., Journal of Catalysis **28** (1973) 498 .

[90] Brückman, K., Haber, J., and Wiltowski, T., Journal of Cataysis **106** (1987) 188 .

[91] Millet, J. M. M., Ponceblanc, H., Coudurier, G., Herrmann J. M., and Vedrine J. C., Journal of Catalysis **142** (1993) 381.

[92] Outokumpu Technology, *HSC Chemistry v4.1*, Outokumpu Technology.

[93] Maione, A. and Devillers, M., Journal of Solid State Chemistry **177** (2004) 2339 .

[94] Stern, D. and Grasselli, R., Journal of Catalysis **167** (1997) 550 .

[95] Yoon, Y. S., Fujikawa, N., Ueda, W., Moro-oka, Y., and Lee, K. W., Catalysis Today **24** (1995) 327.

[96] Carrazan, S. R. G., Martin, C., Rives, V., and Vidal, R., Applied Catalysis A: General **135** (1996) 95.

[97] Trifiro, F., Caputo, G., and Villa, P. L., Journal of the Less Common Metals **36** (1974) 305.

[98] Ueda, W., Moro-oka, Y., and Ikawa, T., Journal of Catalysis **70** (1981) 409.

[99] Anderson, A. B., Ewing, D. W., Kim, Y., and Grasselli, R. K., Journal of Catalysis **96** (1985) 222.

[100] Wolfs, M. W. J. and Batist, P. H. A., Journal of Catalysis **32** (1974) 25.

[101] Matsuura, I., Mizuno, S., and Hashiba, H., Polyhedron **5** (1986) 111.

[102] Gaigneaux, E. M., Dayem, H. M. A., Godard, E., and Ruiz, P., Applied Catalysis A: General **202** (2000) 265.

[103] Abon, M. et al., Journal of Catalysis **134** (1992) 542.

[104] Volta, J. and Tatibouet, J., Journal of Catalysis **93** (1985) 467.

[105] Dury, F., Meixner, S., Clement, D., and Gaigneaux, E. M., J. Mol. Catal. A: Chem. **237** (2005) 9 .

[106] Dewez, J., Doren, A., Schneider, Y.-J., Legras, R., and Rouxhet, P., Surface study of new microporous polymeric membranes used as a substratum for animal cell culture, in *Interfaces in New Materials*, edited by Grange, P. and Delmon, B., Elsevier Applied Science, 1991.

[107] Gerin, P., Dengis, P., and Rouxhet, P., Journal de Chimie Physique et de physico-chimie biologique **92** (1995) 1043 .

[108] Dupin, J., Gonbeau, D., Vinatier, P., and Levasseur, A., Physical Chemistry Chemical Physics **2** (2000) 1319 .

[109] Jimenez, V., Fernandez, A., Espinos, J., and Gonzalezelipe, A., Journal of Electron Spectroscopy and Related Phenomena **71** (1995) 61 .

[110] McCormick, R. L. and Schrader, G. L., Journal of Catalysis **113** (1988) 529.

[111] Barreca, D., Rizzi, G. A., and Tondello, E., Thin Solid Films **333** (1998) 35.

[112] Fun, H. K., Yang, P., Sasaki, M., Inoue, M., and Kadomatsu, H., Acta Crystallographica Section C-Crystal Structure Communications **55** (1999) 841.

[113] Brandt, B. and Skapsi, A., Acta Chem. Scand **21** (1967) 661.

[114] Kleykamp, H. and Supawan, A., Journal of the Less-Common Metals **63** (1979) 237.

[115] Ehrenberg, H. et al., Journal of Magnetism and Magnetic Materials **150** (1995) 371 .

[116] Courtine, P., Cord, P. P., Pannetier, G., Daumas, J. C., and Montarnal, R., Bulletin de le Société Chimique de France **12** (1968) 4816 .

[117] Ono, T., Ogata, N., and Miyaryo, Y., Journal of Catalysis **161** (1996) 78 .

[118] Harrison, W., Materials Research Bulletin **30** (1995) 1325 .

[119] Ono, T., Utsumi, K., Kataoka, M., Tanaka, Y., and Noguchi, F., Catalysis Today **91-92** (2004) 181 .

[120] van den Elzen, A. F. and Rieck, G. D., Acta Cryst. **B29** (1973) 2433 .

[121] Nihtianova, D., Ganev, V., Khaltakova, N., and Gospodinov, M., Comptes rendus de l'Académie bulgare des Sciences **56** (2003) 53 .

Appendix C

Titres récents de la collection :

2001

Département des sciences du milieu et de l'aménagement du territoire

N°1. Auquiere, Eric, SAR temporal series interpretation and backscattering modeling for maize growth monitoring.

Département de biologie appliquée et des productions agricoles

N°2. Debier, Cathy, A study of the dynamics of vitamin A, vitamin E and PCBs in seals during lactation.

2002

Département des sciences du milieu et de l'aménagement du territoire

N°7. Kruyts, Nathalie, Influence de la nature des constituants du sol sur la mobilisation rhizosphérique du radiocésium dans quelques sols forestiers.

N°8. Mounir, Fouad, Conception d'un système d'information géographique pour l'aménagement et la gestion forestière au Maroc. Intégration des critères et indicateurs du développement durable: Application à la Forêt de la Maâmora.

N°10. Tilmant, Amaury, Sustainable management of reservoir resources using flexible stochastic dynamic programming.

N°11. du Bus de Warnaffe, Gaëtan, Impact des systèmes sylvicoles sur la biodiversité: une approche comparative en Ardenne.

N°13. Kolai, Lounas, Etude d'un écosystème forestier: phytosociologie, phytodiversité, productivité et hydrologie au Bois de Lauzelle.

N°18. Jourez, Benoit, Etude de l'effet d'unstimulus gravitationnel induit artificiellement sur la formation du bois de tension et du bois opposé dans de jeunes pousses de peuplier (Populus auramericana cv 'Ghoy').

N°21. Hang, Peou, Les données pédologiques enrichissent la modélisation de la relation pluie-débit.

N°23. de Wasseige, Carlos, Spatio-temporal characterisation of the sub-equatorial forest canopy based on multiscale approach from field and space observations.

Département de biologie appliquée et des productions agricoles

Graindorge, Céline, Modélisation régionalisée bio-économique du secteur agricole pour l'analyse des politiques durables.

Toyi, Isidore, Politique de libéralisation et efficience des marchés de céréales locales au Burkina Faso.

N°3. Henao-Toro, Martha-Cécilia, Dynamique d'éléments fertilisants dans les sols dérivés de cendres volcaniques de la zone caféière centrale de Colombie, sous culture de bananier plantain.

N°12. Nusura, Hassan, Les stratégies de développement et les politiques de sécurité alimentaire en Afrique sub-saharienne : le poids des incohérences.

N°15. Sqalli Adoui, Driss, Evaluation des effets du Programme d'Ajustement Structurel Agricole sur la petite agriculture irriguée au Maroc.

N°19. Kouam, Emile, L'intégration régionale du Cameroun par la promotion des échanges transfrontaliers des produits agricoles vivriers avec les pays voisins : rôle des marchés frontalier.

N°20. Nchare, Amadou, Effets de la libéralisation économique et de la dévaluation du franc CFA sur l'offre du café arabica et des cultures concurrentes au Cameroun.

Département de chimie appliquée et des bio-industries

Dambly, Stéphanie, The two main plant plasma membrane H(+)-ATPase isoforms differ in their regulatory properties.

N°4. Coulibaly, Lacina, Bioconversion de macromolécules dans un réacteur simulant un écoulement piston en régime transitoire : cas de la bioremédiation d'eaux usées synthétiques par Aspergillus nige.

N°6. Godard, Eric, Hydrogénation de l'anhydride maléique en présence de catalyseurs métalliques supportés sur charbon actif.

N°14. Lermusieau, Guillaume, Influence de la variété de houblon sur les propriétés organoleptiques de la bière.

N°16. Owsianik, Grzegorz, Identification of transcriptional and post-translational pathways linking protein degradation and multiple drug resistance in yeast.

N°17. Grec, Sébastien, Caractérisation du promoteur de transcription de NpABC1, un gène codant pour un transporteur ABC de Nicotiana plumbaginifolia induit en présence d'un diterpène.

N°22. Fetter, Karolina, Functional studies of plasma membrane aquaporins from Zea mays.

N°24. De Cupere, Vinciane, Supramolecular organization of adsorbed collagen layers and nanoscale structure of polymer surfaces.

Faculté des sciences, département de biologie

N°5. Levie, Amandine, Development of a biological control method of wheat aphids, by using Aphidiinae parasitoids (Hymenoptera : Braconidae).

Christian de Duve Institute of Cellular Pathology, Laboratoire de Chimie Physiologique

N°9. Ghislain, Delpierre, Fructosamine 3-kinase, an enzyme involved in protein deglycation.

2003

Département des sciences du milieu et de l'aménagement du territoire

N°25. Goor, François, Processes and dynamics of radio cesium cycling in Chernobyl-contaminated pine forests : a multi-scale approach.

N°28. D'Or, Dimitri, Spatial prediction of soil properties: the Bayesian Maximum Entropy approach.

N°29. Vincke, Caroline, Approche écophysiologique des flux d'eau au sein

d'une chênaie pédonculée (Q. robur L.) dépérissante sur sol à régime hydrique alternatif.

N°37. Lambot, Sébastien, Hydrogeophysical characterization of soil using ground penetrating radar.

N°39. Hupet, François, Estimation of evapotranspiration fluxes at the field-scale: parameter estimation, variability and uncertainties.

Département de biologie appliquée et des productions agricoles

N°26. Oum Eloma, Janvier, Analyse économique comparée de la gestion forestière publique des différentes stratégies de production ligneuse au Cameroun.

N°31. Tilquin, Pierre, Methodological aspects of the mapping of disease resistance loci in livestock.

N°35. Nsengimana, Jérémie, Contribution to the analysis of linkage disequilibrium in livestock : effects of selection and inbreeding.

N°38. Tangni, Emmanuel, Occurrence of mycotoxins in beer, exposure assessment for consumers and development of biological detoxification options for the control of ochratoxin A during brewing.

Département de chimie appliquée et des bio-industries

Di Croce, Pascal, Phillips catalysts for ethylene polymerization : surface organization, active sites and performances.

N°27. Gijs, Laurence, Controlling the minor sulfur compounds in beer.

N°30. Cellier, Caroline, Catalytic removal of nitrogen- and sulfur-containing volatile organic compoundsDestruction.

N°32. Ramazzotti, Anna, Mitochondrial functional interactions between the yeast frataxin Yfh1p and Isu1p, a member of the iron-sulphur cluster assembly machinery in Saccharomyces cerevisiae.

N°34. Stukkens, Yvan, Expression and roles of NpABC1 : a Nicotiana plumbaginifolia ABC transporter involved in the plant-pathogen response.

N°36. Popescu Florea, Mihaela, Relationship between structure and activity of vanadium aluminium oxynitrides in propane ammoxidation.

N°40. Wiame, Hugues, Characterisation and catalytic properties of mixed

vanadium and aluminium oxynitride catalysts: "AlVON".

Faculté des Sciences, département de biologie

N°33. Ducarme, Xavier, Convergences et divergences microadaptatives chez les acariens endogés et cavernicoles.

2004

Département de biologie appliquée et des productions agricoles

N°43. Yankam Njonou, Rabelais, Analyse économique de la réponse du marché du blé différencié aux instruments de l'organisation commune des marchés du secteur des céréales : Le cas de la France.

N°47. Collard, François, Characterization of frutctosamine 3-kinase related protein.

N°49. Ruibal Mendieta, Nike Luisa, Lipids and minerals in spelt (*Triticum aestivum* ssp. *spelta*) and common wheat (*T. aestivum* ssp. *vulgare*): Chemical and nutritional distinction between both cereals.

Département de chimie appliquée et des bio-industries

N°41. Kanczewska, Justyna, Regulation of the plant plasma membrane H^+-ATPase by phosphorylation and 14-3-3 proteins.

N°42. Liégeois, Catherine, Pour un meilleur contrôle du statut pro-oxydant/ antioxydant des matières premières de la bière. Etude de la contribution des différentes étapes de fabrication du moût aux teneurs en *trans*-2-nonénal des bières vieillies.

N°44. Counet, Christine, Détermination des structures chimiques des polyphénols du chocolat et étude de leurs principales propriétés fonctionnelles.

N°46. Lefebvre, Benoît, Plant H^+-ATPase targeting to the plasma membrane is not by default and requires cytosolic structural determinants.

N°50. Dries Jan, Development and comparison of different multifunctional permeable reactive barrier (MPRB) concepts for the treatment of groundwater contaminated by pollutant mixtures.

N°51. Cranenbrouck, La culture monoxénique, un outil privilégié pour la systématique des champignons mycorhiziens à arbuscules et l'étude de leurs relations symbiotiques avec la plante hôte.

N°52. Callewaert Maïté, Surface modification by stimuli-responsive polymers : from model systems to stainless steel cleanability.

Département des sciences du milieu et de l'aménagement du territoire

N°45. Javaux, Mathieu, Solute transport in a heterogeneous unsaturated subsoil: experiments and modeling.

N°48. Fontenelle, Jean-Philippe, Dynamiques agraires, irrigation et institutions dans le delta du Fleuve rouge (Viêt-nam).

2005

Département de biologie appliquée et des productions agricoles

N°53. Nkunzimana, Tharcisse, Une filière agro-industrielle en mutation. Cas de la filière théicole au Burundi.

N°55. Meunier, Alexandre, Detection of rhizomania in Belgium: Diversity and characterization of Beet necrotic yellow vein virus RNAs-2 and –3.

N°56. Grissa Kaouthar, Étude de la dynamique des populations et du contrôle des acariens ravageurs dans les vergers de pommiers tunisiens.

Département de chimie appliquée et des bio-industries

N° 57. Vermeulen Catherine, Synthèse et caractérisation organoleptique de thiols polyfonctionnels Recherche de leur présence dans la bière.

N°58. Van Wilder Valérie, Phosphorylation des aquaporines de la membrane plasmique de maïs.

Département des sciences du milieu et de l'aménagement du territoire

N°54. Romanowicz, Agnieszka Aleksandra, The impacts of environmental change on water resources: A case study in the Dyle catchment (Belgium) in support of the implementation of the Water Framework Directive.

N°59. Delfosse Thomas, Acid Neutralisation and Sulphur Retention in S-Impacted Andosols

N°60. Titeux Hugues, Transfert de carbone organique dissous et de métaux dans des sols forestiers acides: influence du fonctionnement de la litière et des réserves minérales du sol.

Pour plus d'informations, visitez http://edoc.bib.ucl.ac.be/